

Rare Kaon Decays:

Matching Long and Short Distance Physics In $K \rightarrow \pi e^+ e^-$

THESIS SUBMITTED FOR THE DEGREE OF

Doctor of Philosophy

BY

Atanu Nath

CYCLE: XXVIII

UNDER THE SUPERVISION OF

Dr. Giancarlo D'Ambrosio



DIPARTIMENTO DI FISICA "ETTORE PANCINI"

Università degli Studi di Napoli Federico II

SESSION 2013-16

Dedicated to

Pritam Bhattacharjee, the friend who lost his life to pursue science. He went through so much torment and in the end lost his life in the hands of goons who will never know the beauty of a Feynman diagram. He inspired and will always inspire me to continue asking "why" and never give up.

Rare Kaon Decays: Matching Long and Short Distance Physics In $K \rightarrow \pi e^+ e^-$

Atanu Nath

Submitted for the degree of Doctor of Philosophy

March 31, 2016

Abstract

In this thesis we [1] try to understand the non-perturbative regime of QCD through long and short distance matching of the decay amplitude $K \rightarrow \pi e^+ e^-$. The first Chapter contains brief introduction and motivation then in the end we introduce the notations and transformation properties of various quantities and tables of phenomenological parameters. In the second chapter we discuss the Chiral Symmetry and its breaking and the construction of $\Delta S = 0, 1$ Lagrangians. Then we apply chiral Lagrangian to calculate the amplitude of $K^+ \rightarrow \pi^+ \pi^-$ decay at one loop in section 2.7.2 of the second chapter, the approach is a little bit different than that of Ecker, Pick and Raffael [2] but a few tricks introduced by them were used. In section 2.7.3 we introduce the beyond leading order dispersive calculation of the same decay by D'Ambrosio *et al.* [3] where the phenomenological parameters a_i and b_i (that completely fixes the form factor of the decay under study) were introduced and were predicted in the last chapter. In chapter 3 we start with a brief discussion of long and short distance matching of QCD and the calculation of Wilson coefficients. Then we introduce in reasonable detail the Bardeen, Buras and Gérard (BBG) [4, 5, 6] scheme of matching which plays the central role in our work. In the last chapter we apply BBG scheme to calculate the form factor of the decay $K \rightarrow \pi e^+ e^-$, first in section 4.0.4 without vector meson resonances and find values which are extremely small compared to the experimental values then in section 4.1 we introduce the resonances through Hidden Local Symmetry (HLS) and construct

the weak chiral Lagrangian containing vector coupling based on the Gilman-Wise[7, 8] $\Delta S = 1$ Hamiltonian, we then use it to calculate the appropriate extension of the BBG long distance evolution operator introduced in chapter 3 and calculate the a_i and b_i parameters. Vector inclusion shows huge enhancements in both parameters, where a_+ and a_S are very close to the experimental values but b_+ still lacks a factor of 2, the possible reasons for this were also discussed. We provide detailed evaluations of the loop integrals in Appendix B, Feynman rules and other conventions are presented in Appendix A and in Appendix C we present the large N structure of relevant Wilson coefficients. Notations, symbols and transformation properties of quantities along with various phenomenological parameters and their values are provided in the end of the introductory chapter. We preferred to provide the references in the end of each Chapter.

Bibliography

- [1] E. Coluccio et al. In: (2016). eprint: [arXiv:1522770](https://arxiv.org/abs/1522770).
- [2] G. Ecker, A. Pich, and E. de Rafael. In: *Nuclear Physics B* 291 (1987), pp. 692–719.
- [3] G. D’Ambrosio et al. In: *Journal of High Energy Physics* 1998 (1988). URL: <http://iopscience.iop.org/article/10.1088/1126-6708/1998/08/004>.
- [4] W. A. Bardeen, A. J. Buras, and J. -M. Gerard. In: *Nucl.Phys. B* 293 (1987), p. 787.
- [5] W. A. Bardeen, A. J. Buras, and J. -M. Gerard. In: *Nucl.Phys. B* 192 (1987), p. 138.
- [6] A. J. Buras, J. -M Gerard, and W. A. Bardeen. In: *Eur. Phys. J. C* 74 (2014), p. 2871.
- [7] F. J. Gilman and M. B. Wise. In: *Phys. Rev. D* 20 (1979), p. 2392.
- [8] F. J. Gilman and M. B. Wise. In: *Phys. Rev. D* (1980).

Declaration

The work in this thesis is based on research carried out by me under the supervision of Dr. Giancarlo D'Ambrosio, in the Department of Physical Sciences, Università degli Studi di Napoli Federico II, Naples, Italy. No part of this thesis has been submitted elsewhere for any other degree or qualification and it contains my own work in collaboration with Dr. David Greynat and Dr. Estefania Coluccio unless referenced to the contrary in the text.

Copyright © 2016 by Atanu Nath.

“The copyright of this thesis rests with the author. No quotations from it should be published without the author’s prior written consent and information derived from it should be acknowledged”.

Acknowledgements

I express my heartfelt gratitude to my supervisor Dr. Giancarlo D'Ambrosio for his unique way of teaching through passionate and involved black-board discussions. He always encouraged to prove him wrong, although I could not achieve that but this gesture alone carries the true scientific spirit. I am thankful to him for putting up with all my shortcomings and guiding me through. His vast knowledge and intuition inspires me all the time.

I express my immense respect for Dr. Luigi Cappiello whom I always found welcoming my doubts and questions, he spent long periods of time listening to however naive things I had to say and cleared my doubts.

I can never forget the wonderful teacher and friend that I found in my colleague Dr. David Greynat. I owe a great deal of my knowledge to him for all those little as well as day long discussions that we had and the volume of knowledge that I acquired from him because of his always humble and welcoming nature. I would also very much like to thank my colleague Dr. Estefania Coluccio for helping me organize the schedule to write down the thesis in a very short time.

My heartfelt thanks to my referees Prof. Fedele Lizzi and Dr. Giulia Ricciardi for being patient with me and for keeping faith in my work.

I would like to thank Prof. Velotta, he was always kind to me and understood and helped me whenever I was in trouble.

I owe my PhD to my wife Amrita who took care of literally everything despite the pressure of her own research. I can honestly confess that nothing would be possible without her constant understanding, support and above all her unconditional love

and friendship.

I cannot possibly forget the beautiful life that I have here in Napoli all because of my wonderful friends. Their constant support, care and understanding, I cannot pay any of this back ever.

Students come and go from different parts of this world but they all meet one common friend in Napoli. The friend, the saviour, the kindest and purest of the hearts our secretary Mr. Guido Celentano who does not realize what a rarest breed of human he is. I awe so much to him that words may fall short to describe how I feel.

I will be forever thankful to my mother for inspiring and supporting me to pursue science since my very childhood and thanks to my father for understanding me for whatever choices I made.

Thanks to bella *Napoli*, I will treasure you in my heart not just for Pizza, but for all the beautiful people and the way they live and leave memories behind.

Contents

| | |
|--|-----------|
| Abstract | ii |
| Declaration | v |
| Acknowledgements | vi |
| 1 Introduction | 1 |
| 1.1 Notations and Symbols | 4 |
| 1.1.1 Definitions of Parameters and Values | 5 |
| 1.2 Transformation Properties of Various Quantities | 6 |
| 2 Chiral Perturbation Theory | 9 |
| 2.1 Spontaneous Breakdown of Chiral Symmetry and Mesons | 9 |
| 2.1.1 Parametrization of The Coset Space | 11 |
| 2.2 The Leading Order Chiral Lagrangian $\mathcal{L}_{p^2}^{\Delta S=0}$ | 14 |
| 2.2.1 The Chiral Currents | 15 |
| 2.2.2 Weinberg's Power Counting | 19 |
| 2.2.3 Classical Sources and The Explicit Breaking of Chiral Symmetry | 20 |
| 2.3 $O(p^4)$ Strong Lagrangian | 23 |
| 2.3.1 The Low Energy Constants (LEC)'s | 24 |
| 2.4 Application of The Strong Lagrangian | 26 |

| | | |
|----------|---|-----------|
| 2.4.1 | Wavefunction Renormalization (WFR) | 26 |
| 2.4.2 | Off-Shell Pion and Kaon Electromagnetic Form Factors | 28 |
| 2.5 | Weak Chiral Lagrangian and The Kaons | 30 |
| 2.5.1 | Leading Order $\Delta S = 1$ Lagrangian | 32 |
| 2.6 | $O(p^4)$ Weak Lagrangian | 32 |
| 2.7 | Kaon Decays In ChPT | 33 |
| 2.7.1 | $K \rightarrow \pi\pi$ and The $\Delta I = 1/2$ Rule | 34 |
| 2.7.2 | $K \rightarrow \pi l^+ l^-$ Decay | 35 |
| 2.7.3 | Unitarity and $O(p^6)$ Calculation of $K \rightarrow \pi\gamma^*$ Form Factor | 42 |
| 3 | Long and Short Distance Matching | 49 |
| 3.1 | RG Evolution and Operator-Mixing | 50 |
| 3.1.1 | $K \rightarrow \pi e^+ e^-$ Effective Hamiltonian Due To Gilman and Wise | 52 |
| 3.2 | Bardeen-Buras-Gèrard Matching Scheme | 53 |
| 3.2.1 | Part-I: Short Distance Evolution of Wilson Coefficients and Large N | 54 |
| 3.2.2 | Part-II: Long Distance Evolution of Matrix Elements and The Chiral Large $N \sim f^2$ | 58 |
| 3.2.3 | The Matching of Quark and Meson Evolution | 65 |
| 3.3 | Inclusion of Vector Mesons In The BBG Scheme | 67 |
| 3.3.1 | Vector Improved Chiral Expansion Parameter $f(M^2)$ | 70 |
| 3.3.2 | Vector Contributions To $\langle Q_{\pm} \rangle$ | 71 |
| 3.3.3 | Improved LD-SD Matching | 72 |
| 4 | Application of BBG Scheme | 75 |
| 4.0.4 | Long Distance Mixing (Without Vectors) | 77 |
| 4.0.5 | $K^+ \rightarrow \pi^+ e^+ e^-$ Matrix Elements (No Vectors) | 79 |

| | | |
|----------|--|------------|
| 4.0.6 | a Parameter and LD-SD Matching | 84 |
| 4.1 | Inclusion of Vector Meson Through Hidden Local Symmetry | 87 |
| 4.1.1 | Construction of The Lowest Order Lagrangian | 88 |
| 4.1.2 | $K^+ \rightarrow \pi^+ e^+ e^-$ Matrix Elements (With Vectors) | 94 |
| 4.1.3 | $K_S \rightarrow \pi^0 e^+ e^-$ | 105 |
| 5 | Conclusion | 107 |
| | Appendix | 110 |
| A | Rules and Conventions | 110 |
| A.1 | Lagrangian Pieces and Feynman Rules For Chapter 2 | 111 |
| A.1.1 | Relevant Lagrangian Pieces Before Diagonalization | 111 |
| A.2 | Simultaneous Diagonalization of Kinetic and Mass Terms | 112 |
| A.2.1 | Relevant Weak Lagrangian Pieces After Diagonalization | 114 |
| A.3 | Lagrangian Pieces and Feynman Rules For Chapter 4 | 116 |
| A.3.1 | Relevant Lagrangian Pieces Before Diagonalization | 118 |
| A.4 | Diagonalization In Chapter 4 | 119 |
| A.5 | Rules and Conventions After Vector Inclusion | 120 |
| A.5.1 | Relevant Lagrangian Pieces Before Diagonalization | 120 |
| A.6 | Diagonalization In Chapter 4: HLS | 123 |
| B | Loop Integrals and Functions | 127 |
| B.1 | Notations Specific To Loop Integrations | 127 |
| B.2 | List of Relevant Analytic Functions | 128 |
| B.2.1 | Behavior of The Functions Around $z = 0$ | 128 |
| B.3 | Loop Integrals | 128 |

| | | |
|----------|--|------------|
| B.3.1 | Definitions of All The Integrals | 128 |
| B.3.2 | The Values of The Integrals In Dimensional Regularization (DR) | 129 |
| B.3.3 | The Values of The Integrals In Naive Cut-off Regularization (NCR) | 130 |
| B.3.4 | Integrals in Symmetry Preserving Cut-off Regularization (SPCR) | 132 |
| C | Large N Structure of Wilson Coefficients | 136 |

List of Figures

| | | |
|-----|--|----|
| 2.1 | Loop contribution to $\pi^+-\pi^0$ elastic scattering. | 18 |
| 2.2 | A generic loop at $O(p^n)$ | 19 |
| 2.3 | Loop contribution to wavefunction renormalization. | 26 |
| 2.4 | Mass of ρ from a pole fit of the pion EM form factor. | 30 |
| 2.5 | List of all possible diagrams before diagonalization of bilinear terms in the leading order chiral Lagrangian. | 38 |
| 2.6 | Type-I diagrams that do not provide q^2 | 39 |
| 2.7 | Type-II diagrams that do provide q^2 | 39 |
| 2.8 | One loop function $\chi(z)$ and $\chi(z/r_\pi^2)$ | 42 |
| 3.1 | Loop contribution to pion and kaon decay constants. | 62 |
| 3.2 | Loop contributions to $K \rightarrow \pi\pi$ process. | 63 |
| 4.1 | Variation of g_8 with scale M (in GeV). | 82 |
| 4.2 | Schematic representation of LD-SD matching through a quadratic divergence. | 86 |
| 4.3 | Long and short distance matching through $a_+(M^2)$. b_+ has been also shown (red) on this plot. | 87 |
| 4.4 | Type-I ^{hls} diagram contributing to $\langle Q_-^{hls} \rangle$ in HLS. | 95 |
| 4.5 | Type-II ^{hls} diagram contributing to $\langle Q_-^{hls} \rangle$ in HLS. V stands for ρ, ω and ϕ | 95 |

| | | |
|------|--|-----|
| 4.6 | Type-A diagrams that just corrects the external meson propagators. | 98 |
| 4.7 | Type-B diagrams are just $F_V(z)$ corrected versions of first two diagrams of Type-I diagrams of ChPT. | 99 |
| 4.8 | Type-C diagrams that upgrades the Type-I diagrams of ChPT. | 99 |
| 4.9 | Type-D diagrams that upgrades the Type-II diagrams of ChPT. | 99 |
| 4.10 | Type-E diagram that does not have a version in ChPT (after diagonalization of $K\pi$ terms). | 100 |
| 4.11 | Long and short distance matching through vector upgraded $a_+(M^2)$. b_+ has also been plotted (red). The shaded region shows the matching range. | 104 |

List of Tables

| | | |
|-----|--|-----|
| 1.1 | Masses of particles. | 5 |
| 1.2 | Decay constants and Λ_{QCD} | 5 |
| 1.3 | Values of other phenomenological parameters. | 5 |
| 2.1 | Renormalized LEC's in units of 10^{-3} at the scale $\mu = m_\rho$ | 25 |
| 2.2 | Experimental values of the parameters a_i and b_i | 44 |
| 3.1 | The amplitudes for the processes $K \rightarrow \pi\pi$ in the units of 10^{-8} GeV for different values of m_s | 67 |
| 3.2 | Variation of f^2 with the scale, with and without vector inclusion. | 71 |
| A.1 | Propagators of all the relevant particles. | 110 |
| A.2 | Vertex symbols. | 110 |

Chapter 1

Introduction

It is well known that QCD can be treated perturbatively at very high energy scale (scale $\gg 1$ GeV) due to the beautiful property called asymptotic freedom [1, 2, 3] that non-Abelian gauge theories enjoy but they also become non-perturbative (typically around and below 1 GeV) at the low energy scale because the coupling constant becomes too large ($O(1)$)! Because of this we have very good understanding of the high energy (short distance) region of the Standard Model (SM). On the other had at very low energy sale (long distance), typically at the scale of pion mass, we have a wonderful effective field theory called Chiral Perturbation Theory (ChPT) [4, 5, 6, 7, 8, 9, 10, 11, 12] built upon the symmetries of the standard model. ChPT is capable of predicting processes involving strong and weak interactions at the pion scale. In principle ChPT is capable of producing perfect results even at a scale very close to 1 GeV, but as we will discuss it in Chapter 2 that as we go up in energy scale more and more counter terms are needed [4, 13, 14, 15] to kill the loop divergences and hence renormalize the theory and ChPT loses the predicting power. To fix the values of large number of unknown coefficients (LEC's) large number of experiments on different scattering processes are needed leading to more input than the output ! So practically speaking, ChPT is perfect only at the pseudo-scalar meson scales. Hence we have two extreme regions where we understand physics well but no clear understanding of the region in between. As we will see in Chapter 3 how one can come down from the W boson mass scale to almost 1 GeV using Operator Product Expansion and Renormalization Group improved perturbation theory [16]. On the

other hand using ChPT we can reach up to a scale slightly below the first vector resonance ρ mass (775 MeV), starting from zero. But the region 0.7-1 GeV is a purely non-perturbative. In the time of LHC when we want to see physics beyond standard model it is necessary that we must have SM results ready to be tested but unfortunately that is not the case when look at the long distance region of SM because of the reasons discussed above. So we must be very efficient to choose the processes that are accessible and manageable theoretically. Decays of Kaons offer one of the best channels to do exactly that.

Among various available attempts (for example [17, 18, 19, 20, 21, 22, 23, 24, 25, 26, 27]) to understand non-perturbative QCD, a relatively simple but interesting framework based on the large $N_c (= N)$ structure of long and short distance QCD is the one developed by Bardeen, Buras and Gérard (BBG) [28, 29, 30] is partially successful in explaining a long standing puzzle called $\Delta I = 1/2$ rule that we will discuss in section 2.7.1 of Chapter 2. The ϵ/ϵ' Their results are also backed well by lattice collaboration [RBC-UKQCD]. We will review this (BBG) framework in reasonable details in Chapter 3.

As the title “...*Matching Long and Short Distance Physics* ” says, we are interested to understand the SM at any energy scale in the cotext of “*Rare Kaon Decays*” especially “ $K \rightarrow \pi e^+ e^-$ ” and eventually predict the values of phenomenological parameters a_i and b_i introduced in section 2.7.3 of Chapter 2. The motivation is to test this framework on experimentally well understood processes so that if it passes the test we can finally produce SM based theoretical predictions. The decay that we are studying is especially important because if we understand the form factor well, it can be used to look for the Universal Lepton Flavour Violation [31]. As our work discussed in Chapter 4 suggests, BBG framework looks promising and in such a case we can look for deviations from the standard model if any. Fortunately NA62 [refer] experiment will study at accuracy.... s/n... this is a great window of opportunity, we can produce numbers and test in the experiment to look for new physics.

The approach is the following: one uses RG improved perturbation theory to

come down from very high energy scale to 1 GeV (keeping the large N structure of the anomalous dimension matrix manifest) where the short distance information gets encoded in the Wilson Coefficients then using a hard momentum cut-off (M) regularized long distance effective theory (such as ChPT) develops an RG like evolution (and so an analogous anomalous dimension matrix with large N structure) of the matrix elements and looks for a range of M where the short distance logarithmic divergence gets numerically cancelled by the quadratic divergence of the long distance theory and amplitude becomes scale independent. This obtained scale is the matching scale where physical quantities can be reliably evaluated and corresponding cross-sections can be matched with the experiment.

Our work is available here [32]. We have also calculated the low energy constant L_9 in the BBG approach which is not included in this thesis but will be published shortly. We are currently also working ¹ on a more formal approach to match the long and short distance QCD through Functional Bosonization method which will be sent for publication soon.

¹In collaboration with M. Knecht.

1.1 Notations and Symbols

Symbols

| | |
|--|--|
| G | The chiral symmetry group $SU(3)_L \times SU(3)_R$ |
| H | The unbroken symmetry group $SU(3)_V$ |
| $\mathcal{C}, \mathcal{P}, \mathcal{T}$ | Charge conjugation, parity and time-reversal transformations respectively |
| Σ | Exponential representation of mesons. |
| Π | Meson octet. |
| $\mathfrak{L}, \mathfrak{R}$ and \mathcal{V} | Left, right and vector transformations of $SU(3)_L$, $SU(3)_R$ and $SU(3)_V$ respectively. |
| λ_a, T^a | Gell-mann matrices and $SU(3)$ generators with $a = 1, \dots, 8$ |
| v_μ, a_μ | External Vector and axial-vector fields respectively. |
| $s, p, \chi = s + ip$ | External scalar fields. |
| l_μ, r_μ | Left and right handed gauge fields of the chiral group $SU(3)_L, SU(3)_R$ respectively |
| $\mathcal{L}_\mu, \mathcal{R}_\mu$ | Noether's currents corresponding to the left and right chiral symmetry. |
| $\mathcal{L}_{\mu\nu}, \mathcal{R}_{\mu\nu}$ | Field strength tensors corresponding to l_μ, r_μ |
| $\mathcal{L}_{p^n}^{\Delta S=0,1}$ | $O(p^n)$ strong and $\Delta S = 1$ weak chiral Lagrangians respectively. |
| $m_K, m_\pi, m_\eta, m_\rho$ | Masses of kaon, pion, η and ρ mesons respectively |
| \tilde{m} | Is the mass parameter introduced by Bardeen, Buras and Gerard in [30]. |
| M_W | Mass of W Boson |
| m_q | Mass of $q = u, d, s, c, b, t$ quarks. |
| M | Momentum cut-off of loop integrals |
| $\alpha_s^{(f)}(\mu)$ | QCD running coupling constant at the $\bar{M}S$ scale μ where f is the number of active flavours |
| α_e | QED coupling constant $= \frac{e^2}{4\pi}$ |

1.1.1 Definitions of Parameters and Values

$$\begin{aligned}
r_i &= m_i/m_K \\
z_i &= z/r_i^2 \\
z_K &= z = q^2/m_K^2 \\
z_M &= q^2/M^2
\end{aligned}
\tag{1.1.1}$$

List of values of parameters are given in Table. 1.2 and 1.3.

Everything is in GeV.

| m_c | m_b | m_t | M_W | m_π | m_K | m_V | m_η | \tilde{m} |
|-------|-------|-------|-------|---------|-------|-------|----------|-------------|
| 1.3 | 4.4 | 170 | 80.3 | 0.139 | 0.494 | 0.775 | 0.546 | 0.3 |

Table 1.1: Masses of particles.

Everything is in MeV.

| F_π | F_K | Λ_{QCD} |
|---------|-------|-----------------|
| 93 | 120 | 300 |

Table 1.2: Decay constants and Λ_{QCD} .

α and β are in the units of 10^{-8} and G_F has a factor of 10^{-5}

| G_F (GeV ⁻²) | z_0 | α_+ | β_+ | α_S | β_S |
|-----------------------------|-------|-----------------|----------------|----------------|----------------|
| 1.17 | 0.41 | -20.6 ± 0.5 | -2.8 ± 1.2 | -5.2 ± 0.5 | -0.5 ± 1.3 |

Table 1.3: Values of other phenomenological parameters.

1.2 Transformation Properties of Various Quantities

Transformation of Σ and It's Covariant Derivative

$$\begin{aligned}
(\Sigma, D_\mu \Sigma) &\stackrel{G}{\mapsto} \mathfrak{L}(\Sigma, D_\mu \Sigma) \mathfrak{R}^\dagger \\
(\Sigma, D_\mu \Sigma) &\stackrel{C}{\mapsto} (\Sigma^\dagger, D_\mu \Sigma^\dagger) \\
&\stackrel{P}{\mapsto} (\Sigma^T, D_\mu \Sigma^T) \\
&\stackrel{T}{\mapsto} (\Sigma, D_\mu \Sigma), \text{ if } T\Pi T^{-1} = \Pi
\end{aligned}$$

Transformation of External Vector Fields

$$\begin{aligned}
(l_\mu, r_\mu) &\stackrel{\mathfrak{L}}{\mapsto} \mathfrak{L}(l_\mu, r_\mu) \mathfrak{L}^\dagger + i \mathfrak{L} \partial_\mu \mathfrak{L}^\dagger \\
(l_\mu, r_\mu) &\stackrel{\mathfrak{R}}{\mapsto} \mathfrak{R}(l_\mu, r_\mu) \mathfrak{R}^\dagger + i \mathfrak{R} \partial_\mu \mathfrak{R}^\dagger \\
l_\mu \stackrel{C}{\leftrightarrow} -r_\mu^T, \quad l_\mu \stackrel{P}{\leftrightarrow} r^\mu, \quad (l_\mu, r_\mu) \stackrel{T}{\leftrightarrow} -(l^\mu, r^\mu)
\end{aligned}$$

Transformation of Left and Right Field-Strength Tensors

$$\begin{aligned}
(\mathcal{L}_{\mu\nu}, \mathcal{R}_{\mu\nu}) &\stackrel{\mathfrak{L}}{\mapsto} \mathfrak{L}(\mathcal{L}_{\mu\nu}, \mathcal{R}_{\mu\nu}) \mathfrak{L}^\dagger \\
(\mathcal{L}_{\mu\nu}, \mathcal{R}_{\mu\nu}) &\stackrel{\mathfrak{R}}{\mapsto} \mathfrak{R}(\mathcal{L}_{\mu\nu}, \mathcal{R}_{\mu\nu}) \mathfrak{R}^\dagger \\
\mathcal{L}_{\mu\nu} \stackrel{C}{\leftrightarrow} -\mathcal{R}_{\mu\nu}^T, \quad \mathcal{L}_{\mu\nu} \stackrel{P}{\leftrightarrow} \mathcal{R}^{\mu\nu}, \quad (\mathcal{L}_{\mu\nu}, \mathcal{R}_{\mu\nu}) \stackrel{T}{\leftrightarrow} (\mathcal{L}^{\mu\nu}, \mathcal{R}^{\mu\nu})
\end{aligned}$$

Transformation of Chiral Currents

$$\begin{aligned}
(\mathcal{L}_\mu, \mathcal{R}_\mu) &\stackrel{\mathfrak{L}}{\mapsto} \mathfrak{L}(\mathcal{L}_\mu, \mathcal{R}_\mu) \mathfrak{L}^\dagger \\
(\mathcal{L}_\mu, \mathcal{R}_\mu) &\stackrel{\mathfrak{R}}{\mapsto} \mathfrak{R}(\mathcal{L}_\mu, \mathcal{R}_\mu) \mathfrak{R}^\dagger \\
\mathcal{L}_\mu \stackrel{C}{\leftrightarrow} -\mathcal{R}_\mu^T, \quad \mathcal{L}_\mu \stackrel{P}{\leftrightarrow} \mathcal{R}^\mu, \quad (\mathcal{L}_\mu, \mathcal{R}_\mu) \stackrel{T}{\leftrightarrow} (\mathcal{L}^\mu, \mathcal{R}^\mu)
\end{aligned}$$

Transformation of External Scalar Fields

χ transforms exactly like Σ .

Bibliography

- [1] D. J. Gross and F. Wilczek. In: *Phys. Rev. Lett.* 30 (1973), pp. 1343–1346.
- [2] H. D. Politzer. “Reliable Perturbative Results for Strong Interactions?” In: *Phys. Rev. Lett.* 30 (1973), pp. 1346–1349.
- [3] D. J. Gross. In: *Nucl. Phys. B Proceedings Supplements* 74 (1999), pp. 426–446. eprint: [hep-th/9809060](#).
- [4] J. Gasser and H. Leutwyler. In: *Nucl. Phys. B* 250.465 (1985).
- [5] S. Weinberg. In: *Physica A* 96 (1979), pp. 327–340.
- [6] G. Ecker. In: *Prog. Part. Nucl. Phys.* 35.1 (1995). eprint: [hep-ph/9501357](#).
- [7] A. Pich. In: *Prog. Prog. Phys.* 58.563 (1995). eprint: [hep-ph/9502366](#).
- [8] A. Pich. In: (). eprint: [hep-ph/9806303](#).
- [9] S. Scherer. “Introduction to Chiral Perturbation Theory”. In: (2002). eprint: [hep-ph/0210398](#).
- [10] J. Gasser. In: *Lect. Notes. Phys.* 629.1 (2004). eprint: [hep-ph/0312367](#).
- [11] J. Bijnens. In: *Prog. Prat. Phys.* 58.521 (2007). eprint: [hep-ph/0604043](#).
- [12] J. F. Donoghue. *Dynamics of the Standard Model*. Ed. by E. Golowich and B. R. Holstein. 5th ed. Cambridge Monographs on Particle Physics, Nuclear Physics and Cosmology, 1992.
- [13] J. Wess and B. Zumino. In: *Phys. Lett. B* 37.95 (1971).
- [14] E. Witten. In: *Nucl. Phys. B* 223.422 (1983).
- [15] J. Bijnens and J. Prades. In: *JHEP* 9901.023 (1999). eprint: [hep-ph/9811472](#).

- [16] F. J. Gilman and M. B. Wise. In: *Phys. Rev. D* (1980).
- [17] M. Knecht, S. Peris, and E. de Rafael. In: *Phys. Lett. B* 508 (2001), p. 117.
- [18] M. Knecht, S. Peris, and E. de Rafael. In: *Phys. Lett. B* 457 (1999), p. 227.
- [19] A. Pich, B. Guberina, and E. de Rafael. In: *Nucl. Phys. B* 277 (1986), p. 197.
- [20] B. Guberina, A. Pich, and E. de Rafael. In: *Phys. Lett. B* 163 (1985), p. 198. eprint: [hep-th/9809060](#).
- [21] M. Jamin and A. Pich. In: *Nucl. Phys. B* 425 (1994), p. 15. eprint: [hep-ph/9402363](#).
- [22] J. Laiho and R. S. Van de Water. In: *PoS Latt. 2010* (2010), p. 312.
- [23] C. H. Kim, C. Sachrajda, and T. In: *Phys. Rev. D* 81 (2010), p. 114506.
- [24] E. J. Goode and M. Lightman. In: *PoS. Latt. 2010* (2010), p. 313.
- [25] Colangelo and *et al.* In: *Eur. Phys. J. C* 71 (2011), p. 1695. eprint: [1101.5579\[hep-lat\]](#).
- [26] P. Boyle and *et al.* In: *PoS. Latt. 2010* (2010), p. 307. eprint: [1101.5579\[hep-lat\]](#).
- [27] P. Boucaud et al. In: *Nucl. Phys. B* 721 (2005), p. 175. eprint: [hep-lat/0412029](#).
- [28] W. A. Bardeen, A. J. Buras, and J. M. Gerard. In: *Phys.Lett. B* 180 (1986), p. 133.
- [29] W. A. Bardeen, A. J. Buras, and J. -M. Gerard. In: *Nucl.Phys. B* 293 (1987), p. 787.
- [30] W. A. Bardeen, A. J. Buras, and J. -M. Gerard. In: *Nucl.Phys. B* 192 (1987), p. 138.
- [31] A. Crivellin et al. In: (2016). eprint: [arXiv:1601.00970](#).
- [32] E. Coluccio et al. In: (2016). eprint: [arXiv:1522770](#).

Chapter 2

Chiral Perturbation Theory

2.1 Spontaneous Breakdown of Chiral Symmetry and Mesons

Let us begin with writing down the quark part of the mass-less QCD Lagrangian:

$$\mathcal{L}_q^0 = i\bar{q}\not{\partial}q \quad (2.1.1)$$

where q is the quark spinor that also contains different flavors and colors but for the moment we will just consider the lightest ones that is u and d . This Lagrangian enjoys so called Chiral symmetry $SU(2)_L \times SU(2)_R \times U(1)_V \times U(1)_A$ ¹, that will become apparent when we write down the Lagrangian in terms of Weyl spinors:

$$\mathcal{L}_q^0 = iq_L^\dagger \bar{\sigma}^\mu \partial_\mu q_L + iq_R^\dagger \sigma^\mu \partial_\mu q_R = i\bar{q}_L \not{\partial} q_L + i\bar{q}_R \not{\partial} q_R \quad (2.1.2)$$

where, $\sigma^\mu = (1, \sigma^i)$ and $\bar{\sigma}^\mu = (1, -\sigma^i)$ and

$$\gamma^\mu = \begin{pmatrix} \bar{\sigma}^\mu & 0 \\ 0 & \sigma^\mu \end{pmatrix} \quad (2.1.3)$$

¹ 2×2 because we are considering only the lightest family of quarks. And V and A stand for vector and axial.

The Lagrangian is symmetric under the independent transformations:

$$q_L \mapsto \mathfrak{L} q_L, \quad q_R \mapsto \mathfrak{R} q_R, \quad \mathfrak{L}, \mathfrak{R} \in SU(2)_{L,R} \quad (2.1.4)$$

In practice there is a mass term,

$$\mathcal{L}_q^m = -m_q \bar{q} q = -m_q (\bar{q}_L q_R + \bar{q}_R q_L) \quad (2.1.5)$$

that breaks the independent left-right symmetry but preserves the vector symmetry, that is the subgroup $SU(2)_V$ whose elements are $\mathfrak{L} = \mathfrak{R} = \mathcal{V}$ is still a symmetry known as the isospin symmetry which is of course approximate because $m_u \neq m_d$. This whole scheme can be upgraded to 3-flavor case (u, d, s) and the symmetry group will become $SU(3)_L \times SU(3)_R \times U(1)_V \times U(1)_A$. For the moment if we consider the masses of u, d and s quarks to be zero which is justified in comparison to Λ_{QCD} (almost true for u and d though) but it has been shown that [1] $U(1)_A$ is an anomaly of the quantum theory while $U(1)_V$ is a symmetry and it leads to baryon number conservation. So let us talk about the rest that is $SU(3)_L \times SU(3)_R$. But QCD vacuum condensate $\langle \bar{q} q \rangle \neq 0$ breaks the chiral symmetry $SU(3)_L \times SU(3)_R$ down to $SU(3)_V$, the mechanism of which is not known but it is strongly believed that the breakdown is a dynamical one [2] and the 8 broken generators create an octet of massless Nambu-Goldstone bosons [3, 4] living in the coset space $SU(3)_L \times SU(3)_R / SU(3)_V$. From $\langle q \bar{q} \rangle$ we see that we need spin zero, isospin 1, parity odd 8 Goldstone bosons and in nature we have an octet of light mesons (π 's, K 's and η_8 ²) that has this exact quantum numbers. In practice, $u, d,$ and s are very light but not massless making the original chiral symmetry an approximate one which is the reason why mesons are light but not massless. So here we see two steps of symmetry breaking:

- Massless QCD chiral symmetry spontaneously breaking down and creating massless Goldstone bosons.

²the 9th meson, η kills everything because it is too heavy ($m_{\eta'} \simeq 1$ GeV), but we will not discuss that here.

- Quarks acquire masses through Higgs mechanism leading to further and explicit breaking of the chiral symmetry that finally gives masses to the original Goldstone bosons (mesons).

Based on only these facts and parametrizing the coset space, a theory of very low energy QCD, that is the theory of mesons [5, 6, 7, 8, 9, 10, 11, 12, 13, 14]. We will consider the most popular parametrization, and start with the beautiful and the most successful theory of mesons, that is the **Chiral Perturbation Theory**.

2.1.1 Parametrization of The Coset Space

There are infinite ways we can parametrize the coset space of course because there are infinite directions the vacuum can choose that ultimately breaks the global symmetry, hence there are infinitely many ways the mesons can be parametrized and of course it's consistent with the equivalence theorem.³ That may sound depressing but there's a beautiful formalism called CCWZ [15, 16] which can save us (A review on this worth mentioning can be found here [17]). We will talk about this now and then will cherry-pick two most popular parametrizations.

CCWZ Formalism

In a theory where the global symmetry group G breaks down to a subgroup H , the vacuum manifold is the coset space G/H , in our case $G = SU(3)_L \times SU(3)_R$, $H = SU(3)_V$ and the coset space is also isomorphic to $SU(3)$. We would like to choose a set of coordinates to describe the local orientation of the vacuum for small fluctuation around the standard vacuum. Let us say $\Xi(x) \in G$ be the element that rotates the standard vacuum configuration to the local field configuration. But as H is a residual symmetry, that is symmetry of the standard vacuum, hence $\Xi(x)\mathfrak{h}$ where $\mathfrak{h} \in H$ also plays the same role as $\Xi(x)$ does. CCWZ procedure is to pick a set of broken generators X^a and parametrize the coset space as:

³Field redefinitions that preserves symmetries and 1-particle states allow classical EOM to simplify local EFT operators without affecting the observables.

$$\Xi(x) = e^{iX^a\pi^a(x)} \quad (2.1.6)$$

where $\pi^a(x)$ are the pseudo-scalar meson fields. Under a global transformation $\mathbf{g} \in G$, $\Xi(x) \mapsto \mathbf{g}\Xi(x)$ and is not in the standard form any more and can be expressed as:

$$\mathbf{g}\Xi(x) = \Xi'(x)\mathfrak{h} \implies \Xi(x) \mapsto \mathbf{g}\Xi(x)\mathfrak{h}^{-1}(g, \Xi(x)) \quad (2.1.7)$$

Since $\mathbf{g}\Xi(x)$ and $\Xi'(x)\mathfrak{h}$ describe the same field configuration differ by H , this \mathfrak{h} is non-trivial because the Goldstone boson manifold G/H is curved. 2.1.6 and 2.1.7 together define the CCWZ parametrization. Any other parametrization (infinitely many of them) will yield the same physics (S-matrix elements).

The generators of chiral symmetry ($G = SU(3)_L \times SU(3)_R$) are T_L^a and T_R^a and that of the unbroken group ($H = SU(3)_V$) are $T_L^a + T_R^a$. There are two commonly used bases for writing down the effective Lagrangian called the ξ and the Σ , meaning, there are two choices of broken generators that provides two most popular parametrizations of the coset space in terms of which chiral effective Lagrangian describing the dynamics of the goldstone bosons (8 mesons in this case) can be written down and we will discuss them now.

The ξ Basis

This basis is defined by the choice $X^a = T_L^a - T_R^a$. If the G is represented in a block diagonal form then any $\mathbf{g} \in G$ can be written as:

$$\mathbf{g} = \begin{pmatrix} \mathfrak{L} & 0 \\ 0 & \mathfrak{R} \end{pmatrix} \quad (2.1.8)$$

where $\mathfrak{L} \in SU(3)_L$ and $\mathfrak{R} \in SU(3)_R$, the unbroken group (H) then can be represented by,

$$\mathfrak{h} = \begin{pmatrix} \mathcal{V} & 0 \\ 0 & \mathcal{V} \end{pmatrix} \quad (2.1.9)$$

With $\mathfrak{L} = \mathfrak{R} = \mathcal{V}$. Then by CCWZ scheme we can parametrize the mesons as:

$$\Xi(x) = e^{iX \cdot \pi(x)} = \exp \left\{ i \begin{pmatrix} T^a \pi^a(x) & 0 \\ 0 & -T^a \pi^a(x) \end{pmatrix} \right\} = \begin{pmatrix} \xi(x) & 0 \\ 0 & \xi^\dagger(x) \end{pmatrix} \quad (2.1.10)$$

where T^a are the $SU(3)$ generators, can be Gell-Mann matrices and $\xi = e^{iT^a \pi^a}$ and the transformation law is:

$$\begin{pmatrix} \xi(x) & 0 \\ 0 & \xi(x) \end{pmatrix} \mapsto \begin{pmatrix} \mathfrak{L} & 0 \\ 0 & \mathfrak{R} \end{pmatrix} \begin{pmatrix} \xi(x) & 0 \\ 0 & \xi^\dagger(x) \end{pmatrix} \begin{pmatrix} \mathcal{V}^{-1} & 0 \\ 0 & \mathcal{V}^{-1} \end{pmatrix}$$

That gives:

$$\xi(x) \mapsto \mathfrak{L} \xi(x) \mathcal{V}^{-1}(x) = \mathcal{V}(x) \xi(x) \mathfrak{R}^\dagger \quad (2.1.11)$$

which defines \mathcal{V} in terms of \mathfrak{L} and ξ .

The Σ Basis

In Σ basis, the left generators are chosen as broken and so CCWZ gives:

$$\Xi(x) = e^{iX \cdot \pi(x)} = \exp \left\{ i \begin{pmatrix} T^a \pi^a(x) & 0 \\ 0 & 0 \end{pmatrix} \right\} = \begin{pmatrix} \Sigma(x) & 0 \\ 0 & 1 \end{pmatrix} \quad (2.1.12)$$

where $\Sigma = e^{iT \cdot \pi}$ and the transformation law takes the form:

$$\begin{pmatrix} \Sigma(x) & 0 \\ 0 & \Sigma(x) \end{pmatrix} \mapsto \begin{pmatrix} \mathfrak{L} & 0 \\ 0 & \mathfrak{R} \end{pmatrix} \begin{pmatrix} \Sigma(x) & 0 \\ 0 & \Sigma(x) \end{pmatrix} \begin{pmatrix} \mathcal{V}^{-1} & 0 \\ 0 & \mathcal{V}^{-1} \end{pmatrix}$$

That means,

$$\Sigma(x) \mapsto \mathfrak{L}\Sigma(x)\mathfrak{R}^\dagger \quad (2.1.13)$$

Comparing this with Eq. (2.1.11) we can see that:

$$\Sigma(x) = \xi^2(x) \quad (2.1.14)$$

2.2 The Leading Order Chiral Lagrangian $\mathcal{L}_{p^2}^{\Delta S=0}$

From here on we will choose the Σ parametrization of the mesons unless it is specified otherwise. Goldstone boson fields are angular variables and so dimensionless but to write a Lagrangian for the mesons we need mass dimension 1 fields hence we cast Σ in terms of a mass dimension 1 constant quantity f such that Σ is dimensionless and the most popular parametrization is:

$$\Sigma(x) = e^{2i\Pi(x)/f} \quad (2.2.15)$$

where $\Pi(x) = T^a \pi^a(x)$ and $\text{tr}[T^a T^b] = \delta^{ab}/2$. For $T^a = \lambda^a/2$ meson matrix takes the form:

$$\Pi = \frac{1}{\sqrt{2}} \begin{pmatrix} \pi^0/\sqrt{2} + \eta_8/\sqrt{6} & \pi^+ & K^+ \\ \pi^- & -\pi^0/\sqrt{2} + \eta_8/\sqrt{6} & K^0 \\ K^- & \bar{K}^0 & -2\eta_8/\sqrt{6} \end{pmatrix} \quad (2.2.16)$$

We will soon see that f is the pion decay constant (~ 93 MeV) and is related to the quark condensate. Following points will guide us to construct a Lagrangian:

- The Lagrangian must be an invariant function of $\Sigma(x)$, invariant both under the chiral symmetry group and Lorentz group and must have right transformation properties under \mathcal{C} and \mathcal{P} .

- As it describes a low energy theory of mesons, it must have an expansion in terms of external momenta, that is equivalent to say that there will be increasing number of derivatives at each higher order.

$O(p^0)$ order is just a function of $\Sigma\Sigma^\dagger$ hence an uninteresting constant moreover, there cannot be odd orders of momenta because of Lorentz invariance, hence:

$$\mathcal{L}^{\Delta S=0} = \mathcal{L}_{p^2}^{\Delta S=0} + \mathcal{L}_{p^4}^{\Delta S=0} + \dots \quad (2.2.17)$$

At $O(p^2)$ there is only one choice⁴

$$\mathcal{L}_{p^2}^{\Delta S=0} = \frac{f^2}{4} \text{tr}[\partial^\mu \Sigma \partial_\mu \Sigma^\dagger] \quad (2.2.18)$$

where the trace is in the flavor space of 3×3 matrices, pre-factor f^2 ensures that the kinetic terms of pions and kaons have the right coefficients. This Lagrangian can be used to calculate tree level amplitudes like π - π scattering etc. But before that let us convince ourselves that f indeed is the pion decay constant.

2.2.1 The Chiral Currents

Noether left and right currents associated with $SU(3)_{L,R}$ can be obtained by considering infinitesimal left and right transformation of Σ by $\mathfrak{L} = 1 + i\epsilon_L^a(x)T^a + O(\epsilon^2)$ under the left transformation $\Sigma \mapsto \Sigma + i\epsilon_L^a T^a \Sigma$ putting this in Eq. (2.2.18) we can obtain the change in Lagrangian:

$$\delta \mathcal{L}_{p^2}^{\Delta S=0} = \mathcal{L}_{p^2}^{\Delta S=0} + \frac{if^2}{4} \text{tr}[2T^a \Sigma \partial^\mu \Sigma^\dagger] \partial_\mu \epsilon_L^a + \frac{if^2}{4} \text{tr}[T^a (\partial^\mu \Sigma \partial_\mu \Sigma^\dagger - \partial_\mu \Sigma^\dagger \partial_\mu \Sigma)] \epsilon_L^a \quad (2.2.19)$$

Taking derivative of the change in Lagrangian with respect to $\partial_\mu \epsilon_L^a$ we obtain:

⁴As Σ is dimensionless and we are still in the chiral limit so no masses either, hence at $O(p^2)$ only double derivative term that counts right and this is the only one.

$$\mathcal{L}_\mu^a = \frac{if^2}{2} \text{tr}[T^a \Sigma \partial_\mu \Sigma^\dagger] \quad (2.2.20)$$

When we expand Σ we find:

$$\begin{aligned} \mathcal{L}_\mu^a &= \frac{if^2}{2} \text{tr}[T^a \mathbb{1} T^b \frac{-2i}{f} \partial_\mu \pi^b] + \dots \\ &= \frac{f}{2} \partial_\mu \pi^a \end{aligned} \quad (2.2.21)$$

And so

$$\langle 0 | \mathcal{L}_\mu^a | \pi^b(p) \rangle = -i \frac{f}{2} p_\mu \delta^{ab} + \dots \quad (2.2.22)$$

which proves that f is indeed the pion decay constant at leading order and we call $f|_{p^2} = F_\pi$. Measuring the decay $\pi \rightarrow \mu\nu$ we can fix $f \sim 93$ MeV at this order. Similarly under right transformation we get:

$$\mathcal{R}_\mu^a = \frac{if^2}{2} \text{tr}[T^a \Sigma^\dagger \partial^\mu \Sigma] \quad (2.2.23)$$

The axial current in terms of pion fields appears as:

$$j_A^{\mu a} = \mathcal{R}^{\mu a} - \mathcal{L}^{\mu a} \quad (2.2.24)$$

$$= \frac{if^2}{2} \text{tr}[T^a (\Sigma^\dagger \partial^\mu \Sigma - \Sigma \partial^\mu \Sigma^\dagger)] \quad (2.2.25)$$

$$= \frac{if^2}{2} \text{tr}[T^a (\mathbb{1} \frac{2i}{f} T^b \partial^\mu \pi^b + \mathbb{1} \frac{2i}{f} T^b \partial^\mu \pi^b)] + \dots$$

$$= -2f \text{tr}[T^a T^b] \partial^\mu \pi^b + \dots$$

$$= -f \partial^\mu \pi^a + \dots \quad (2.2.26)$$

Before dealing with the masses let us pause for a moment and try to understand whatever we have achieved till now. Two questions:

1. This Lagrangian has an expansion in low momenta, but low with respect to what ?

2. It is an infinite series with all possible diagrams, how do we determine what are the relevant contributions ?
3. What about perturbative unitarity and loops and so divergences ?

We have to understand the counting rules to answer these questions. At first we will take a naive approach and then will introduce more formal analysis [7].

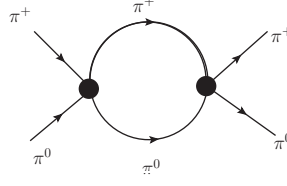
Low Momentum Expansion and Naive Dimensional Counting

As we have already seen that the chiral Lagrangian is a series in number of derivatives involved so from dimensional counting we expect that coefficient of a term involving n numbers of derivatives will behave like Λ_χ^{4-n} , where Λ_χ is the scale of our chiral EFT. Therefore, such a vertex will look like p^n/Λ_χ^{n-4} , so if we restrict ourselves to momenta $p \ll \Lambda_\chi$ we just have to consider a few terms in the momentum expansion of the Lagrangian and needless to say \mathcal{L}_{p^2} will be the leading term with first correction coming from \mathcal{L}_{p^4} and so on.

Loops and Chiral Symmetry Breaking Scale Λ_χ

At a first glance it would appear that our dimensional counting logic is shattered by the loops ! For example we may expect that at $O(p^4)$, two of momenta are external and two internal that gets integrated leading to a disastrous behavior p^2/Λ_χ^{4-4} ! Fortunately, that never happens. Let us consider an example to illustrate this before going into a more formal proof.

Let us consider the loop diagram of Fig. 2.1 that contributes to $\pi^+\pi^0$ scattering: If we use $O(p^2)$ vertices then we have one f^2 pre-factor in each vertex from the Lagrangian and $1/f$ coming with each pion field from the expansion of Σ hence an overall factor of $1/f^4$ and for simplicity let us take all the external momenta to be equal (p let us say). In that case each vertex will give us a set of terms like $(p^2, p \cdot l, l^2)$ which will provide an overall numerator in the amplitude of the following form:


 Figure 2.1: Loop contribution to $\pi^+-\pi^0$ elastic scattering.

$(p^4, p^2(p_\mu l^\mu), p^2 l^2, p_\mu p_\nu l^\mu l^\nu, p_\mu l^\mu l^2, l^4)$ and then we have two denominators, if we want to look at the UV divergence then let us consider the loop momenta to be very high, that is $l^2 \gg p^2$, in that case:

$$\begin{aligned}
 \langle \pi_+ \pi_0 | \mathcal{L}_{p^2}^{\Delta S=0} | \pi_+ \pi_0 \rangle_{loop} &\sim \frac{1}{f^4} \int \frac{d^4 l}{l^4} \left(p^4, p^2 p_\mu l^\mu, p^2 l^2, p_\mu p_\nu l^\mu l^\nu, p_\mu l^\mu l^2, l^4 \right) \\
 &\sim \left(\frac{p}{f} \right)^4 \int \left(\frac{d^4 l}{l^4}, \frac{p_\mu}{p^2} \frac{d^4 l l^\mu}{l^4}, \frac{1}{p^2} \frac{d^4 l}{l^2}, \frac{p_\mu p_\nu}{p^4} \frac{d^4 l l^\mu l^\nu}{l^4}, \frac{p_\mu}{p^4} \frac{d^4 l l^\mu}{l^2}, \frac{d^4 l}{p^4} \right)
 \end{aligned}$$

All these terms inside the parenthesis are visibly dimensionless and the only quantity that has a dimension is p , hence the integral of the parenthesis must be expressible in terms of a dimensionless function of the external momenta.

$$\langle \pi_+ \pi_0 | \mathcal{L}_{p^2}^{\Delta S=0} | \pi_+ \pi_0 \rangle_{loop} \sim \left(\frac{p}{f} \right)^4 f(p^2/\mu^2) \quad (2.2.27)$$

where μ is some momentum scale, now if we would have used dimensional regularization with space-time dimension d then we had to use:

$$\int d^4 l \rightarrow \mu^{(4-d)} \int d^d l \quad (2.2.28)$$

And so we would have found that function $f(p^2/\mu^2)$ to be a logarithm plus dimensionless numbers and pole type divergence. Hence we can see that this loop does behave like p^4 and not p^2 . With each $1/f^2$ factor entering at each vertex enters a p^2 to maintain the dimensionless nature of the amplitude, a higher order loop will have more vertices so more such $1/f^2$ factors hence more p^2 factors too, therefore the initial notion of counting rule is ok. We will come up with a more formal proof in a moment but let us estimate the scale of our EFT.

The scale Λ_χ : Considering a tree diagram we can see $\langle \pi_+ \pi_0 | S | \pi_+ \pi^0 \rangle_{tree} \sim p^2/f^2$ while the loop result as we have seen shows a behavior p^4/f^4 that means the loop is suppressed by a factor of p^2/f^2 and of course $1/16\pi^2$ is always there with every loop, hence a loop is suppressed by a factor of $p^2/(4\pi f)^2$ and so we can guess $\Lambda_\chi \sim 4\pi f \sim 1$ GeV.

2.2.2 Weinberg's Power Counting

A general diagram at order p^n will look like the one shown in Fig. 2.2, which has m_i vertices coming from $\mathcal{L}_{p^i}^{\Delta S=0}$ where $i = 2, 4 \dots$, it has l number of loops, \mathfrak{I} number of internal lines.

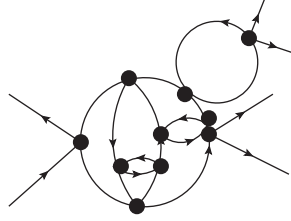


Figure 2.2: A generic loop at $O(p^n)$.

Corresponding generic amplitude will have the following form:

$$\mathcal{A} = \int (d^4 p)^l \frac{1}{(p^2)^{\mathfrak{I}}} \prod_n (p^n)^{m_n} \quad (2.2.29)$$

where p is a generic momentum. In mass independent subtraction scheme (MS , \overline{MS} etc), external momenta are the only dimensional parameters so $\mathcal{A} \sim p^{\mathfrak{D}}$, where,

$$\mathfrak{D} = 4l - 2\mathfrak{I} + \sum_n n m_n \quad (2.2.30)$$

But number of internal lines is related to the number of vertices and loops by the following relation:

$$\sum_n \mathbf{m}_n - \mathfrak{J} + \mathfrak{l} = 1 \quad (2.2.31)$$

Combining Eq. (2.2.30) and (2.2.31) we have,

$$\mathfrak{D} = 2 + 2\mathfrak{l} + \sum_n (n-2)\mathbf{m}_n \quad (2.2.32)$$

The Lagrangian series starts at $O(p^2)$ so of course $n \geq 2$, and hence Eq. (2.2.32) contains only non-negative terms so only finite number of terms are needed at any fixed momentum order, which is the EFT definition of renormalization.

Summary:

- At $O(p^2)$ of course there can only be tree level contributions.
- Unitarity demands loops that comes at $O(p^4)$, vertices in the loop will come from \mathcal{L}_{p^2} while there will be tree contributions from \mathcal{L}_{p^4} which will renormalize the loop diagrams.

2.2.3 Classical Sources and The Explicit Breaking of Chiral Symmetry

So far we have been treating the quarks (u, d and s) as massless and the effective theory was also built on chiral symmetry, but in nature this symmetry is only approximate, the fact that these three quarks are very light can be used to treat the mass term in QCD as a perturbation but then this breaking of the chiral symmetry will manifest itself in the long distance theory, the chiral perturbation theory, as a breaking of the symmetry there too generating masses of the mesons.

The Spurion Trick

The trick is to plug in a classical and external gauge field (or a bunch of them if necessary) to the QCD Lagrangian and replacing the partial derivatives with corre-

sponding covariant derivatives in such a way that the chiral symmetry is preserved, this scheme then will be translated down to the EFT and everything will be fine until we freeze the gauge field leading to an explicit breaking of the chiral symmetry, this field then will be re-interpreted as the quark mass matrix in the QCD Lagrangian which will generate the meson masses too in the low energy effective theory.

Let's start with the QCD Lagrangian with a triplet of light quarks ($q = u, d, s$):

$$\begin{aligned}\mathcal{L}_{QCD} &= \mathcal{L}_{QCD}^0 + \bar{q}\gamma^\mu(v_\mu + a_\mu\gamma_5)q - \bar{q}(s + ip\gamma_5)q \\ &= \mathcal{L}_{QCD}^0 + \bar{q}_L\gamma^\mu l_\mu q_L + \bar{q}_R\gamma^\mu r_\mu q_R - \bar{q}_R(s + ip)q_L \\ &\quad - \bar{q}_L(s - ip)q_R\end{aligned}\tag{2.2.33}$$

where \mathcal{L}_{QCD}^0 is the QCD Lagrangian when quark masses are zero, v_μ , a_μ , l_μ , r_μ , s and p are classical Hermitian 3×3 matrices:

$$r_\mu = v_\mu + a_\mu, \quad l_\mu = v_\mu - a_\mu\tag{2.2.34}$$

Through r_μ and l_μ gauge fields QCD achieves now $SU(3)_L \times SU(3)_R$ gauge symmetry where these fields are also the sources of the Noether currents. This theory is invariant under the following transformations:

$$\begin{aligned}q_R &\mapsto \mathfrak{R} q_R \\ q_L &\mapsto \mathfrak{L} q_L\end{aligned}\tag{2.2.35}$$

Transformation of the vector and scalar fields and related quantities are listed in section 1.2 of Chapter 1. Same symmetry can be carried out to the low energy EFT by letting these classical source fields to interact with the low energy theory through minimal coupling, that is:

$$\partial^\mu \Sigma \mapsto D^\mu \Sigma = \partial^\mu \Sigma - il^\mu \Sigma + i\Sigma r^\mu, \quad D^\mu \Sigma^\dagger = \partial^\mu \Sigma^\dagger - ir^\mu \Sigma^\dagger + i\Sigma^\dagger l^\mu\tag{2.2.36}$$

We already know the Noether's currents corresponding to this gauge symmetry but we can identify again by using the covariant derivative in the effective Lagrangian and then looking for the currents that couple to the left and right gauge fields and we can cast them in the following form:

$$(\mathcal{L}_\mu)_{ij} = \frac{if^2}{2} [(\partial_\mu \Sigma) \Sigma^\dagger]_{ji} \quad (2.2.37)$$

$$(\mathcal{R}_\mu)_{ij} = \frac{if^2}{2} [(\partial_\mu \Sigma^\dagger) \Sigma]_{ji} \quad (2.2.38)$$

here i, j are the flavor indices and to achieve the above results we used the cyclic property of trace and the fact that Σ is unitary.

Mesons Acquiring Masses

To introduce masses we have to break this symmetry and we know what breaks the chiral symmetry in QCD it is the mass term $\bar{q}_L M_q q_R + h.c.$, where:

$$M_q = \begin{pmatrix} m_u & 0 & 0 \\ 0 & m_d & 0 \\ 0 & 0 & m_s \end{pmatrix} \quad (2.2.39)$$

As s and p always enters as $s \pm ip$ we can name these two combinations χ and χ^\dagger . Now at the lowest order we can create the unique invariant that can be added to the chiral Lagrangian:

$$\mathcal{L}_{p^2}^\chi = \mathfrak{B}_0 \text{tr}[\Sigma^\dagger \chi + \chi^\dagger \Sigma] \quad (2.2.40)$$

Setting $s = M_q, p = 0$ produces the mass term in QCD Lagrangian and of course breaks the chiral symmetry because S and P do not transform any more. This one the other hand generates meson masses in the chiral Lagrangian and \mathfrak{B}_0 is proportional to the quark condensate $\langle \bar{q}q \rangle$. Expanding Σ in terms of meson fields we can obtain their masses:

$$\begin{aligned}
m_\pi^2 &= 4\frac{\mathfrak{B}_0}{f^2}m + O((m_u - m_d)^2) \simeq m \mathcal{B}_0 \\
m_k^2 &= 2\frac{\mathfrak{B}_0}{f^2}(m + m_s) + O((m_u - m_d)^2) \simeq \frac{1}{2}m_s \mathcal{B}_0 \\
m_\eta^2 &= 4\frac{\mathfrak{B}_0}{f^2}\left(\frac{m}{3} + 2\frac{m_s}{3}\right) + O((m_u - m_d)^2) \simeq \frac{2}{3}m_s \mathcal{B}_0
\end{aligned} \tag{2.2.41}$$

Here we have used the following substitution: $4\mathfrak{B}_0/f^2 = \mathcal{B}_0$. Eq. (2.2.41) recovers the Gell-Mann Okubo relation [18, 19, 20] :

$$3m_\eta^2 + m_\pi^2 = 4m_K^2 \tag{2.2.42}$$

We have considered the isospin limit⁵ $m_u = m_d = m$ and ignored weak and electromagnetic effects and assumed isospin invariance. At the leading order, chiral Lagrangian takes the following form:

$$\mathcal{L}^{\Delta S=0} = \mathcal{L}_{p^2}^{\Delta S=0} = \frac{f^2}{4} \left(\text{tr}[D^\mu \Sigma D_\mu \Sigma^\dagger] + \mathcal{B}_0 \text{tr}[\Sigma \chi^\dagger + \Sigma^\dagger \chi] \right) \tag{2.2.43}$$

$s = M_q, p = 0 \implies \chi = M_q$ choice no longer allows the fields to transform and hence breaks the chiral symmetry explicitly through gauge fixing, this choice reproduces the mass term in QCD and leads to mass term in chiral effective theory too. We have new expansion parameters in our theory, the quark masses and before we move on we should specify the counting powers of the new source fields in general, l_μ and r_μ counts like derivatives ($O(p)$) can be understood from their transformations and from the masses of mesons we can see χ is $O(p^2)$.

We are now ready to discuss the next to leading order Lagrangian with which comes loops and of course the renormalization that deserves a separate section.

2.3 $O(p^4)$ Strong Lagrangian

As discussed in the last section, we need loops for unitarity and indeed loops can be constructed using $O(p^2)$ vertices but these are divergent hence we need counter-

⁵A chiral limit would be $m_u = m_d = m_s = 0$

terms which is why we need $O(p^4)$ Lagrangian. Based on the arguments that drove to the leading order Lagrangian the most general form of the next to leading order effective Lagrangian can also be obtained that is constructing invariants of $O(p^4)$ out of Σ and χ but at this order field-strength tensors can also be used which was not possible earlier because they are $O(p^2)$ and needs contractions of two indices which is only possible by considering 1) two gauge fields or 2) two derivatives or 3) one field-strength tensor, that precisely means $O(p^4)$. We will not go into the construction but will directly write it down [5]:

$$\begin{aligned}
\mathcal{L}_{p^4}^{\Delta S=0} &= L_1 \left\{ (\text{tr}[D^\mu \Sigma D_\mu \Sigma^\dagger])^2 + L_2 \text{tr}[D_\mu \Sigma D_\nu \Sigma^\dagger] \text{tr}[D^\mu \Sigma D^\nu \Sigma^\dagger] \right. \\
&+ L_3 \text{tr}[D^\mu \Sigma D_\mu \Sigma^\dagger D^\nu \Sigma D_\nu \Sigma^\dagger] + L_4 \text{tr}[D^\mu \Sigma D_\mu \Sigma^\dagger] \text{tr}[\Sigma \chi^\dagger + \chi \Sigma^\dagger] \\
&+ L_5 \text{tr}[D^\mu \Sigma D_\mu \Sigma^\dagger (\Sigma \chi^\dagger + \chi \Sigma^\dagger)] + L_6 (\text{tr}[\Sigma \chi^\dagger + \chi \Sigma^\dagger])^2 \\
&+ L_7 (\text{tr}[\Sigma \chi^\dagger - \chi \Sigma^\dagger])^2 + 4\mu^2 L_8 \text{tr}[\Sigma \chi^\dagger \Sigma \chi^\dagger + \chi \Sigma^\dagger \chi \Sigma^\dagger] \\
&- iL_9 \text{tr}[\mathcal{R}_{\mu\nu} D^\mu \Sigma D_\nu \Sigma^\dagger + \mathcal{L}_{\mu\nu} D^\mu \Sigma^\dagger D_\nu \Sigma] + L_{10} \text{tr}[\Sigma \mathcal{L}_{\mu\nu} \Sigma^\dagger R^{\mu\nu}] \\
&\left. + H_1 \text{tr}[\mathcal{L}_{\mu\nu} \mathcal{L}^{\mu\nu} + \mathcal{R}_{\mu\nu} \mathcal{R}^{\mu\nu}] + 4\mu^2 H_2 \text{tr}[\chi \chi^\dagger] \right\} \quad (2.3.44)
\end{aligned}$$

where $\mathcal{L}_{\mu\nu}, \mathcal{R}_{\mu\nu}$ are the field strength tensors corresponding to the gauge field l_μ, r_μ respectively. As H_i terms involve only external fields they are not physical.

2.3.1 The Low Energy Constants (LEC)'s

The L_i 's and H_i 's are constants and in principle can be derived from the underlying theory that is QCD that requires a “**matching**” which involves non-perturbative QCD, a full calculation of this sort have never been achieved but some QCD inspired models [21, 22, 23, 24], vector meson resonance saturation [25, 26, 27, 28, 29] and lattice calculations [30, 31] along with experiments were able to fix these values to some extent. Although a complete long distance and short distance QCD matching is still unavailable, present work is an attempt to understand and apply one such matching technique that we will discuss later in detail.

LEC's and Renormalization

From Weinberg's counting argument we have already seen that $O(p^2)$ Lagrangian leads to $O(p^4)$ loops hence the divergences cannot be absorbed into the renormalization of the known parameters f and \mathcal{B}_0 ! We need these L_i 's to absorb the divergences of one loop, this has been achieved by Gasser and Leutwyler [5] and they are listed below:

$$L_i = L_i^r + \frac{\Gamma_i}{32\pi^2} R_\varepsilon, \quad i = 1, \dots, 10, \quad (2.3.45)$$

$$(2.3.46)$$

Γ_i 's are listed in the table 2.1 and R_ε is defined in Eq. (B.1.1).

| Coefficient | Experimental Values | Γ_i |
|-------------|---------------------|------------|
| L_1^r | 0.4 ± 0.3 | 3/32 |
| L_2^r | 1.35 ± 0.3 | 3/16 |
| L_3^r | -3.5 ± 1.1 | 0 |
| L_4^r | -0.3 ± 0.5 | 1/8 |
| L_5^r | 1.4 ± 0.5 | 3/8 |
| L_6^r | -0.2 ± 0.3 | 11/144 |
| L_7^r | -0.4 ± 0.2 | 0 |
| L_8^r | 0.9 ± 0.3 | 5/48 |
| L_9^r | 6.9 ± 0.7 | 1/4 |
| L_{10}^r | -5.5 ± 0.7 | -1/4 |

Table 2.1: Renormalized LEC's in units of 10^{-3} at the scale $\mu = m_\rho$ [32]

$\mathcal{L}_{p^4}^{\Delta S=0}$ contains redundant terms that can be eliminated using equations of motion but we will not discuss it here. We will also not discuss Wess-Zumino-Witten action as it is out of the scope of this whole study but this discussion can be found here [11].

2.4 Application of The Strong Lagrangian

Strong chiral Lagrangian can be applied to various processes but we will consider the following examples:

- Wave function renormalization.
- Pion and kaon electromagnetic form factors.

Because these are the ones that we will need in these study. And we will consider only $O(p^2)$ Lagrangian because the reason for this will become clear in Chapter 4. Feynman rules for relevant vertices corresponding to the Lagrangian in Eq. (2.2.43) are given in Appendix A.

2.4.1 Wavefunction Renormalization (WFR)

Diagram that contributes to WFR is shown in Fig. 2.3.

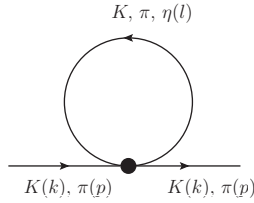


Figure 2.3: Loop contribution to wavefunction renormalization.

At $O(p^4)$ the self-energy of a meson field Π can be expressed in terms of the constants a_Π and b_Π as:

$$\Sigma_\Pi(p^2) = a_\Pi + p^2 b_\Pi \quad (2.4.47)$$

Fig. 2.3 contributes to these constants and they also have tree level contributions from $\mathcal{L}_{p^4}^{\Delta S=0}$ that we will not consider here. b_Π by definition is:

$$\Sigma'_{\Pi}(p^2) = \frac{\partial \Sigma_{\Pi}}{\partial p^2} = B_{\Pi} \quad (2.4.48)$$

where $-i\Sigma_{\Pi}(p^2)$ is all the 1-PI diagrams that contribute at 1-loop level and Π represents any meson field. So we need to multiply all the loop results by i to retrieve a_{Π} and b_{Π} hence Σ_{Π} ⁶.

Wavefunction renormalization constant for the field Π is defined as:

$$Z_{\Pi} = \frac{1}{1 - \Sigma'(M_{\Pi}^2)} \quad (2.4.49)$$

where M_{Π} is the physical mass of the field Π . Although we have carried out this calculation ourselves⁷ but this exists in many reviews including this one [11] so we can directly state the values of a_{Π} and b_{Π} below:

$$\begin{aligned} b_{\pi} &= \frac{1}{3f^2} [A(m_K^2) + 2A(m_{\pi}^2)] \\ a_K &= \frac{1}{4f^2} \{A(m_{\pi}^2) + I(m_{\eta}^2) + 2A(m_K^2)\} \end{aligned}$$

Hence the pion and kaon wavefunction renormalization (WFR) constants are:

$$\begin{aligned} Z_{\pi} &= \frac{1}{1 - \Sigma'(p^2 = m_{\pi}^2)} = \frac{1}{1 - b_{\pi}} = 1 + b_{\pi} + O(p^4) \\ &\simeq 1 + \frac{1}{3f^2} [A(m_K^2) + 2A(m_{\pi}^2)] \\ Z_K &= \frac{1}{1 - \Sigma'(k^2 = m_K^2)} = \frac{1}{1 - b_K} = 1 + b_K + O(p^4) \\ &\simeq 1 + \frac{1}{4f^2} \{A(m_{\pi}^2) + A(m_{\eta}^2) + 2A(m_K^2)\} \end{aligned}$$

The integral $A(m_i^2)$ is the one-point function defined in [33] and is evaluated in Appendix B. Of course one needs the contributions from tree diagrams coming from

⁶ For the lack of symbols we have to use Σ for both the exponential representation of mesons as well as self energy, but there will be suffix $\Pi = \pi, K$ etc and this ambiguity will be limited to this subsection only

⁷ Unrenormalized.

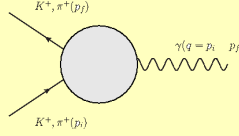
$O(p^4)$ Lagrangian given by Eq. (2.3.44) to remove the divergences, we will come back to this regularization issue in Chapter 4. We will need the quantity $\sqrt{Z_K Z_\pi}$ so we better write it down below in the limit $m_\pi^2 \ll m_K^2$ and up to $O(1/f^2)$:

$$\sqrt{Z_K Z_\pi} = 1 + \frac{1}{(4\pi f)^2} \left\{ M^2 - \frac{5}{12} m_K^2 \log \left(1 + \frac{M^2}{m_K^2} \right) - \frac{1}{8} m_\eta^2 \log \left(1 + \frac{M^2}{m_\eta^2} \right) \right\}$$

(2.4.50)

2.4.2 Off-Shell Pion and Kaon Electromagnetic Form Factors

Pion and kaon electromagnetic form factors are calculated in details in many places for example in [34] and in [14], hence we will write down the un-renormalized results in the following form:



$$= i e \epsilon^*(q) \cdot (p_i + p_f) \left[1 + \frac{1}{(4\pi f)^2} \left(F_0^\Pi(M^2) + z F_1^\Pi(M^2) \right) + \dots \right] + \epsilon^*(q) \cdot q\text{-terms.}$$

(2.4.51)

Where $\Pi = \pi^+, K^+$ the ellipses represent terms higher order in z and $\epsilon \cdot q$ -terms are irrelevant for us. And:

$$F_0^{\pi^+}(M^2) = -M^2 + \frac{1}{3} m_K^2 \log \left(1 + \frac{M^2}{m_K^2} \right) + O(m_\pi^2/M^2) \simeq -M^2$$

$$F_0^{K^+}(M^2) = -M^2 + \frac{m_K^2}{4} \log \left(1 + \frac{M^2}{m_K^2} \right) + \frac{m_\eta^2}{4} \log \left(1 + \frac{M^2}{m_\eta^2} \right) + O(m_\pi^2/M^2) \simeq -M^2$$

(2.4.52)

The fact that F_0 's get killed by WFR is apparent from Eq. (2.4.52) and (2.4.50).

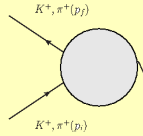
But the following survive:

$$\begin{aligned}
 F_1^{\pi^+}(M^2) &= \frac{m_K^2}{3} \left\{ 4 + \log \left(1 + \frac{M^2}{m_\pi^2} \right) + \frac{1}{2} \log \left(1 + \frac{M^2}{m_K^2} \right) \right\} + O(m_\pi^2/M^2) \\
 F_1^{K^+}(M^2) &= \frac{m_K^2}{3} \left\{ 4 + \log \left(1 + \frac{M^2}{m_K^2} \right) + \frac{1}{2} \log \left(1 + \frac{M^2}{m_\pi^2} \right) \right\} + O(m_\pi^2/M^2)
 \end{aligned} \tag{2.4.53}$$

Where we have used SPCR regularization method discussed in Appendix B and used the correspondence given by Eq. (B.3.27) and (B.3.28) to extract the cut-off (M^2) divergence from dimensionally regularized results of the references mentioned above. In chapter 3 and 4 we will see that the energy range $M = 0.6-0.9$ is of special relevance, and in that range we can approximate:

$$F_1^{K^+}(M^2) \simeq 1.2 F_1^{\pi^+}(M^2) \simeq \frac{m_K^2}{3} \left(4 + \frac{3}{2} \log \frac{M^2}{\tilde{m}^2} \right) \tag{2.4.54}$$

Where $\tilde{m} = 0.3$ GeV. If we apply the WFR, then we have:



$$\begin{aligned}
 &= i e \epsilon^*(q) \cdot (p_i + p_f) \left(1 + \frac{z}{(4\pi f)^2} F_1^\Pi(M^2) \right) + \dots \\
 &\simeq i e \epsilon^*(q) \cdot (p_i + p_f) \frac{r_V^2}{r_V^2 - z}
 \end{aligned} \tag{2.4.55}$$

Where we have approximated the form factors using a pole like function. If we plot this for Pion case (Fig. 2.4) in the range of interest that we mentioned then we obtain the value of $m_V \simeq 0.78$, which is excellent. In fact this tells us why this range of scale is crucial, because this is the scale where vector mesons start to enter the dynamics and so of course this is obvious that exactly around the ρ mass we found the matching with the experimental value of it.

But we will also need the unrenormalized approximate form factor in Chapter 4. So we summarize:

$$\begin{aligned}
 F_0^{\pi^+}(M^2) &\simeq F_0^{K^+}(M^2) \simeq -M^2 = F_0(M^2) \\
 F_1^{\pi^+}(M^2) &\simeq F_1^{K^+}(M^2) \simeq \frac{m_K^2}{3} \left[4 + \frac{3}{2} \log \frac{M^2}{\tilde{m}^2} \right] = F_1(M^2)
 \end{aligned} \tag{2.4.56}$$

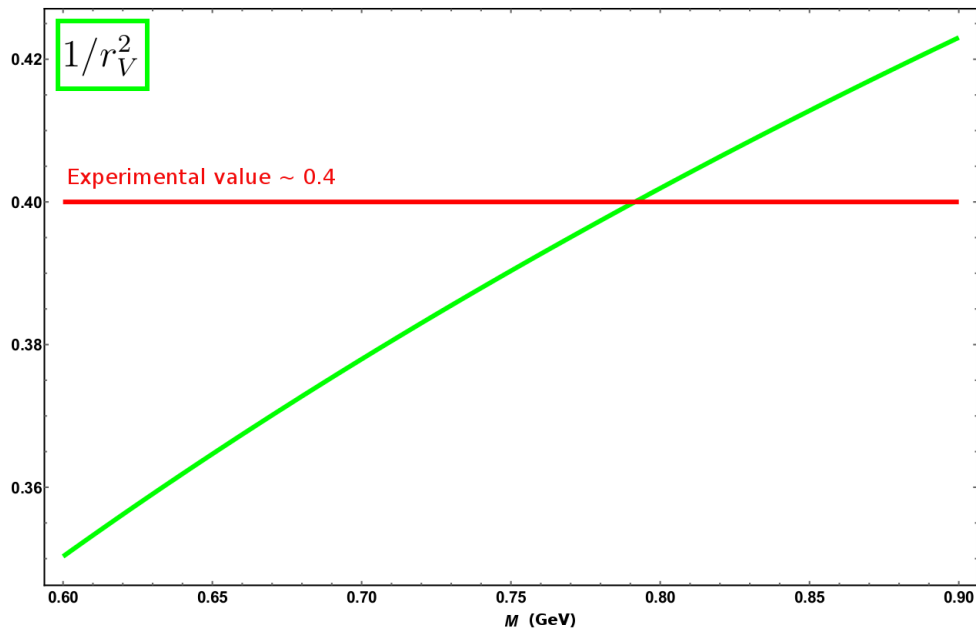


Figure 2.4: Mass of ρ from a pole fit of the pion EM form factor.

Let us end the analysis of strong chiral Lagrangian for now later we will reboot it in the context of long and short distance matching in chapter 4, where it will not be quite the Chiral Perturbation Theory but the core will still be based on it.

2.5 Weak Chiral Lagrangian and The Kaons

In the Standard Model strangeness changing weak processes are mediated by W boson, following the line of Fermi theory we can think of introducing such interactions in the chiral Lagrangian as perturbation through current-current operators that transforms properly under $SU(3) \times SU(3)$. And translating such a current from the Standard Model itself can be carried out in a straight forward way through external source method that we already discussed in section 2.2.3. We will minimally couple W -boson to the chiral Lagrangian through the covariant derivative and identify the currents attached to it both in Standard Model and the chiral Lagrangian. From this current then we can build strangeness changing current-current operators.

In the Standard Model [see Eq. (2.2.33)] quark- W interaction can be introduced via the left handed external field:

$$r_\mu = 0, \quad l_\mu = -\frac{g_2}{2}W_\mu + h.c \quad (2.5.57)$$

where g_2 is the $SU(2)_L$ weak coupling constant and the charged W boson in this basis takes the form:

$$W_\mu = \begin{pmatrix} 0 & \sqrt{2}W_\mu^+V_{ud} & \sqrt{2}W_\mu^+V_{us} \\ \sqrt{2}W_\mu^-V_{ud} & 0 & 0 \\ \sqrt{2}W_\mu^-V_{us} & 0 & 0 \end{pmatrix} \quad (2.5.58)$$

So the interaction Lagrangian looks:

$$\mathcal{L}_{q-W} = -\frac{g_2}{2}\bar{q}_L\gamma^\mu W_\mu q_L \quad (2.5.59)$$

Sum over colors and flavors is understood. And from Eq. (2.2.20) and (2.2.23) we already know what the form of left handed current is that couples to l_μ . Coupling to photons⁸ can be introduced in the usual way by taking:

$$l_\mu = r_\mu = -eQ\mathcal{A}_\mu \quad (2.5.60)$$

where

$$Q = \frac{1}{3} \begin{pmatrix} 2 & 0 & 0 \\ 0 & -1 & 0 \\ 0 & 0 & -1 \end{pmatrix} \quad (2.5.61)$$

is the quark charge matrix and \mathcal{A}_μ is the electromagnetic gauge field, and we need to just do the substitution $\partial_\mu \mapsto D_\mu = \partial_\mu - ie\mathcal{A}_\mu[Q, \cdot]$ everywhere in the effective theory, that is also in the current given by Eq. (2.2.37) and (2.2.38).

⁸Which leads to the familiar form of covariant derivative $D\Sigma = \partial\Sigma + ie\mathcal{A}[Q, \Sigma]$ and $D\Sigma^\dagger = \partial\Sigma^\dagger + ie\mathcal{A}[Q, \Sigma^\dagger]$ in ChPT.

2.5.1 Leading Order $\Delta S = 1$ Lagrangian

We have to again look back to the short distance structures of weak interaction to construct operators in long distance theory, OPE and RG can be used to come down from the top mass scale to a scale $\mu < 1$ GeV [35, 36] construct the $\Delta S = 1$ effective Hamiltonian:

$$\mathcal{H}_{eff}^{\Delta S=1} = \frac{G_F}{\sqrt{2}} V_{ud} V_{us}^* \sum_i C_i(\mu) \mathcal{Q}_i, \quad G_F = \frac{\sqrt{2} g_2^2}{8M_W^2} \quad (2.5.62)$$

The Wilson coefficients (C_i) were evaluated up to two loops so far [35, 37, 38, 39, 40, 41, 42]. The transformation (under $SU(3) \times SU(3)$) properties of the current-current ⁹ $((V - A) \times (V - A))$ four quark operators given in Eq. (3.2.18) guide us to construct two terms with similar transformation properties at the leading order with the current \mathcal{L}_μ and this leads to an interaction Lagrangian:

$$\mathcal{L}_p^{\Delta S=1} = \frac{G_F}{\sqrt{2}} V_{ud} V_{us}^* g_8 \text{tr}[\lambda \mathcal{L}_\mu \mathcal{L}^\mu] + g_{27} \left(\mathcal{L}_{\mu 23} \mathcal{L}_{11}^\mu + \frac{2}{3} \mathcal{L}_{\mu 21} \mathcal{L}_{13}^\mu \right) + h.c \quad (2.5.63)$$

where $\lambda = (\lambda_6 - i\lambda_7)/2$ projects onto $s \rightarrow d$ sector. First term transforms as $(8_L, 1_R)$ and the second as $(27_L, 1_R)$. We have two new LEC's g_8 and g_{27} , short distance analysis shows $g_8 \gg g_{27}$, this is popularly known as the ‘‘octet enhancement’’. Experimentally, $K \rightarrow \pi\pi$ decay fixes $|g_8| \simeq 5.1$ ¹⁰ and $g_{27} \simeq 0.3$, we will hence drop the non-octet part from now on. And we will also introduce the following notation:

$$G_8 = \frac{G_F}{\sqrt{2}} V_{ud} V_{us}^* g_8 \quad (2.5.64)$$

2.6 $O(p^4)$ Weak Lagrangian

It is easy to see that $\mathcal{L}^{\Delta S=0} \sim \text{tr}[\mathcal{L}_\mu \mathcal{L}^\mu] = \text{tr}[\mathcal{R}_\mu \mathcal{R}^\mu]$ which transforms as a singlet, using this property and the transformation properties of $\Delta S = 1$ Lagrangian We

⁹Electroweak penguin operators will be dealt with in the next chapter.

¹⁰We have reproduced this value of g_8 inside our framework pretty reasonably in section 4.0.5 in the next Chapter.

want to construct $O(p^4)$ Lagrangian that also must have the same transformation property, that means $\mathcal{L}_{p^4}^{\Delta S=1}$ must transform as $(8_L, 1_R)$ and $(27_L, 1_R)$. We will not discuss in detail the construction of $O(p^4)$ weak Lagrangian here as in our actual calculation we will not require $O(p^4)$ local terms in the Lagrangian, we will not list down all the possible terms which has been nicely done by [43, 44, 45] but when we discuss a particular weak decay the relevant interaction terms will be used. Here we will try to have a basic idea about how one can construct the Lagrangian from the building blocks which in the current-current sector are:

$$\begin{aligned} \text{The currents } \mathcal{L}_\mu, \mathcal{R}_\mu & \quad \text{which are } O(p) \\ \text{Field strength tensors } \mathcal{L}_{\mu\nu}, \mathcal{R}_{\mu\nu} & \quad \text{are } O(p^2) \end{aligned} \tag{2.6.65}$$

Then we have the matrix $\lambda = (\lambda_6 - i\lambda_7)/2$ that projects onto s - d sector. So we need to contract the Lorentz indices to construct $O(p^4)$ invariants and then project them with λ and take one trace or product of two trace terms. So the Lagrangian will look like:

$$\begin{aligned} \mathcal{L}_{p^4}^{\Delta S=1} \sim & \text{tr}[\lambda \mathcal{L}_\mu \mathcal{L}^\mu \mathcal{L}_\nu \mathcal{L}^\nu] + \text{tr}[\lambda \mathcal{L}_\mu \mathcal{L}_\nu \mathcal{L}^{\mu\nu}] + \text{tr}[\lambda \mathcal{L}_{\mu\nu} \mathcal{L}^{\mu\nu}] \\ & + \text{double trace terms} + \text{all possible distinct permutations} \end{aligned}$$

The full list of all the $O(p^4)$ $\Delta S = 1$ terms are derived by [46, 43] which we will not discuss in detail here and we also do not need them for the present study.

2.7 Kaon Decays In ChPT

There are so many reasons that motivate us to study the decay of kaons, in fact kaons played the key role in the construction and development of the Standard Model and it is the window to new physics too. In the discovery of Strangeness [47, 48], parity violation [49, 50], meson-antimeson mixing [51, 52], quark mixing [53, 54], CP violation [55], suppression of FCNC and the GIM mechanism [56], kaon decays played the most important role. A comprehensive review was done [57] but they did not include processes forbidden under SM while rare decays are discussed in [58, 59].

2.7.1 $K \rightarrow \pi\pi$ and The $\Delta I = 1/2$ Rule

Bose symmetry tells us that in the decays $K \rightarrow \pi\pi$, the S -wave final state has two basic modes: total isospin 0 or 2, hence such decays can be parametrized as:

$$\mathcal{A}(K^0 \rightarrow \pi^+\pi^-) = \mathcal{A}_{+-} = \mathcal{A}_0 e^{i\chi_0} + \frac{1}{\sqrt{2}} \mathcal{A}_2 e^{i\chi_2} \quad (2.7.66)$$

$$\mathcal{A}(K^0 \rightarrow \pi^0\pi^0) = \mathcal{A}_{00} = \mathcal{A}_0 e^{i\chi_0} - \sqrt{2} \mathcal{A}_2 e^{i\chi_2} \quad (2.7.67)$$

$$\mathcal{A}(K^+ \rightarrow \pi^+\pi^0) = \mathcal{A}_{+0} = \frac{3}{2} \mathcal{A}_2^+ e^{i\chi_2^+} \quad (2.7.68)$$

We have three kinds of basic amplitudes here, \mathcal{A}_0 corresponds to $I = 0$ final state where as we have two different amplitudes describing $I = 2$ state, latter two are equal if there is no $\Delta I = 5/2$ contribution which is expected to come from electromagnetic corrections, but if we neglect electromagnetic corrections then $\mathcal{A}_0 = \mathcal{A}_{+0}$, experiment suggests:

$$|\mathcal{A}(K^0 \rightarrow \pi^+\pi^-)| = 5.56 \times 10^{-7} m_K \quad (2.7.69)$$

$$|\mathcal{A}(K^0 \rightarrow \pi^0\pi^0)| = 5.28 \times 10^{-7} m_K \quad (2.7.70)$$

$$|\mathcal{A}(K^+ \rightarrow \pi^+\pi^0)| = 3.72 \times 10^{-8} m_K \quad (2.7.71)$$

Experimental fit of $\pi - \pi$ scattering suggests $\delta_0 - \delta_2 \simeq 45^\circ$ and in this case there is a $\Delta i = 5/2$ contribution but for $\delta_0 - \delta_2 \simeq 57^\circ$ it is not there. If we consider only the isospin amplitudes then

$$\boxed{\left| \frac{\mathcal{A}_0}{\mathcal{A}_2} \right| \simeq 22} \quad (2.7.72)$$

This dominance of $\Delta I = 1/2$ amplitude is known as the $\Delta i = 1/2$ rule [60, 61, 62, 63, 64, 65, 66]. The origin of this rule can be traced back to the short distance dynamics that is QCD, and we will attempt to understand this in the next chapter.

2.7.2 $K \rightarrow \pi l^+ l^-$ Decay

This process have been calculated at $O(p^4)$ by [67] but we have used a different method which makes the problem simpler, the trick was suggested by them but used in another problem [68] not in this one. It is well known that this decay is dominated by photon exchange, that is $K \rightarrow \pi \gamma^* \rightarrow K \rightarrow \pi l^+ l^-$ which is why this is forbidden at leading order Chiral Perturbation Theory even if the photon is off-shell. Leading order Lagrangian describing this process is of course:

$$\mathcal{L}_{p^2} = \mathcal{L}_{p^2}^{\Delta S=0} + \mathcal{L}_{p^2}^{\Delta S=1} \quad (2.7.73)$$

No $O(p^2)$ Amplitude: Reason-I

Consider the most general form of the amplitude allowed by Lorentz and gauge invariance:

$$\mathcal{A}(K(k) \rightarrow \pi \gamma^*(q)) = eW(q^2) (\epsilon^\mu(q)q^\nu - \epsilon^\nu(q)q^\mu) (k_\mu p_\nu - k_\nu p_\mu) \quad (2.7.74)$$

where $W(q^2)$ is the dynamical unknown lorentz invariant function of photon momentum. We can clearly see that the amplitude requires three external momenta but leading order chiral Lagrangian can only offer only two !

No $O(p^2)$ Amplitude: Reason-II

If we diagonalize the kinetic and mass term simultaneously¹¹ by a transformation that mixes kaons and pions then gauge invariance removes also $k\pi\gamma$ vertex¹² vertex as a consequence. Hence there's no tree level vertex present in our leading order Lagrangian to ask for a contribution ! This is the trick that we will use to simplify the problem.

¹¹Which can always be done and is well known.

¹²Because kinetic term involves covariant derivatives through which photon field couples to mesons.

$O(p^4)$ Calculation

The amplitude given by Eq. (2.7.74) can be cast into a more convenient form as:

$$\mathcal{A}(K(k) \rightarrow \pi\gamma^*(q)) = e \frac{W(z)}{(4\pi)^2} [z(k+p)^\mu - (1 - r_\pi^2)q^\mu] \epsilon_\mu^*(q) \quad (2.7.75)$$

r_π , z are defined in Eq. (1.1.1). Ecker, Pick and de Rafael [67] argued the following that we are going to apply too:

1. In Lorentz (Landau) gauge, terms proportional to q^μ do not contribute to the process $K \rightarrow \pi l^+ l^-$ so we can drop all the diagrams and terms that are proportional to q^μ and consider only those who provides us with $(k+p)^\mu$ component.
2. We can also restrict ourselves to the diagrams that can give us factors of q^2 because of the form of the amplitude given by Eq. (2.7.75).
3. Diagonalizing the kinetic and mass terms simultaneously in the Lagrangian (see Eq. (2.7.73)) we can remove all the bilinear mixed terms that is $K\pi$ -terms and through co-variant derivative $K\pi\mathcal{A}_\mu$ terms will also disappear leading to no diagrams involving $k\pi$ and $k\pi\gamma$ vertices.

These two arguments reduces a lot of diagrams and leaves us with just two and also in these two diagrams q^μ can be dropped, furthermore, $q^\mu q^\nu$ term in the photon propagator will not contribute either. So the final amplitude will look like:

$$\langle l^+(p_+) l^-(p_-) \pi(p) | \mathcal{L}_{p^2} | K(k) \rangle = -\frac{\alpha_e}{4\pi m_K^2} W(z) (k+p)^\mu [\bar{u}_l(p_-) \gamma^\mu v_l(p_+)]$$

(2.7.76)

where $\alpha = \frac{e^2}{4\pi}$.

All possible loop diagrams are shown in Fig. 2.5 and then by the diagonalization argument we can remove the diagrams that involve K - π and/or K - π - γ vertices, finally we will list the remaining diagrams in two categories:

- **Type-I:** Diagrams that do not provide a factor of q^2 shown in Fig. 2.6
- **Type-II:** Diagrams that a factor of q^2 shown in Fig. 2.7

Question of Gauge Invariance

One might ask, Type-I diagrams are not zero and if we do not calculate them then how come ward identity will be satisfied by Type-II diagrams alone ? The answer is, we will not explicitly calculate Type-I diagrams but they will not be discarded completely but will be included indirectly by the virtue of another trick used in [67] that we will discuss and describe now. If we consider the first diagram of the Type-I (Fig. 2.7), the photon vertex can only contain terms like $\epsilon^* \cdot (k, p)$ and the four-meson vertex can be either be proportional to square of either the loop momentum (l^2) or the external momentum (p^2), other kinds will vanish due to Lorentz invariance. Now the non-zero terms coming from the second diagram of Type-I contains just one vertex that has to be of the form $\epsilon^* \cdot (k, p)$ that is why they do not produce a factor of q^2 while Type-II can have both q^2 and q^2 -less terms, so schematically we can write:

$$\text{Type-I} \propto (k+p)^\mu f_0(m_\pi, m_K) + \dots \quad (2.7.77)$$

$$\text{Type-II} \propto (k+p)^\mu [f_1(m_\pi, m_K) + q^2 f_2(m_\pi, m_K)] + \dots \quad (2.7.78)$$

Ellipsis represent the q^μ terms which will not contribute in the end and f, g and h are some functions of the masses, exact forms of which are not important at the moment. So the amplitude will be:

$$i \langle \gamma^*(q) \pi(p) | \mathcal{L}^{\Delta S=1} | K(k) \rangle \propto \text{Type-I} + \text{Type-II} \quad (2.7.79)$$

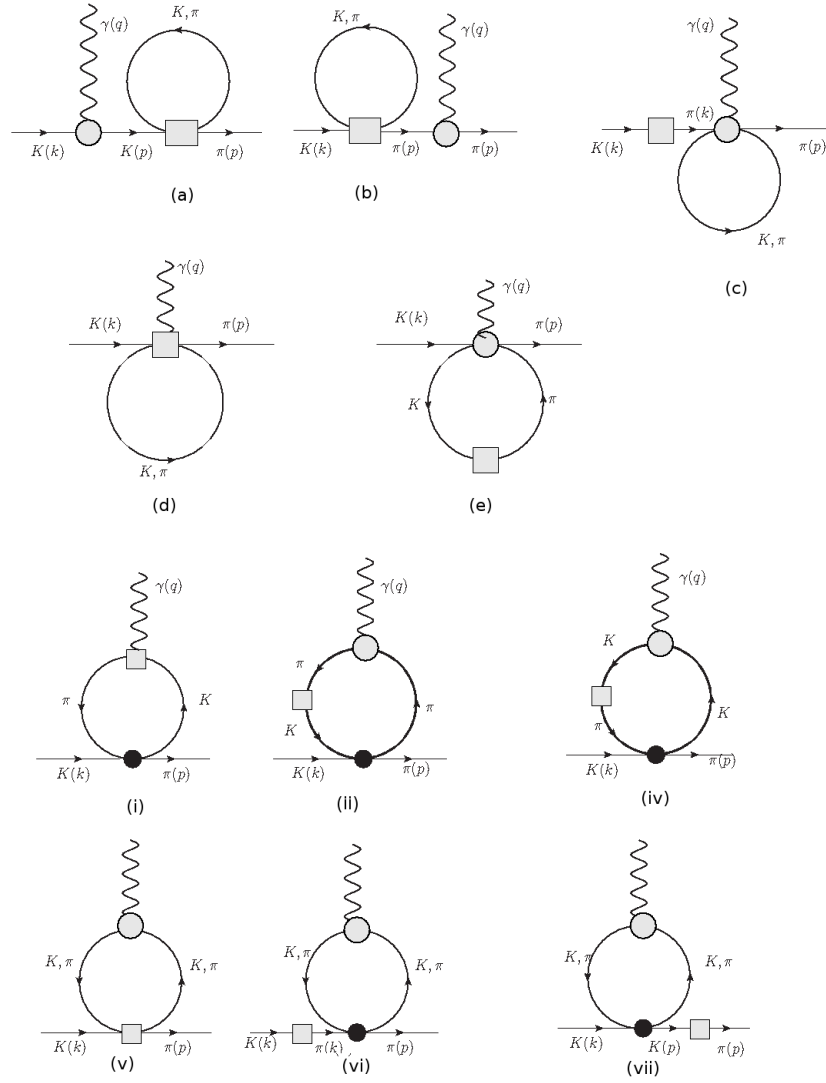


Figure 2.5: List of all possible diagrams before diagonalization of bilinear terms in the leading order chiral Lagrangian.

And gauge invariance requires $\lim_{q^2 \rightarrow 0} i \langle \gamma^*(q) \pi(p) | \mathcal{L}^{\Delta S=1} | K(k) \rangle = 0$, this suggests:

$$\begin{aligned}
 \lim_{q^2 \rightarrow 0} \text{Type-I} &= - \lim_{q^2 \rightarrow 0} \text{Type-II} \\
 \implies \text{Type-I} &= - \lim_{q^2 \rightarrow 0} \text{Type-II}
 \end{aligned} \tag{2.7.80}$$

Last line is true because Type-I does not have any q^2 in it so does not get effected by the limit. This result is remarkable, because we can now substitute Type-I contribution in terms of Type-II in Eq. (2.7.81) and get:

$$\mathcal{A}(K \rightarrow \pi\gamma^*) \propto \text{Type-II} - \lim_{q^2 \rightarrow 0} \text{Type-II} \quad (2.7.81)$$

Which of course says that the function $f_0 = -f_1$, but we just proved that we do not need them we only need to find the function f_2 . This is exactly the trick that we promised above to describe.

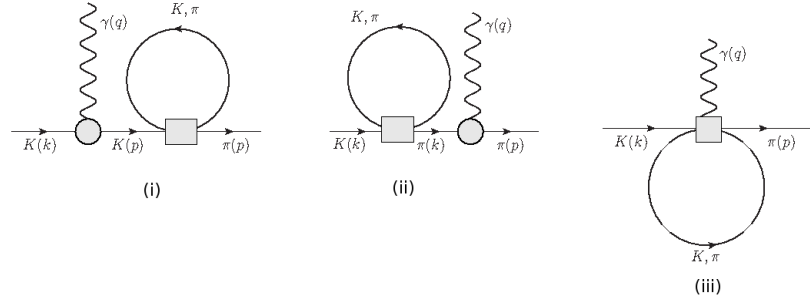


Figure 2.6: Type-I diagrams that do not provide q^2 .

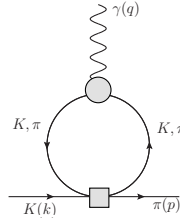


Figure 2.7: Type-II diagrams that do provide q^2 .

Loop Calculations

Contribution of the Type-II diagrams can be written down as:

$$i \langle \pi^+(p) \gamma^*(q) | \mathcal{L}_{p^2} | K^+ \rangle = \int \frac{d^4 l}{(2\pi)^4} i \frac{\text{Diagram (i)}}{l^2 - m_\pi^2 + i0_+} \times i \frac{\text{Diagram (ii)}}{(l-q)^2 - m_\pi^2 + i0_+} \quad (2.7.82)$$

Another trick: Before we actually calculate this we must consider another trick that simplifies the problem further. Let us consider the general structures of the

two relevant vertices:

$$\begin{array}{c} \pi^+(p) \\ \swarrow \\ \square \\ \swarrow \quad \searrow \\ K^+(k) \quad K^+, \pi^+(l) \end{array} \quad \sim \quad a_0 + a_1 (k+p)_\mu l^\mu + a_2 l^2 \quad (2.7.83)$$

$$\begin{array}{c} K^+, \pi^+(l-q) \\ \swarrow \\ \circ \\ \swarrow \quad \searrow \\ K^+, \pi^+(l) \quad \gamma(q) \end{array} \quad \sim \quad \epsilon_\nu^* (b_0 q^\nu + b_1 l^\nu) \quad (2.7.84)$$

where a's and b's are l -independent Lorentz invariant constants. The product of the above vertices will enter the integral (Eq. (2.7.82)), and except the product of terms linear in the loop momenta coming from both vertices, every other term will finally be proportional to $\epsilon_\mu^* q^\mu$ which as we discussed earlier, does not have any contributions in the end. So we just need to consider only the terms in the two vertices which can give just one l_μ , then the product of two vertices will be $l_\mu l_\nu$ kind which when integrated can produce the important term proportional to $g_{\mu\nu}$ and another irrelevant term proportional to $q_\mu q_\nu$. Hence it is also clear that any term in the Lagrangian that does not contain any derivative will not contribute either, such an irrelevant term could appear from the (symmetry breaking) mass term of the strong Lagrangian, that is the χ term in Eq. (2.2.43) due to the field redefinition discussed in section A.2. In fact this is the reason we did not provide any Feynman rules in Appendix A.

Using the vertex rules given by Eq. (A.2.14) and (A.1.6) we have:

$$\begin{aligned} \langle \pi^+(p) \gamma^*(q) | \mathcal{L}_{p^2} | K^+ \rangle &= -2e G_8 (k+p)_\mu \epsilon_\nu^* \\ &\times \int \frac{d^4 l}{(4\pi)^4} \frac{l^\mu l^\nu}{[l^2 - m_\pi^2 + i0_+][(l-q)^2 - m_\pi^2 + i0_+]} \quad (2.7.85) \\ &= -2e G_8 (k+p)_\mu \epsilon_\nu^* q^2 g^{\mu\nu} \left[B_{21}(q^2, m_\pi^2) \right. \\ &\quad \left. + B_{21}(q^2, m_K^2) \right] \end{aligned}$$

here we have dropped the $q \cdot \epsilon^*$ terms. The function $B_{21}(q, m_1^2, m_2^2)$ of one and two point functions [33] have been evaluated in Appendix B. Of course Eq. (2.7.85) is not the full contribution to the one loop amplitude, we need to apply the trick discussed in section 2.7.2 that is we need to subtract from the above result its $q^2 \rightarrow 0$ limit. Hence finally the one loop contribution to the amplitude $K^+(k) \rightarrow \pi^+(p) \gamma^*(q)$ (without counter terms) is given by:

$$\begin{aligned} \langle \pi^+(p) \gamma^*(q) | \mathcal{L}_{p^2} | K^+ \rangle = & - 2 e G_8 (k+p)_\mu \epsilon^{*\mu} \left\{ q^2 \sum_{i=\pi, K} B_{21}(q^2, m_i^2) \right. \\ & \left. - \lim_{q^2 \rightarrow 0} \left[q^2 \sum_{i=\pi, K} B_{21}(q^2, m_i^2) \right] \right\} \end{aligned} \quad (2.7.86)$$

Comparing this with Eq. (2.7.75) we can extract the one loop contribution to the form factor(unrenormalized):

$$\begin{aligned} W_+(z) = & - G_8 \frac{32\pi^2}{z} \left\{ q^2 \sum_{i=\pi, K} B_{21}(q^2, m_i^2) \right. \\ & \left. - \lim_{q^2 \rightarrow 0} \left[q^2 \sum_{i=\pi, K} B_{21}(q^2, m_i^2) \right] \right\} \\ = & - m_K^2 G_8 \left(\chi(z/r_\pi^2) + \chi(z) + \frac{1}{3} \log \frac{m_\pi m_K}{M^2} - 2\theta \right) \end{aligned} \quad (2.7.87)$$

where θ is a constant that depends on the regularization scheme, for example $\theta = 5/18, 1/6, 0$ in *Naive Momentum Cut-off Regularization* (NCR), *Symmetry Preserving Cut-off Regularization* (SPCR)¹³ and *Dimensional Regularization* respectively. We will keep this general form so that one can use whatever regularization method and replace the loop integrals inside B_{21} (Appendix B) and we are not interested in renormalizing the results yet by using the counter term Lagrangian given by Eq. (2.3.44), the reason for this is discussed in section 3.2 of Chapter 3. For completeness though we would like to write down the following form of the form factor:¹⁴

$$W_+(z) = - m_K^2 G_8 \left(\chi(z/r_\pi^2) + \chi(z) + \frac{1}{3} \log \frac{m_\pi m_K}{M^2} \right) \quad (2.7.88)$$

where the function $\chi(z)$ is given in Eq. (B.2.4) of Appendix B. One can easily obtain the loop contribution to the final amplitude for the process $K^+ \rightarrow \pi^+ e^+ e^-$ by plugging in $W_+(z)$ given by Eq. (2.7.87) in Eq. (2.7.76).

¹³Details can be found in Appendix B.

¹⁴Here dimensional regularization was used hence $\theta = 0$

Before we end this chapter we need to discuss a very beautiful calculation of the above amplitude at $O(p^6)$ (partial) by using the unitarity property of the S -matrix element. And in fact this dispersive calculation and its results play the most crucial role in our whole work.

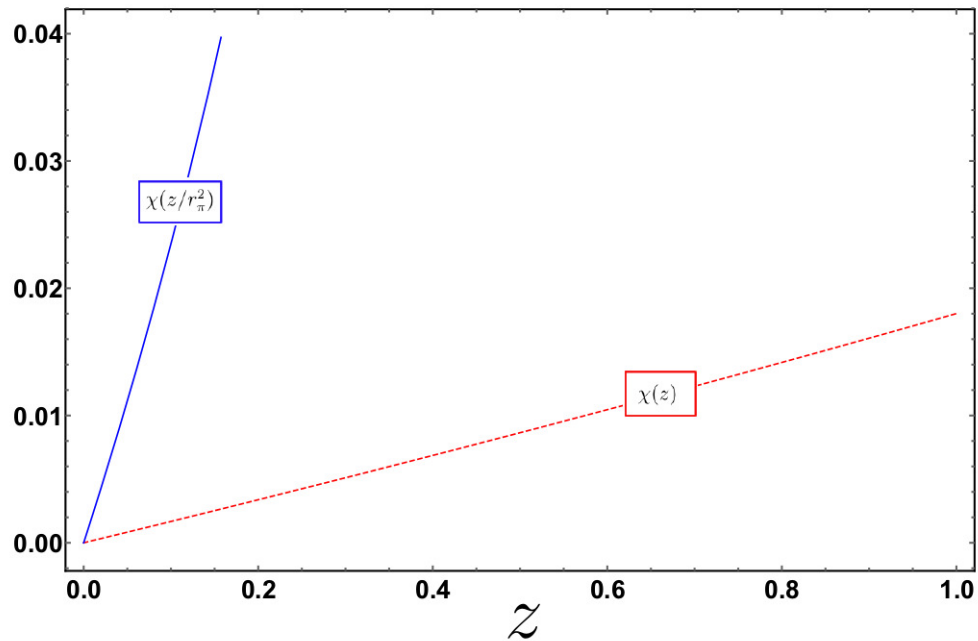


Figure 2.8: One loop function $\chi(z)$ and $\chi(z/r_\pi^2)$.

2.7.3 Unitarity and $O(p^6)$ Calculation of $K \rightarrow \pi\gamma^*$ Form Factor

As the form factors W_i ($i = +, S, L$) are analytic functions of complex variable z and they have the branch-cut that obviously starts at $z = 4r_\pi^2$ because the decay $K \rightarrow \pi\gamma^*$ starts at one loop and the lightest particles allowed to run in the loop are the pions, and the leading contribution needs two pions in the loop, hence $4r_\pi^2$. Because the final state is an electron-positron pair, the biggest contribution to the amplitude should come from lightest pseudo meson pair: $\pi^+\pi^-$ intermediate state. D'Ambrosio *et al.* (DEIP) [69] used this argument and gave this *ansatze* for the

form factor:

$$W_i(z) = G_F m_K^2 W_i^{pol}(z) + W_i^{\pi\pi}(z) \quad (2.7.89)$$

where they also argued that the contribution of massive intermediate states can all be expressed as a low order polynomial in z encoded in the function $W_i^{pol}(z)$ and $W_i^{\pi\pi}(z)$ is understandably the dominant pion-loop contribution. At the leading order the polynomial part will be a constant although a tiny term linear in z will be there for the kaon-loop and in fact we have already seen that the $\chi(z)$ function (Eq. (B.2.4)) coming from the kaon loop is negligible (See Fig. 2.8) in the allowed region (approximately 0-1) in comparison to $\chi(z/r_\pi^2)$ coming from pion loop, this is because the range gets enhanced by the huge factor of $1/r_\pi^2$. This is all well understood at $O(p^4)$ in the chiral expansion. But their result has information of higher orders and also of higher degrees of freedom entering through a_i and b_i , the expansion parameters they used to parametrize the polynomial part of the form factor:

$$W_i^{pol}(z) = a_i + b_i z, \quad (i = +, S) \quad (2.7.90)$$

They used the pion loop diagram of the Type-II diagrams shown in Fig. 2.7 using using $K \rightarrow \pi\pi\pi$ amplitude expanded up to $O(p^4)$ to replace the $K\pi\pi\pi$ vertex. The physical $K \rightarrow \pi\pi\pi$ amplitude expansion are given by:

$$\begin{aligned} A(K^+(k) \rightarrow \pi^+(p_1)\pi^+(p_2)\pi^-(p_3)) &= 2 \mathbf{a}_c + (\mathbf{b}_c + \mathbf{b}_2) Y + 2 \mathbf{c}_c \left(Y^2 + \frac{X^2}{3} \right) \\ &\quad + (\mathbf{d}_c + \mathbf{d}_2) \left(Y^2 - \frac{X^2}{3} \right) \\ A(K_S(k) \rightarrow \pi^+(p_1)\pi^-(p_2)\pi^0(p_3)) &= \frac{2}{3} \mathbf{b}_2 X - \frac{4}{3} \mathbf{d}_2 X Y \end{aligned} \quad (2.7.91)$$

where,

$$X = \frac{1}{m_\pi^2}(s_1 - s_2), \quad Y = \frac{1}{m_\pi^2}(s_3 - s_0), \quad s_i = (k - p_i)^2, \quad s_0 = \frac{1}{3}(s_1 + s_2 + s_3)$$

As this vertex is $O(p^4)$ of course the other vertex has to be taken up to that order too to calculate a consistent amplitude at the order $O(p^6)$, and at $O(p^4)$ the pion electromagnetic form factor can be written down as [14, p.174]:

$$F_V(z) = \frac{r_V^2}{r_V^2 - z} = 1 + \frac{z}{r_V^2} + O(z^2/r_V^4) \quad (2.7.92)$$

where V stands for the vector meson and so for the lightest vector meson ρ , $r_V = m_\rho/m_K \simeq 1.6$.

$O(p^6)$ amplitude corresponding to the pion loop diagram of Type-II diagrams (Fig. (2.7)) can be evaluated using dispersive integral up to a polynomial of the form given in Eq. (2.7.90):

$$W_i^{\pi\pi}(z) = \frac{1}{3r_\pi^4} [3r_\pi^2(\alpha_i - \beta_i) + \beta_i(3z - 1)] F_V(z) \chi\left(\frac{z}{r_\pi^2}\right) \quad (2.7.93)$$

$\chi(z)$ is the one loop function given in Eq. (B.2.4) and the values of the parameters α_i , β_i are given in Table 1.3. Experimentally found [70, 71, 72, 73] values of the DEIP [69] parameters for $K \rightarrow \pi l^+ l^-$ are given in Table 2.2.

| l | a_+ | b_+ | $ a_S $ |
|-------|-------------------|-------------------|------------------------|
| e | 0.578 ± 0.016 | 0.779 ± 0.066 | $1.06_{-0.21}^{+0.26}$ |
| μ | 0.578 ± 0.016 | 0.779 ± 0.066 | $1.54_{-0.32}^{+0.40}$ |

Table 2.2: Experimental values of the parameters a_i and b_i .

Let us end this chapter here with an announcement that we have used the long and short distance matching of the standard model through a matching scheme that we will discuss in the next chapter and predicted the values of the a , b parameters in Chapter 4 which are in good agreement with the experimental values.

Bibliography

- [1] G. 't. Hooft. In: *Phys.Rept* 142 (1986), pp. 357–387.
- [2] G. 't. Hooft. In: *NATO Sci.Ser.B* 59.135 (1980).
- [3] Y. Nambu. In: *Phys. Rev.* 117.648 (1960).
- [4] J. Goldstone. In: *Il Nuovo Cimento* 19.1955-1965 (1961).
- [5] J. Gasser and H. Leutwyler. In: *Nucl. Phys. B* 250.465 (1985).
- [6] S. Weinberg. In: *Phys. Rev. Lett.* 17 (1966), p. 616.
- [7] S. Weinberg. In: *Physica A* 96 (1979), pp. 327–340.
- [8] G. Ecker. In: *Prog. Part. Nucl. Phys.* 35.1 (1995). eprint: [hep-ph/9501357](#).
- [9] A. Pich. In: *Prog. Prog. Phys.* 58.563 (1995). eprint: [hep-ph/9502366](#).
- [10] A. Pich. In: (). eprint: [hep-ph/9806303](#).
- [11] S. Scherer. “Introduction to Chiral Perturbation Theory”. In: (2002). eprint: [hep-ph/0210398](#).
- [12] J. Gasser. In: *Lect. Notes. Phys.* 629.1 (2004). eprint: [hep-ph/0312367](#).
- [13] J. Bijnens. In: *Prog. Prat. Phys.* 58.521 (2007). eprint: [hep-ph/0604043](#).
- [14] J. F. Donoghue. *Dynamics of the Standard Model*. Ed. by E. Golowich and B. R. Holstein. 5th ed. Cambridge Monographs on Particle Physics, Nuclear Physics and Cosmology, 1992.
- [15] C. Callan et al. In: *Phys. Rev.* 177 (1969), p. 2247.
- [16] S. Coleman, J. Wess, and B. Zumino. In: *Phys. Rev.* 177 (1969), p. 2239.

- [17] A. V. Manohar. “Effective field theories”. In: *Lecture Notes in Physics, Springer* 479 (2007), pp. 311–362. eprint: [hep-ph/9606222](#).
- [18] M. Gell-Mann. *The Eightfold Way: A Theory of Strong Interaction Symmetry*. 1961.
- [19] S. Okubo. In: *Progress of Theoretical Physics* 27.5 (1962), pp. 949–966.
- [20] S. Okubo. In: *Progress of Theoretical Physics* 28.1 (1962), pp. 24–32.
- [21] D Ebert and H Reinhardt. In: *Nucl. Phys. B* 271.188 (1986).
- [22] D. Espiriu, E. D. Rafael, and J. Taron. In: *Nucl. Phys. B* 345.22 (1990).
- [23] D. Ebert et al. In: *Int. J. Mod. Phys. A* 8.1313 (1993).
- [24] J. Bijnens, C. Bruno, and E. de Rafael. In: *Nucl. Phys. B* 390.501 (1993).
- [25] G. Ecker et al. In: *Phys. Lett. B* 223.425 (1989).
- [26] G. Ecker et al. In: *Nucl. Phys. B* 321.311 (1989).
- [27] J. F. Donoghue, C. Ramirez, and G. Valencia. In: *Phys. Rev. D* 39.1947 (1947).
- [28] M. Knecht and A. Nyffeler. In: *Eur. Phys. J. C* 21.659 (2001).
- [29] S. Leupold. In: (2001). eprint: [hep-ph/0111204](#).
- [30] S. Myint and C. Rebbi. In: *Nucl. Phys. Proc. Suppl.* 34 (1994), p. 213.
- [31] M. Golterman. In: (2000). eprint: [hep-ph/0011084](#).
- [32] J. Bijnens, G. Ecker, and J. Gasser. *The Second DAΦNE Physics Handbook*. Ed. by L. Maiani, G. Pancheri, and N. Paver. 5th ed. Frascati, Italy: Cambridge Monographs on Particle Physics, Nuclear Physics and Cosmology, 1995.
- [33] G. ‘t Hooft and M Veltman. In: *Nucl. Phys. B* 153.365-401 (1979).
- [34] T. E. Rudy, H. W. Fearing, and S. Scerer. In: *Phys. Rev. C* 50 (1994), p. 447. eprint: [hep-ph/9401302](#).
- [35] A. J. Buras, M. Jamin, and M. E. Lautenbacher. In: *Nucl. Phys. B* 400 (1993), pp. 75–102. eprint: [hep-ph/9211321](#).
- [36] F. J. Gilman and M. B. Wise. In: *Phys. Rev. D* 20 (1979), p. 2392.

- [37] A. J. Buras, M. Jamin, and M. E. Lautenbacher. In: *Nucl.Phys. B* 408 (1993), p. 209. eprint: [hep-ph/9303284](#).
- [38] A. J. Buras, M. Jamin, and M. E. Lautenbacher. In: *Phys. Lett. B* 389 (1996), p. 749. eprint: [hep-ph/9608365](#).
- [39] M. Ciuchini et al. In: *Phys. Lett. B* 301 (1993), p. 263. eprint: [hep-ph/9212203](#).
- [40] M. Ciuchini et al. In: *Phys. Lett. B* 415 (1994), p. 403. eprint: [hep-ph/9304257](#).
- [41] M. Ciuchini et al. In: *Z. Phys. C* 68 (1995), p. 239. eprint: [hep-ph/9501265](#).
- [42] G. Buchalla, A. J. Buras, and E. M. Lautenbacher. In: *Rev.Mod.Phys.* 68 (1996), pp. 1125–1144. eprint: [hep-ph/9512380](#).
- [43] G. Ecker, J. Kambor, and D. Wyler. In: *Nucl.Phys. B* 394 (1993), pp. 101–138.
- [44] G. D’Ambrosio and J. Portoler. In: *Phys. Lett. B* 389 (1996), p. 403. eprint: [hep-ph/9606213](#).
- [45] G. D’Ambrosio and J. Portoler. In: *Nucl. Phys. B* 492 (1997), p. 417. eprint: [hep-ph/9610244](#).
- [46] J. Kambor, J. Missimer, and D. Wyler. In: *Nucl.Phys. B* 346 (1990), pp. 17–64.
- [47] M. Gell-Man. In: *Phys. Rev.* 92 (1953), p. 833.
- [48] A. Pais. In: *Phys. Rev.* 86 (1952), p. 663.
- [49] R. H. Dalitz. In: *Phys. Rev.* 94 (1954), p. 1046.
- [50] T. D. Lee and C. -N. Yang. In: *Phys. Rev.* 104 (1956), p. 254.
- [51] K. Lande. In: *Phys. Rev.* 103 (1956), p. 1901.
- [52] W. F. Fry, J. Schneps, and M. S. Swami. In: *Phys. Rev.* 103 (1956), p. 1904.
- [53] N. Cabibbo. In: *Phys. Rev.* 10 (1963), p. 531.
- [54] M. Kobayashi and T. Maskawa. In: *Prog. Theor. Phys.* 49 (1973), p. 652.
- [55] J. H. Christenson et al. In: *Phys. Rev. Lett.* 13 (1964), p. 138.

- [56] S. L. Glashow, J. Iliopoulos, and L. Maiani. In: *Phys. Rev. D* 2 (1970), p. 1285.
- [57] V. Cirigliano et al. In: *Rev. Mod. Phys.* 84 (2012), p. 399. eprint: [1107.6001 \[hep-ph\]](#).
- [58] G. D'Ambrosio and G. Isidori. In: (2013). eprint: [hep-ph/9611284](#).
- [59] G. Buchalla and A. J. Buras. In: *Nucl. Phys. B* 548 (1999), pp. 309–327. eprint: [hep-ph/9901288](#).
- [60] W. A. Bardeen, A. J. Buras, and J. -M. Gerard. In: *Nucl. Phys. B* 293 (1987), p. 787.
- [61] W. A. Bardeen, A. J. Buras, and J. M. Gerard. In: *Phys. Lett. B* 180 (1986), p. 133.
- [62] A. J. Buras and J. -M. Gerard. In: *Nucl. Phys. B* 264 (1986), p. 371.
- [63] E. Pallante and A. Pich. In: *Phys. Rev. Lett.* 84 (2000), p. 2568. eprint: [hep-ph/9911233](#).
- [64] E. Pallante and A. Pich. In: *Nucl. Phys. B* 592 (2001), p. 294. eprint: [hep-ph/0007208](#).
- [65] J. Kambor, J. Missimer, and D. Wyler. In: *Phys. Lett. B* 261 (1991), p. 496.
- [66] J. Bijnens and J. Prades. In: *JHEP* 9901.023 (1999). eprint: [hep-ph/9811472](#).
- [67] G. Ecker, A. Pich, and E. de Rafael. In: *Nuclear Physics B* 291 (1987), pp. 692–719.
- [68] G. Ecker, A. Pich, and E. de Rafael. In: *Nucl. Phys. B* 303 (1988), pp. 665–702.
- [69] G. D'Ambrosio et al. In: *Journal of High Energy Physics* 1998 (1988). URL: <http://iopscience.iop.org/article/10.1088/1126-6708/1998/08/004>.
- [70] et al. (NA48/1) Batley J. R. In: *Phys. Lett. B* 576 (2003), p. 43.
- [71] et al. (NA48/1) Batley J. R. In: *Phys. Lett. B* 599 (2004), p. 197.
- [72] et al. (NA48/2) Batley J. R. In: *Phys. Lett. B* 677 (2009), p. 246.
- [73] et al. (NA48/2) Batley J. R. In: *Phys. Lett. B* 697 (2011), p. 107.

Chapter 3

Long and Short Distance Matching

What we did in the last chapter was an example of “Bottom Up” effective field theory, that is we start at a very low energy (long distance) scale and construct a Lagrangian looking at the symmetry and symmetry breaking structure of a theory that lies at very high energy (short distance) scale. One might ask, “There could be many such high energy theories who share the same symmetry structure with QCD then how is our effective theory unique ?” The answer is, it is indeed not unique, there are unknown low energy parameters (LECs) that can assume different values that will connect them to different high energy theories. But once we fix them by fitting with experiments or matching the EFT with one of the high energy theory, it becomes unique.

Now we will do exactly the opposite, we will start with QCD and will come down step by step in energy scale and will construct a “Top Down” effective field theory based on the method called Operator Product Expansion (OPE). Our aim will be to construct $\Delta S = 1$ Lagrangian at a scale as low as ~ 1 GeV, which is possible because of the nice asymptotic freedom of QCD that will allow us to treat it perturbatively at high energy scales (m_t down to ~ 1 GeV). We will be using \overline{MS} regularization scheme in this chapter and all the quantities like QCD running coupling constant, Λ_{QCD} etc will be in \overline{MS} , furthermore we will be solely working within the leading logarithmic approximation.

The scheme is as follows:

- At the scale of (let us say $\mu = m_t$), where we can neglect the QCD corrections, there are a few operators (just one in some cases), that contributes to a particular process.
- Then we include corrections due to hard-gluons which brings new operators into the picture. This is the so called “operator-mixing”.
- Integrate out heavier particles as we come down the energy scale step by step and in each step we impose certain continuity conditions.

The above mentioned continuity condition is that at each step where we integrate out a particle we impose the continuity of the running coupling constant $\alpha_s^{(f)}(\mu)$, where f is the number of active quark flavors. For example, if we start with $f(\mu) = f_i$ number of flavors at an energy scale $\mu > \mu_i$ and come down below the scale μ_i by integrating out the heaviest among these quarks then the following condition must be obeyed:

$$\alpha_s^{(f_i)}(\mu_i) = \alpha_s^{(f_i-1)}(\mu_i) \quad (3.0.1)$$

This is called the matching condition and this must be imposed at each step. If we are coming down from m_t to $\mu < m_c$ then we will have the following three matching conditions at subsequent steps:

$$\alpha_s^{(6)}(m_t) = \alpha_s^{(5)}(m_t), \quad \alpha_s^{(5)}(m_b) = \alpha_s^{(4)}(m_b), \quad \alpha_s^{(4)}(m_c) = \alpha_s^{(3)}(m_c) \quad (3.0.2)$$

At a scale μ where only f flavors are active, we have:

$$\begin{aligned} \alpha_s^{(f)}(\mu) &= \frac{4\pi}{\beta_0^{(f)}} \frac{1}{\log(\mu^2/\Lambda^2)} \\ \beta_0^{(f)} &= \frac{11N-2f}{3}, \text{ where } N \text{ is the number of colors} \end{aligned} \quad (3.0.3)$$

3.1 RG Evolution and Operator-Mixing

Let us consider an example [1] of $c \rightarrow s\bar{u}\bar{d}$, at the scale of M_W QCD corrections can be neglected and the amplitude is simply,

$$A(c \rightarrow s\bar{u}\bar{d}) = i \frac{G_F}{\sqrt{2}} V_{cs}^* V_{ud} (\bar{s}_\alpha c_\alpha)_{V-A} (\bar{u}_\beta d_\beta)_{V-A} + O\left(\frac{k^2}{M_W^2}\right) \quad (3.1.4)$$

where k is the momentum flow through the W -boson and is much smaller than M_W . This amplitude can be calculated using an effective Hamiltonian:

$$\mathcal{H}_{eff} = \frac{G_F}{\sqrt{2}} V_{cs}^* V_{ud} \mathcal{O}_2 + \dots \quad (3.1.5)$$

where ellipses mean higher than dimension 6 operators which are sub-leading and we will not consider here and,

$$\mathcal{O}_2 = (\bar{s}_\alpha c_\alpha)_{V-A} (\bar{u}_\beta d_\beta)_{V-A} \quad (3.1.6)$$

where $(\bar{\psi}_1 \psi_2)_{V-A} (\bar{\psi}_3 \psi_4)_{V-A} \equiv [\bar{\psi}_1 \gamma^\mu (1 - \gamma_5) \psi_2] [\bar{\psi}_3 \gamma_\mu (1 - \gamma_5) \psi_4]$. Here specifically in this example we are using the notation $\mathcal{O}_{1,2}$ for operators to distinguish them from $\mathcal{Q}_{1,2}$ of Chapter 2 which involve only light quarks but we will get back to \mathcal{Q}_i notation later.

If we now include the hard-gluon correction then we can see that a gluon can link up the two distinct color singlet currents in the operator to mix the colors keeping the flavor structure intact, that is because of the color algebra of the generators ($T_{\alpha\beta}^a$):

$$T_{\lambda_1 \lambda_2}^a T_{\lambda'_2 \lambda'_1}^a = -\frac{1}{2N} \delta_{\lambda_1 \lambda_2} \delta_{\lambda'_1 \lambda'_2} + \frac{1}{2} \delta_{\lambda_1 \lambda'_2} \delta_{\lambda_2 \lambda'_1} \quad (3.1.7)$$

Due to which a new operator will enter the picture:

$$\mathcal{O}_1 = (\bar{s}_\alpha c_\beta)_{V-A} (\bar{u}_\beta d_\alpha)_{V-A} \quad (3.1.8)$$

Which means we have to modify our effective Hamiltonian now to explain physics at this slightly lower scale where hard-gluon exchange is significant:

$$\mathcal{H}_{eff} = \frac{G_F}{\sqrt{2}} V_{cs}^* V_{ud} (C_1 \mathcal{O}_1 + C_2 \mathcal{O}_2) \quad (3.1.9)$$

In the beginning we had $C_1 = 0$ and $C_2 = 1$ now both are non zero ! Now if we calculate the same amplitude it will be given by:

$$A(c \rightarrow s u \bar{d}) = -i \frac{G_F}{\sqrt{2}} V_{cs}^* V_{ud} (C_1 \langle \mathcal{O}_1 \rangle + C_2 \langle \mathcal{O}_2 \rangle) \quad (3.1.10)$$

Because a physical amplitude must be independent of scale we can calculate the amplitude at very high scale which is given by Eq. (3.1.4) and then we can calculate

the matrix elements of \mathcal{O}_1 and \mathcal{O}_2 and plug them into Eq. (3.1.10) then equating the two amplitudes we can extract the values of C_1 and C_2 which will of-course depend on the scale so will $\langle \mathcal{O}_i \rangle$'s but the amplitude of course will not. This is an example of matching the effective long distance theory with the full theory at short-distance through OPE where C_i 's are the Wilson [2] coefficients.

3.1.1 $K \rightarrow \pi e^+ e^-$ Effectice Hamiltonian Due To Gilman and Wise

We will consider the simpler 4-quark case of effective Hamiltonian relevant for the decay $K \rightarrow \pi e^+ e^-$, where one considers an effective region where only four quarks ($q = u, d, s$ and c) and W boson, are active and when one comes down from $\mu > M_W$ to $\mu < M_W$ considering W as much heavier than those four quarks then the Hamiltonian describing this decay is given by:

$$\mathcal{H}_{GW} = -\frac{G_F}{\sqrt{2}} V_{ud}^* V_{us} \left[C_+^{(4)}(\mu) \mathcal{Q}_+(\mu) + C_-^{(4)}(\mu) \mathcal{Q}_-(\mu) \right] + h.c \quad (3.1.11)$$

GW stands for Gilman and Wise [3]. $C_{\pm}^{(f)}(\mu)$ are given in Eq. (3.2.29) and the operators are defined in Eq. (3.2.16), (3.2.15). They also considered another operator relevant for this process namely:

$$\mathcal{Q}_7 = \alpha_e [\bar{s}_\alpha \gamma^\mu (1 - \gamma_5) d_\alpha] [\bar{e} \gamma_\mu e] \quad (3.1.12)$$

This operator involves the conserved vector current hence does not need renormalization and hence will be scale independent. When we come down below the charm quark mass, all the operators mix among themselves and they obtained the final effective Hamiltonian:

$$\mathcal{H}_{GW}^{eff} = -\frac{G_F}{\sqrt{2}} V_{ud}^* V_{us} \left[\tilde{C}_+(\mu) \mathcal{Q}_+(\mu) + \tilde{C}_-(\mu) \mathcal{Q}_-(\mu) + \tilde{C}_7(\mu) \mathcal{Q}_7(0) \right] + h.c$$

$$(3.1.13)$$

where,

$$\begin{aligned}
\tilde{C}_+(\mu) &= \frac{1}{2} \left[\frac{\alpha_s^{(4)}(m_c^2)}{\alpha_s^{(3)}(\mu^2)} \right]^{\frac{2}{9}} \left[\frac{\alpha_s^{(4)}(M_W^2)}{\alpha_s^{(4)}(m_c^2)} \right]^{\frac{6}{25}} \\
\tilde{C}_-(\mu) &= \frac{1}{2} \left[\frac{\alpha_s^{(4)}(m_c^2)}{\alpha_s^{(3)}(\mu^2)} \right]^{\frac{4}{9}} \left[\frac{\alpha_s^{(4)}(M_W^2)}{\alpha_s^{(4)}(m_c^2)} \right]^{\frac{12}{25}} \\
\tilde{C}_7(\mu) &= \frac{16}{99\alpha_s^{(4)}(m_c^2)} \left\{ \left(1 - \left[\frac{\alpha_s^{(4)}(m_c^2)}{\alpha_s^{(3)}(\mu^2)} \right]^{\frac{11}{9}} \right) \left[\frac{\alpha_s^{(4)}(M_W^2)}{\alpha_s^{(4)}(m_c^2)} \right]^{\frac{6}{25}} \right\} \\
&\quad - \frac{16}{90\alpha_s^{(4)}(m_c^2)} \left\{ \left(1 - \left[\frac{\alpha_s^{(4)}(m_c^2)}{\alpha_s^{(3)}(\mu^2)} \right]^{-\frac{5}{9}} \right) \left[\frac{\alpha_s^{(4)}(M_W^2)}{\alpha_s^{(4)}(m_c^2)} \right]^{\frac{12}{25}} \right\}
\end{aligned}$$

As we explained above, Q_7 is scale independent while $C_i(\mu)$'s ($i = +, -, 7$) and Q_{\pm} are all scale dependent and because $\langle \pi e^+ e^- | \mathcal{H}_{GW}^{eff} | K \rangle$ has to be scale independent, the scale dependence of $\sum_{i=-,+} C_i \langle Q_i \rangle$ must be cancelled by the scale dependence of $C_7(\mu)$ alone. Gilman and Wise did not keep the large N structure of their analysis explicit but we have obtained the large N structure of $C_7(\mu)$ and is presented in Appendix C, large N structure of C_{\pm} are of course available due to Bardeen, Buras and Gèrard [4] that we will discuss in section 3.2.1.

This Hamiltonian will be used in the next chapter when we present our own work in the study of the long and short distance matching of QCD in the context of the same decay $K \rightarrow \pi e^+ e^-$ using the Bardeen, Buras and Gèrard scheme that we are going to introduce now.

3.2 Bardeen-Buras-Gèrard Matching Scheme

Bardeen, Buras and Gèrard [5, 4, 6] devised a scheme to match short and long distance QCD that can be summarized in the following way:

1. One starts with a truncated chiral Lagrangian and calculate loops with hard-momentum cut-off M . Matrix elements of Q_i 's are evaluated using such UV

truncated loops such that they are now M dependent: $\langle \mathcal{Q}_i \rangle \mapsto \langle \mathcal{Q}_i(M) \rangle$ and mixing among the matrix elements is obtained through the RG-like (“meson-evolution”) evolution: $\langle \mathcal{Q}_i(M) \rangle = \mathcal{E}_{ij}(M^2) \langle \mathcal{Q}_j(0) \rangle$ where “0” stands for tree level calculation in the meson theory. In this “meson-evolution” a long-distance anomalous dimension matrix is obtained that serves the purpose of mixing the $\langle \mathcal{Q}_i \rangle$ s and shown to have a large N structure.

2. Usual short distance RG improved perturbation theory is used with explicit large N structure to come down (“quark-evolution”) from a scale $\mu \sim M_W$ to $\mu \sim 1\text{GeV}$.
3. UV scale of the long distance theory M is identified with the short distance (\overline{MS}) IR scale μ appearing in the Wilson coefficients.
4. Large N structure of long and short distance anomalous dimension matrices are shown to be consistent. The matching have been studied in the range $M = 0.6 - 1 \text{ GeV}$.

Let us elaborate a bit. The whole scheme is divided into two broad parts:

3.2.1 Part-I: Short Distance Evolution of Wilson Coefficients and Large N

At a scale way above the W mass where strong-interaction is practically absent they [4] start with $\Delta S = 1$ Hamiltonian given by:

$$\mathcal{H}^{\Delta S=1} = -\frac{G_F}{\sqrt{2}} V_{ud}^* V_{us} [(\mathcal{Q}_2^u - \mathcal{Q}_2^c) + \tau(\mathcal{Q}_2^c - \mathcal{Q}_2^t)] \quad (3.2.14)$$

where

$$\mathcal{Q}_2^q = [\bar{s}_\alpha \gamma^\mu (1 - \gamma_5) q_\alpha] [\bar{q}_\beta \gamma_\mu (1 - \gamma_5) d_\beta], \quad \tau = -\frac{V_{ts}^* V_{td}}{V_{us}^* V_{ud}} \quad (3.2.15)$$

For completeness we also define:

$$\mathcal{Q}_1^q = [\bar{s}_\alpha \gamma^\mu (1 - \gamma_5) d_\alpha] [\bar{q}_\beta \gamma_\mu (1 - \gamma_5) q_\beta] \quad (3.2.16)$$

then they [4] consider the OPE method as discussed in the beginning of this chapter to come down to a scale $\mu \sim 1$ GeV and as expected new operators are generated (“mixing”) and the new effective Hamiltonian at this scale takes the following form:

$$\mathcal{H}^{\Delta S=1} = \frac{G_F}{\sqrt{2}} V_{ud}^* V_{us} \sum_i C_i(\mu) \mathcal{Q}_i(\mu) \quad (3.2.17)$$

where

$$\begin{aligned} \mathcal{Q}_1 &= [\bar{s}_\alpha \gamma^\mu (1 - \gamma_5) d_\alpha] [\bar{u}_\beta \gamma_\mu (1 - \gamma_5) u_\beta] \\ \mathcal{Q}_2 &= [\bar{s}_\alpha \gamma^\mu (1 - \gamma_5) u_\alpha] [\bar{u}_\beta \gamma_\mu (1 - \gamma_5) d_\beta] \\ \mathcal{Q}_3^q &= [\bar{s}_\alpha \gamma^\mu (1 - \gamma_5) d_\alpha] [\bar{q}_\beta \gamma_\mu (1 - \gamma_5) q_\beta] \\ \mathcal{Q}_4^q &= [\bar{s}_\alpha \gamma^\mu (1 - \gamma_5) q_\alpha] [\bar{q}_\beta \gamma_\mu (1 - \gamma_5) u_\beta] \\ \mathcal{Q}_5^q &= [\bar{s}_\alpha \gamma^\mu (1 - \gamma_5) d_\alpha] [\bar{q}_\beta \gamma_\mu (1 + \gamma_5) q_\beta] \\ \mathcal{Q}_6^q &= -8(\bar{s}_{\alpha L} q_{\alpha R})(\bar{q}_{\beta R} d_{\beta L}) \end{aligned} \quad (3.2.18)$$

here $q = u, d, s$ only and all of \mathcal{Q}_i s are not independent because of the relation:

$$\mathcal{Q}_4 = \mathcal{Q}_2 + \mathcal{Q}_3 - \mathcal{Q}_1 \quad (3.2.19)$$

And the Wilson coefficients are given by:

$$C_i(\mu) = z_i(\mu) + \tau y_i(\mu), \quad (3.2.20)$$

The difference between their method of short distance analysis and that of Gilman and Wise [7] is that they have considered the large N structure of the anomalous dimension matrix to reduce work significantly. Consider the 6×6 anomalous dimension matrix γ^{QG} written in the \mathcal{Q}_i ($i = 1 - 6$) basis and defined as:

$$M^2 \frac{\partial}{\partial M^2} \langle \mathcal{Q}_i(M^2) \rangle = -\frac{1}{2} \gamma_{ij}^{QG} \langle \mathcal{Q}_j(M^2) \rangle \quad (3.2.21)$$

with

$$\gamma^{QG} = \frac{g^2}{8\pi^2} \begin{pmatrix} -\frac{3}{N} & 3 & 0 & 0 & 0 & 0 \\ 3 & -\frac{3}{N} & -\frac{1}{3N} & \frac{1}{3} & -\frac{1}{3N} & \frac{1}{3} \\ 0 & 0 & -\frac{11}{3N} & \frac{11}{3} & -\frac{2}{3N} & \frac{2}{3} \\ 0 & 0 & (3 - \frac{f}{3N}) & (\frac{f}{3} - \frac{3}{N}) & -\frac{f}{3N} & \frac{f}{3} \\ 0 & 0 & 0 & 0 & \frac{3}{N} & -3 \\ 0 & 0 & -\frac{f}{3N} & \frac{f}{3} & -\frac{f}{3N} & (\frac{f}{3} + \frac{3}{N} - 3N) \end{pmatrix} \quad (3.2.22)$$

As we defined in the beginning of this chapter, f is the number of active flavors, in this case $f = 5, 4, 3$. If one considers the LO in large N expansion then only \mathcal{Q}_6 operator will survive and there will be no mixing between \mathcal{Q}_2 and other operators but for the evolution we need this mixing because \mathcal{Q}_2 is the operator that we start with at very short distance, hence we need to consider the NLO terms. They argued that the long evolution from M_W scale down to 1 GeV will compensate for this $1/N$ suppression from NLO in the \mathcal{Q}_1 - \mathcal{Q}_2 sector. On the other hand \mathcal{Q}_2 - \mathcal{Q}_i ($i \neq 1, 2$, the penguins) mixing is GIM suppressed up to the scale m_c and hence considering LO will be sufficient, for the same reason mixing within the penguin sector and the diagonal evolution of $\mathcal{Q}_{3,4,5}$ are also neglected. This leads to a 4×4 anomalous dimension matrix:

$$\gamma^{QG} = \frac{g^2}{8\pi^2} \begin{pmatrix} -3/N & 3 & 0 & 0 \\ 3 & -3/N & 1/3 & 1/3 \\ 0 & 0 & 0 & 0 \\ 0 & 0 & 0 & -3N \end{pmatrix} \quad (3.2.23)$$

With active operators \mathcal{Q}_1 , \mathcal{Q}_2 , \mathcal{Q}_4 and \mathcal{Q}_6 only. In fact they have shown in their long distance calculation that at the leading order in $N \simeq \Lambda_x^2$ the matrix elements of only these four operators survive and here we have already started to see the consistency between long and short distance behaviors of the anomalous dimension matrix under large N . The Wilson coefficients can be calculated from the evolution relation [8]:

$$\langle \mathcal{Q}_i(M_W^2) \rangle = U_{ij}(M_W^2, \mu^2) \langle \mathcal{Q}_j(\mu^2) \rangle \quad (3.2.24)$$

where the $U(M_W^2, \mu^2)$ is the evolution operator that relates the four-quark operators at the scales M_W and μ and is given by:

$$U(\mu_1^2, \mu_2^2) = \text{T} \left\{ \exp \left[- \int_{\mu_2^2}^{M_W^2} \frac{dp^2}{2p^2} \gamma^{QG}(\alpha_s^{(f)}(p^2)) \right] \right\} \quad (3.2.25)$$

where T defines the momentum order products of $\gamma^{QG}(\alpha_s^{(f)})$ matrices so that f is taken as 5, 4, 3 in successive steps as we come down in momentum scale. The penguin operators are of course important here in their (BBG) study but it is out of

the scope of this thesis so far so we will drop them from our discussion from now on and it is not so bad because the evolution of $\mathcal{Q}_{1,2}$ is unaffected by the presence of the penguins. We will also not consider the CP violating y_i part of the Wilson coefficients.

In this sector (\mathcal{Q}_1 - \mathcal{Q}_2) the following $\mathcal{Q}_\pm = \mathcal{Q}_2 \pm \mathcal{Q}_1$ operators diagonalize the anomalous dimension matrix. Corresponding Wilson coefficients will then take the form $C_\pm = (C_2 \pm C_1)/2$ and this makes the calculation of C_1 and C_2 fairly simple. The anomalous dimension matrix in this sector becomes:

$$\gamma^{QG} = \frac{g^2}{8\pi^2} \begin{pmatrix} \gamma^{QG+} & 0 \\ 0 & \gamma^{QG-} \end{pmatrix} \quad (3.2.26)$$

where,

$$\gamma^{QG\pm} = \pm 3 - 3/N \quad (3.2.27)$$

Evolution matrix then can be written as:

$$U(M_W^2, \mu^2) = \begin{pmatrix} C_+^{(f)}(M_W^2, \mu^2) & 0 \\ 0 & C_-^{(f)}(M_W^2, \mu^2) \end{pmatrix} \quad (3.2.28)$$

Eq. (3.2.25), (3.2.26) and (3.2.27) then leads to:

$$C_\pm^{(f)}(M_W^2, \mu^2) = \exp \left[- \int_{\mu^2}^{M_W^2} \frac{dp^2}{4\pi p^2} \gamma^{QG\pm}(\alpha_s^{(f)}(p^2)) \right] = \left[\frac{\alpha_s^{(f)}(M_W^2)}{\alpha_s^{(f)}(\mu^2)} \right]^{a_\pm^{(f)}} \quad (3.2.29)$$

It must be noted here that when the scale jump is done, that is crossing $\mu = M_W$, $\alpha_s^{(f)}$ is kept fixed, that means in Eq.(3.2.29) f remains fixed. $\alpha_s^{(f)} = g^2/4\pi$ had been used in the derivation above and,

$$a_\pm^{(f)} = \frac{3\gamma^{QG\pm}}{11N - 2f} \quad (3.2.30)$$

We can now write down the final $\Delta S = 1$ effective Lagrangian valid at ~ 1 GeV:

$$\mathcal{H}_{eff}^{\Delta S=1} = -\frac{1}{\sqrt{2}} V_{ud}^* V_{us} \left(C_+^{(f)}(\mu) Q(\mu) + C_-^{(f)}(\mu) Q(\mu) \right) + \text{Penguins} \quad (3.2.31)$$

here we have used the short notation in the argument of the Wilson coefficients, that is just (μ) instead of (M_W^2, μ^2) . It is now time to proceed to the next part of the game, that is the long distance meson-evolution picture.

3.2.2 Part-II: Long Distance Evolution of Matrix Elements and The Chiral Large $N \sim f^2$

In the long distance part (below 1 GeV) they [6] start with the following effective Lagrangian:

$$\mathcal{L}_{BBG}^{\Delta S=0} = \frac{f^2}{4} \left\{ \text{tr}[D^\mu \Sigma D_\mu \Sigma^\dagger] + \mathcal{B}_0 \text{tr}[M_q(\Sigma + \Sigma^\dagger)] \right\} + \mathcal{L}^\Lambda \quad (3.2.32)$$

where,

$$\mathcal{L}^\Lambda = -\frac{f^2}{4} \frac{\mathcal{B}_0}{\Lambda^2} \text{tr}[M_q(D^2 \Sigma + D^2 \Sigma^\dagger)] \quad (3.2.33)$$

This Lagrangian possesses the following features:

1. It is a truncated chiral Lagrangian that does not have extra LECs ¹ other than the typical $O(p^2)$ parameters f and \mathcal{B}_0 and as we will see apparently the third parameter Λ will be a function of pion and kaon decays constants Λ sets the scale of the higher order terms. F_π and F_K respectively. Still this Lagrangian should be treated like a full theory and loops should be considered,
2. because It is valid up to a scale M which is the hard momentum cut-off imposed on the loop integrals so that it explains the physics lying below M which is expected to be smaller than Λ .
3. This provides a bosonization of QCD at very low energy ($\sim m_\pi$).
4. The large N expansion is achieved through tree (LO in $1/N$), one-loop (NLO in $1/N$), ...

¹But in their later work they have included resonances that saturate the LECs indeed.

Bosonization of the four-quark operators and hence eventually of the effective Hamiltonian given by Eq. (3.2.31) can be achieved through the left chiral current given in Eq. (2.2.37) plus an extra term coming from Eq. (3.2.33). Procedure is simple if we use the fact that left currents couple to W boson in the standard model then we can gauge the chiral covariant derivative and identify the left current coming from the truncated chiral Lagrangian, this time we have to just use this extra piece of Lagrangian to recover term (\mathcal{L}_μ^Λ let us say.) that should be added to the already derived left current given by Eq. (2.2.37).

Considering the term linear in l_μ :

$$\mathcal{L}^\Lambda = -\frac{if^2}{4} \frac{\mathcal{B}_0}{\Lambda^2} \text{tr} [l^\mu (M_q(\partial_\mu \Sigma^\dagger) - (\partial_\mu \Sigma)M_q)] + O(l^2) + O(l^0) \quad (3.2.34)$$

and the same in Eq. (2.2.33) and evaluating the following at $l^\mu = W^\mu$:

$$\frac{\delta \mathcal{L}^\Lambda}{\delta l^\mu} = \frac{\delta \mathcal{L}_{QCD}}{\delta l^\mu} \quad (3.2.35)$$

we extract:

$$\mathcal{L}_{\mu ij}^\Lambda + \dots = \bar{q}_L^j \gamma_\mu q_L^j = -\frac{if^2}{4} \frac{\mathcal{B}_0}{\Lambda^2} [M_q(\partial_\mu \Sigma^\dagger) - (\partial_\mu \Sigma)M_q]_{ji} + \dots \quad (3.2.36)$$

Ellipsis represent the term coming from \mathcal{L}^Λ subtracted part of the Lagrangian in Eq. (3.2.32). Adding this piece of the current to the left current given in Eq. (2.2.37) we obtain the full current:

$$(\mathcal{L}_\mu^{BBG})_{ij} = \bar{q}_L^i \gamma_\mu q_L^j = \mathcal{L}_{ij} + \mathcal{L}_{\mu ij}^\Lambda \quad (3.2.37)$$

Hence the bosonized current-current operators are²

$$\mathcal{Q}_1 = 4(\mathcal{L}_\mu^{BBG})_{32}(\mathcal{L}^{BBG\mu})_{11} \quad (3.2.38)$$

$$\mathcal{Q}_2 = 4(\mathcal{L}_\mu^{BBG})_{31}(\mathcal{L}^{BBG\mu})_{12} \quad (3.2.39)$$

These then imply:

$$\mathcal{Q}_\pm = 4 \left[(\mathcal{L}_\mu^{BBG})_{31}(\mathcal{L}^{BBG\mu})_{12} \pm (\mathcal{L}_\mu^{BBG})_{32}(\mathcal{L}^{BBG\mu})_{11} \right] \quad (3.2.40)$$

²Here we have used $(1 \pm \gamma_5)^2 = 2(1 \pm \gamma_5)$ and $(1 \pm \gamma_5) : \psi \mapsto 2\psi_{R,L}$.

And finally we can plug them in Eq. (3.2.31) to obtain the $\Delta S = 1$ effective Hamiltonian that governs the dynamics of the region below the scale Λ . Before we proceed to calculate the matrix elements we need to estimate the value of Λ as we promised above.

Pion and Kaon Decay Constants and Λ

Like we did in the last chapter, we can expand Σ in terms of pion and kaon fields to obtain their decay constants by looking at the coefficients of $\partial_\mu\pi$ and $\partial_\mu K$ in the left current but let us do it a little bit differently in not so elegant way just for fun. The decay constants must be of the following form:

$$F_{\pi,K} = f \left(1 + \frac{a_{\pi,K}^2}{\Lambda^2} \right) \quad (3.2.41)$$

The first term is coming from \mathcal{L}_μ piece of \mathcal{L}_μ^{BBG} while the correction should come from the \mathcal{L}_μ^Λ piece. The constants $a_{\pi,K}$ should be proportional to $\mathcal{B}_0 M_q$ and they can be guessed studying the structural similarity of the two pieces of the current. Notice that,

$$\begin{aligned} \mathcal{L}^\mu &= \frac{if^2}{2} [(\partial^\mu \Sigma) \Sigma^\dagger] \\ &= \frac{if^2}{4} [(\partial^\mu \Sigma) \Sigma^\dagger - \Sigma (\partial^\mu \Sigma^\dagger)] \\ &= -\frac{if^2}{4} [\mathbb{1} (\partial^\mu \Sigma^\dagger) - (\partial^\mu \Sigma) \mathbb{1}] \end{aligned}$$

This will look exactly like \mathcal{L}^Λ if we do the following substitution:

$$\mathbb{1} \mapsto \frac{\mathcal{B}_0}{\Lambda^2} M_q$$

In the pion sector $M_q = m \mathbb{1}_{2 \times 2}$ which implies $a_\pi = \frac{\mathcal{B}_0 m}{\Lambda^2} = \frac{m_\pi^2}{\Lambda^2}$ and in the limit of isospin symmetry, that is $m_\pi = m_K$ we must have $F_\pi = F_K$ and this enforces $a_\pi = a_K$, in the isospin limit hence we must have $a_K = \frac{m_K^2}{\Lambda^2}$ or $a_K = \frac{m_\pi^2}{\Lambda^2}$, but we know that the isospin symmetry is broken hence the later choice is not possible. One could argue that there could be possibilities like $a_K = 2m_K^2 - m_\pi^2$ etc, but notice that M_q is diagonal and if you look at the component of the left current “ $\mathcal{L}_{3i,i3,i \neq 3}^\Lambda$ ” then

only m_s will enter the picture giving rise to m_K^2 . Here we have used Eq. (2.2.41) to express the meson masses in terms of quark masses.

Hence,

$$F_{\pi,K} = f \left(1 + \frac{m_{\pi,K}^2}{\Lambda^2} \right) \quad (3.2.42)$$

and indeed this is the leading order large N expression provided by Bardeen, Buras and Gèrard in [4], they also evaluated the ratio to estimate Λ ,

$$\frac{F_K}{F_\pi} = 1 + \frac{m_K^2 - m_\pi^2}{\Lambda^2} + O\left(\frac{1}{\Lambda^4}\right) + O\left(\frac{1}{N}\right) \quad (3.2.43)$$

Experimentally this ratio is 1.28 and if we impose the large N limit then this implies $\Lambda \simeq 0.9$ GeV, so indeed this theory lies beneath the scale where perturbative QCD fails. The aim is to match this theory to the lower limit of OPE-obtained QCD governed by the Hamiltonian given by (3.2.31). They calculated the matrix elements of the four-quark operators in the tree level [4] we will just list down $\langle Q_{1,2} \rangle$ here,

$$\langle \pi^+ \pi^0 | \mathcal{Q}_{1,2}(0) | K^+ \rangle = X/\sqrt{2} \quad (3.2.44)$$

$$\langle \pi^+ \pi^- | \mathcal{Q}_2(0) | K^0 \rangle = -\langle \pi^0 \pi^0 | \mathcal{Q}_1(0) | K^0 \rangle = X \quad (3.2.45)$$

All other matrix elements of $\mathcal{Q}_{1,2}$ are zero and

$$X = \sqrt{2} F_\pi (m_K^2 - m_\pi^2) \simeq 0.03 \text{ GeV}^3 \quad (3.2.46)$$

Loops And $O(1/N)$ Corrections

$1/N$ correction to the matrix elements and decay constants are achieved through one-loop calculations done with the momentum cut-off M in [6], we will list them below. The pion and kaon decay constants at one loop (Fig. 3.1) are given by:

$$\begin{aligned} F_\pi &= f \left[\left(1 + \frac{m_\pi^2}{\Lambda^2} \right) - \frac{1}{2f^2} \left(2A_0(M^2, m_\pi^2) + A_0(M^2, m_K^2) \right) \right] \\ F_K &= f \left[\left(1 + \frac{m_K^2}{\Lambda^2} \right) - \frac{3}{8f^2} \left(2A_0(M^2, m_K^2) + A_0(M^2, m_\pi^2) \right. \right. \\ &\quad \left. \left. + A_0(M^2, m_\eta^2) \right) \right] \end{aligned} \quad (3.2.47)$$

where the extra argument M^2 in A_0 means that the usual one point function [9] has been calculated in a cut-off regularization (please check Eq. (B.3.17) and

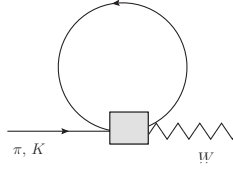


Figure 3.1: Loop contribution to pion and kaon decay constants.

(B.3.29)) scheme instead of dimensional regularization. Scale dependence of the expansion parameter f is given by:

$$f^2 = f^2(M^2) = F_\pi^2 + 2A_0(M^2, m_\pi^2) + A_0(M^2, m_K^2) \quad (3.2.48)$$

Comparing Eq. (3.2.47) with Eq. (3.2.42), we can see the N -structure of decay constants:

$$F_{K,\pi} = F_{K,\pi} + O\left(\frac{1}{N}\right) \quad (3.2.49)$$

And also their ratio have the same structure which is at one loop takes the form:

$$\frac{F_K}{F_\pi} = \left(1 + \frac{m_K^2 - m_\pi^2}{\Lambda^2}\right) - \frac{1}{8f^2} \left(2A_0(M^2, m_K^2) - 5A_0(M^2, m_\pi^2) + 3A_0(M^2, m_\eta^2)\right) \quad (3.2.50)$$

and it is well understood [10] that low energy theory of interacting mesons is dual to QCD and so they both should have the same N structure and this structure is the basis of BBG matching scheme. We now list the one loop (Fig. (3.2)) correction terms to the matrix elements of $\mathcal{Q}_{1,2}$.

$$\langle \pi^+ \pi^- | \mathcal{Q}_1 | K^0 \rangle = X_1 \quad (3.2.51)$$

$$\langle \pi^+ \pi^- | \mathcal{Q}_2 | K^0 \rangle = X_2 \quad (3.2.52)$$

$$\langle \pi^0 \pi^0 | \mathcal{Q}_1 | K^0 \rangle = X_3 \quad (3.2.53)$$

$$\langle \pi^0 \pi^0 | \mathcal{Q}_2 | K^0 \rangle = X_4 \quad (3.2.54)$$

$$\langle \pi^+ \pi^0 | \mathcal{Q}_{1,2} | K^+ \rangle = X_5 \quad (3.2.55)$$

Where,

$$\left. \begin{aligned}
 X_1 &= \frac{X}{(4\pi f)^2} \frac{f}{F_\pi} \left\{ -2M^2 \left(\frac{m_K^2}{4} + \frac{19}{9} m_\pi^2 \right) \log \left(1 + \frac{M^2}{\tilde{m}^2} \right) \right\} \\
 X_2 &= X \left\{ \left[1 + \frac{f}{F_\pi} \left(\frac{F_K}{F_\pi} - 1 \right) \frac{m_\pi^2}{m_K^2 - m_\pi^2} \right] \right. \\
 &\quad \left. \frac{1}{(4\pi f)^2} \frac{f}{F_\pi} \left[M^2 + \left(m_K^2 - \frac{3}{2} m_\pi^2 \right) \log \left(1 + \frac{M^2}{\tilde{m}^2} \right) \right] \right\} \\
 X_3 &= X \left\{ \left[1 + \frac{f}{F_\pi} \left(\frac{F_K}{F_\pi} - 1 \right) \frac{m_\pi^2}{m_K^2 - m_\pi^2} \right] \right. \\
 &\quad \left. - \frac{1}{(4\pi f)^2} \frac{f}{F_\pi} \frac{8}{9} m_\pi^2 \log \left(1 + \frac{M^2}{\tilde{m}^2} \right) \right\} \\
 X_4 &= \frac{X}{(4\pi f)^2} \frac{f}{F_\pi} \left[3M^2 + \left(\frac{3}{4} m_K^2 - \frac{9}{2} m_\pi^2 \right) \log \left(1 + \frac{M^2}{\tilde{m}^2} \right) \right] \\
 X_5 &= \frac{X}{\sqrt{2}} \left\{ - \left[1 + \frac{f}{F_\pi} \left(\frac{F_K}{F_\pi} - 1 \right) \frac{m_\pi^2}{m_K^2 - m_\pi^2} \right] \right. \\
 &\quad \left. \frac{1}{(4\pi f)^2} \frac{f}{F_\pi} \left[-2M^2 + \left(\frac{1}{4} m_K^2 - 3m_\pi^2 \right) \log \left(1 + \frac{M^2}{\tilde{m}^2} \right) \right] \right\}
 \end{aligned} \right\} \quad (3.2.56)$$

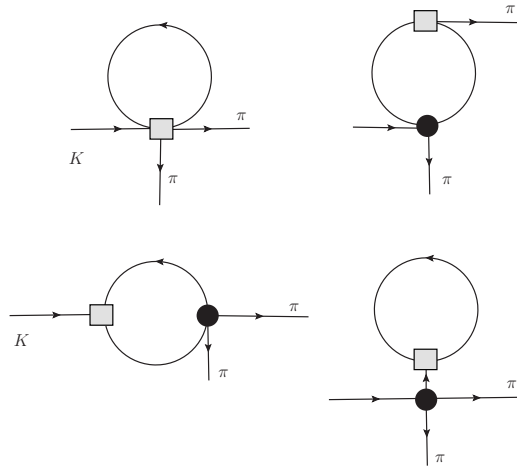


Figure 3.2: Loop contributions to $K \rightarrow \pi\pi$ process.

Long Distance Mixing

Bardeen, Buras and noted that these loop corrections to the matrix elements can be interpreted as an evolution in M from the tree results, much like the short distance RG-evolution that leads to operator mixing. In fact this evolution in M is in tune with the evolution in $1/N$. This becomes apparent when we observe that $M = 0$ leads to all the $1/N$ corrections to vanish which further justifies the notation that the tree matrix elements $\langle \mathcal{Q}_i(0) \rangle$ represents the leading order large N values. Symbolically this fact can be expressed as:

$$\langle \mathcal{Q}_i(M^2) \rangle \equiv \langle \mathcal{Q}_i(0) \rangle + O\left(\frac{M^2}{N}\right) \quad (3.2.57)$$

In fact they showed that in the limit $m_\pi^2 \mapsto 0$, these matrix elements listed in Eq. (3.2.51) can be cast into an operator mixing relations:

$$\begin{aligned} \mathcal{Q}_1(M^2) &= \mathcal{Q}_1(0) - \left[\frac{f}{F_\pi} \right] \frac{c_1(M^2)}{(4\pi f)^2} \mathcal{Q}_2(0) \\ \mathcal{Q}_2(M^2) &= \mathcal{Q}_2(0) - \left[\frac{f}{F_\pi} \right] \frac{c_1(M^2)}{(4\pi f)^2} \mathcal{Q}_1(0) \\ &\quad + \left[\frac{f}{F_\pi} \right] \frac{c_2(M^2)}{(4\pi f)^2} [\mathcal{Q}_2(0) - \mathcal{Q}_1(0)] \end{aligned} \quad (3.2.58)$$

And in terms of \mathcal{Q}_\pm ,

$$\begin{aligned} \mathcal{Q}_+(M^2) &= \left(1 - \left[\frac{f}{F_\pi} \right] \frac{c_1(M^2)}{(4\pi f)^2} \right) \mathcal{Q}_+(0) + \left[\frac{f}{F_\pi} \right] \frac{c_2(M^2)}{(4\pi f)^2} \mathcal{Q}_-(0) \\ \mathcal{Q}_-(M^2) &= \left(1 + \left[\frac{f}{F_\pi} \right] \frac{c_1(M^2) + c_2(M^2)}{(4\pi f)^2} \right) \mathcal{Q}_-(0) \end{aligned} \quad (3.2.59)$$

Where,

$$c_1(M^2) = 2M^2 - \frac{m_K^2}{4} \log\left(1 + \frac{M^2}{\tilde{m}^2}\right) \quad (3.2.60)$$

$$c_2(M^2) = M^2 + m_K^2 \log\left(1 + \frac{M^2}{\tilde{m}^2}\right) \quad (3.2.61)$$

Important thing to notice here is that \mathcal{Q}_- evolves independently while \mathcal{Q}_+ mixes with \mathcal{Q}_- . This mixing is approximately suppressed by a factor of 2 if one looks at the

quadratically divergent term. Another fact is that Q_+ is also numerically suppressed in comparison to Q_- as evident from the above expressions, which is significant because it is consistent with the short distance behavior of the dominance of $C_-(\mu)$ over $C_+(\mu)$. It will be useful later to define the following long-distance evolution operator:

$$\begin{aligned} \mathcal{E}_-(M^2) &= 1 + \left[\frac{f}{F_\pi} \right] \frac{c_1(M^2) + c_2(M^2)}{(4\pi f)^2} \\ &= 1 + \frac{1}{(4\pi f)^2} \left[\frac{f}{F_\pi} \right] \left[3M^2 + \frac{3}{4}m_K^2 \log \left(1 + \frac{M^2}{\tilde{m}^2} \right) \right] \end{aligned} \quad (3.2.62)$$

that evolves Q_- from 0 to M . Here f of course means $f(M^2)$ given by Eq. (3.2.48). We must pause and stress that this result is significant which one can realize when calculating processes where Q_- is the dominant operator. One just will have to calculate the leading order matrix element of Q_- which can be even one loop but still leading order in $1/N$ expansion and can apply $\mathcal{E}_-(M^2)$ to extract the NLO result without taking the trouble of actually calculating NLO that is the next order in loop expansion. In fact we will use this property to calculate the amplitude $K^+ \rightarrow \pi^+ e^+ e^-$ in Chapter 4.

3.2.3 The Matching of Quark and Meson Evolution

So far we have seen that there exist a division between the short and long distance physics, in the SD case the scale μ enters through usual renormalization prescription which in this case must be below the charm mass while the LD scale is the UV cut-off M . They [6] made the identification $\mu = M$ and because they have a quadratic divergence (M^2) in the long distance part it is now possible to have a point $\mu = M$ where the quadratic divergence kills the logarithmic divergence of the Wilson coefficients and that will be the matching scale. Their approach is more general, they evaluated a long distance anomalous dimension matrix, we will consider the

$\mathcal{Q}_{1,2}$ sector of it. Eq. (3.2.58) can be expressed in a renormalization equation form:

$$M^2 \frac{\partial \mathcal{Q}_1(M^2)}{\partial M^2} = - \left[\frac{f}{F_\pi} \right] \frac{M^2}{(4\pi f)^2} \frac{\partial c_1(M^2)}{\partial M^2} \mathcal{Q}_2(0) \quad (3.2.63)$$

$$\begin{aligned} M^2 \frac{\partial \mathcal{Q}_2(M^2)}{\partial M^2} &= - \left[\frac{f}{F_\pi} \right] \frac{M^2}{(4\pi f)^2} \frac{\partial c_1(M^2)}{\partial M^2} \mathcal{Q}_1(0) \\ &+ \left[\frac{f}{F_\pi} \right] \frac{M^2}{(4\pi f)^2} \frac{\partial c_2(M^2)}{\partial M^2} [\mathcal{Q}_2(0) - \mathcal{Q}_1(0)] \end{aligned} \quad (3.2.64)$$

Now if we denote the long distance (meson) anomalous dimension matrix by γ^M then,

$$\gamma_{12}^M = \gamma_{21}^M = 2 \left[\frac{f}{F_\pi} \right] \frac{M^2}{(4\pi f)^2} \frac{\partial c_1(M^2)}{\partial M^2} > 0 \quad (3.2.65)$$

has the same structure as that of its short distance counterpart given by Eq. (3.2.23), the sign and large N structure matches. The only difference is that in long distance case its evolution is much faster because of the quadratic divergence which will become slower due to the inclusion of resonances as we will see later. Furthermore they also calculated the mixing with penguins and so achieved the following ratios for $\mu = M = 0.8$ GeV:

$$\boxed{\frac{\gamma_{12}^M}{\gamma_{26}^M} = 12.2, \quad \frac{\gamma_{12}^{QG}}{\gamma_{26}^{QG}} = 9} \quad (3.2.66)$$

This ratio $\gamma_{12}^M/\gamma_{26}^M$ is closed to 9 when $\mu = M = 0.7$ GeV value is taken. They also showed that in the region 0.6–0.8 GeV the amplitudes are almost scale independent. We quote their results expressed in Table (3.1).

Of course these results involve the penguin operators that we did not discuss here much but the intention of quoting this table was to demonstrate the success of the scheme and hence to build some confidence in this approach. This table produces $T_1/T_3 \simeq 12$ which is encouraging because the experimental value is 15 and shows the promise of finally explaining $\Delta I = 1/2$ rule. And this is motivating enough to apply this scheme to other processes that we will do in the next chapter and also in other processes in the future but with necessary modification to the scheme that we have proposed in our own work in the next chapter and in conclusion.

Here $T_1 = \mathcal{A}(K^0 \rightarrow \pi^+\pi^-)$, $T_2 = \mathcal{A}(K^0 \rightarrow \pi^0\pi^0)$ and $T_3 = \mathcal{A}(K^+ \rightarrow \pi^+\pi^0)$.

| m_s (MeV) | $\mu = M$ (GeV) | T_1 | T_2 | T_3 |
|-------------|-----------------|-------|-------|-------|
| 125 | 0.6 | 22.8 | 20.3 | 1.75 |
| 125 | 0.7 | 22.3 | 20.0 | 1.58 |
| 125 | 0.8 | 22.2 | 20.3 | 1.33 |
| 150 | 0.6 | 20.4 | 17.9 | 1.75 |
| 150 | 0.7 | 20.1 | 17.8 | 1.58 |
| 150 | 0.8 | 20.1 | 18.2 | 1.33 |
| 175 | 0.6 | 19.0 | 16.5 | 1.75 |
| 175 | 0.7 | 18.8 | 16.5 | 1.58 |
| 175 | 0.8 | 18.8 | 17.0 | 1.33 |
| Data | | 27.7 | 26.3 | 1.84 |

Table 3.1: The amplitudes for the processes $K \rightarrow \pi\pi$ in the units of 10^{-8} GeV for different values of m_s .

3.3 Inclusion of Vector Mesons In The BBG Scheme

We will not discuss Hidden Local Symmetry (HLS) that BBG uses to introduce vectors in full detail in this chapter, this is because in fact they did not consider all the technicalities and issues. We will however describe in full details what they did [11] in this chapter and we promise to come back to this topic of Hidden Local Symmetry in the last part of the next chapter where we will take it more seriously and will present it in full detail. For now, let us start where BBG started.

The motivation to include the resonances is straightforward, that is to make the matching scheme smoother that means to shrink the gap between meson and quark sectors. As we have seen in the last section that the typical matching scale was achieved by BBG at around 0.7 GeV which is expected because the next lightest particles are the vector mesons and $\rho(775)$ is in fact lightest among them. The expectation is that when one includes these resonances the drastic M^2 behavior

will start to diminish and will start to get replaced by poles of these resonances together leading towards a logarithmic behavior, which eventually will justify the identification $\mu = M$.

In Sec. 2.1.1 of Chap. 2 we introduced two bases for parametrizing the mesons, Σ and Ξ which are related by the Eq. (2.1.14), this relation hides a $U(3)$ symmetry which is apparent in Eq. (2.1.11) under which Σ is an invariant. Exploiting this hidden gauge symmetry $U(3)$ BBG introduced the corresponding gauge field V which transforms under $\mathfrak{h}(x) \in U(3)$ as:

$$V_\mu \mapsto \mathfrak{h}(x)V_\mu \mathfrak{h}^\dagger(x) + \frac{i}{g_V} \mathfrak{h}(x) \partial_\mu \mathfrak{h}^\dagger(x) \quad (3.3.67)$$

which fixes the covariant derivative:

$$D_\mu \xi = \partial_\mu \xi - ig_V V_\mu \xi, \quad D_\mu \xi^\dagger = \partial_\mu \xi^\dagger - ig_V V_\mu \xi^\dagger \quad (3.3.68)$$

and an associated field strength tensor given by:

$$V_{\mu\nu} = \partial_\mu V_\nu - \partial_\nu V_\mu - ig_V [V_\mu, V_\nu] \quad (3.3.69)$$

They have taken the mass less limit of their Lagrangian 3.2.32 :

$$\mathcal{L}(\pi) = \frac{f^2}{4} \text{tr}[\partial_\mu \Sigma \partial^\mu \Sigma^\dagger] \quad (3.3.70)$$

and had directly wrote down the following Lagrangian as an extension of the above Lagrangian that incorporates the vector (1^{--}) nonet V_μ :

$$\mathcal{L}(\pi, V) = \mathcal{L}(\pi) - a \frac{f^2}{4} \text{tr} \left[\left((\partial_\mu \xi^\dagger) \xi + (\partial_\mu \xi) \xi^\dagger - 2ig_V V_\mu \right)^2 \right] - \frac{1}{4} \text{tr}[V_{\mu\nu} V^{\mu\nu}] \quad (3.3.71)$$

where,

$$V_\mu = T^a V_\mu^a = \frac{1}{\sqrt{2}} \begin{pmatrix} \rho_\mu^0 + \omega_\mu/\sqrt{2} & \rho_\mu^+ & K_\mu^{*+} \\ \rho_\mu^- & -\rho_\mu^0 + \omega_\mu/\sqrt{2} & K_\mu^{*0} \\ K_\mu^{*-} & \bar{K}_\mu^{*0} & \phi_\mu \end{pmatrix} \quad (3.3.72)$$

We will discuss the construction of a Lagrangian based on this ‘‘Hidden Local Symmetry’’ in the next chapter in much more details when we introduce vector mesons

in our own work. We feel like there are issues for example how does one identify this gauge field V as the vector meson field etc that BBG [11] did not address and so we will go on and discuss things presently in their context. They interpret $\mathcal{L}(\pi)$ to be the limiting value of $\mathcal{L}(\pi, V)$ for arbitrary values of the parameter a in the absence of any vector propagation, that is absence of the kinetic term for V in the above Lagrangian. But when vector propagation is considered, $a \simeq 2$ is successful in producing results that are consistent with Vector Meson Dominance. If we consider just ρ^0 vector meson then,

$$V_\mu = \frac{\rho_\mu^0}{2} \lambda_3 \quad (3.3.73)$$

and we can read off the mass of ρ^0 from $\text{tr}[V^2]$ term in Eq. (3.3.71):

$$m_V^2 = af^2 g_V^2 (\rho_\mu^0 \rho^{0\mu}) \quad (3.3.74)$$

Comparing this with the the mass of $\rho = 0.775$ GeV, we get the constraint:

$$\sqrt{ag_V} = 8.33 \quad (3.3.75)$$

And looking at the IIIIV term:

$$\mathcal{L}_{\text{IIIIV}} = iag_V \text{tr} [V_\mu [\partial^\mu \Pi, \Pi]] \quad (3.3.76)$$

we can extract the coupling strength:

$$g_{V\text{III}} = \frac{ag}{2} \quad (3.3.77)$$

Using the experimental value $g_{V\text{III}} \simeq 6.1$, Eq. (3.3.75) and Eq. (3.3.77) we see that,

$$a \simeq 2 \quad (3.3.78)$$

This had been worked out in [12], considering the following term

$$\mathcal{L}_\mu^{ij} = -\frac{af^2}{2} g_V (\xi V_\mu \xi)^{ji} + \text{other terms} \quad (3.3.79)$$

in the left current coming from the above Lagrangian given by Eq. (3.3.71) and calculating the matrix element:

$$\langle 0 | \mathcal{L}_\mu^{ij} | \rho^+ \rangle = -\frac{af^2 g_V}{\sqrt{2}} \varepsilon_\mu + \dots = -\frac{f_V}{2} m_V \varepsilon_\mu + \dots \quad (3.3.80)$$

where ε is the polarization of ρ , they showed that the ρ^+ decay constant $f_V = \sqrt{2a}f$ produces the KSRF [13, 14] relation:

$$f_V = 2f = 2F_\pi, \quad \text{if } a = 2 \quad (3.3.81)$$

We will discuss other virtues of HLS in the next chapter. Let us now proceed to show how inclusion of vector mesons improved the BBG matching scheme by listing the correction to decay constants and matrix elements. And we must emphasize once again that we will just consider those parts of their work which are relevant to our own work which we will present in the next chapter, so we will not go into CP violation pion electro magnetic mass difference and penguins etc that are essential ingredients of their paper [11] basically on which this chapter stands.

3.3.1 Vector Improved Chiral Expansion Parameter $f(M^2)$

Vector-loop corrected tree level decay constants of mass-less scalar mesons described by the Lagrangian Eq. (3.3.71) as calculated by BBG reads:

$$f(M^2, m_V^2) = F_\pi^2 + \frac{3}{(4\pi)^2} \left[\left(1 - \frac{9a}{16}\right) M^2 + \frac{9a}{16} m_V^2 \log \left(a + \frac{M^2}{m_V^2} \right) \right] \quad (3.3.82)$$

In the limit $m_V^2 \gg M^2$ for any value of a they recover $f(M^2 \ll m_V^2) = F_\pi^2$. It has been also discussed that for $a = 16/9$ the M^2 dependence vanishes which shows the virtue of including vector mesons because even if $a \neq 16/9$, it still is close as discussed above and so the quadratic divergence is way weaker than the earlier case of without vectors.

But coming back to the case of $a = 2$ and the massive pseudo scalars described by Eq. (3.2.32) they add the vector-loop correction to the earlier result (Eq. (3.2.48)) and the complete result $f(M^2, m_V^2)$ is:

$$f(M^2) \mapsto f(M^2, m_V^2) = f(M^2) + \Delta f^2(M^2, m_V^2) \quad (3.3.83)$$

where

$$\Delta f^2(M^2, m_V^2) = -\frac{27}{8} A_0(M^2, m_V^2) \quad (3.3.84)$$

where $\Delta f^2(M^2, m_V^2)$ is the correction term. The slower variation of improved chiral coupling constant is apparent from their table that we quote below (Table 3.2):

| M (GeV) | 0.6 | 0.7 | 0.8 | 0.9 | 1.0 |
|-------------------------|-------|-------|-------|-------|-------|
| $f^2(M^2)$ (MeV) | 114.7 | 123.5 | 133.3 | 143.7 | 154.8 |
| $f^2(M^2, m_V^2)$ (MeV) | 107.6 | 112.1 | 116.4 | 120.6 | 124.3 |

Table 3.2: Variation of f^2 with the scale, with and without vector inclusion.

3.3.2 Vector Contributions To $\langle Q_{\pm} \rangle$

Vector contribution to the current current matrix elements was again shown to maintain the same operator mixing structure described in Eq. (3.2.59) where the corrections enter the coefficients only, and so we have the new mixing equations:

$$\begin{aligned} \mathcal{Q}_+(M^2) &= \left(1 - \left[\frac{f}{F_\pi} \right] \frac{c_1(M^2, m_V^2)}{(4\pi f)^2} \right) \mathcal{Q}_+(0) + \left[\frac{f}{F_\pi} \right] \frac{c_2(M^2, m_V^2)}{(4\pi f)^2} \mathcal{Q}_-(0) \\ \mathcal{Q}_-(M^2) &= \left(1 + \left[\frac{f}{F_\pi} \right] \frac{c_1(M^2, m_V^2) + c_2(M^2, m_V^2)}{(4\pi f)^2} \right) \mathcal{Q}_-(0) \end{aligned}$$

(3.3.85)

By f we mean $f(M^2, m_V^2)$ given by Eq. (3.3.83) and

$$\begin{aligned} c_1(M^2, m_V^2) &= c_1(M^2) + \Delta c_1(M^2, m_V^2) \\ c_2(M^2, m_V^2) &= c_2(M^2) + 0 \end{aligned} \quad (3.3.86)$$

And

$$\Delta c_1(M^2, m_V^2) = 4\pi^2 \left[\frac{9}{2} A_0(M^2, m_V^2) - 3m_V^2 B_0(M^2, 0, m_V^2) \right] \quad (3.3.87)$$

where B_0 is the 't Hooft-Veltman two point function [9] evaluated in cut-off regularization and is given in Eq. (B.3.19) and Eq. (B.3.30) of Appendix B. Meson evolution operator that we defined in Eq. (3.2.62) a correction:

$$\mathcal{E}_-(M^2) \mapsto \mathcal{E}_-(M^2, m_V^2) + \Delta \mathcal{E}_-(M^2, m_V^2) \quad (3.3.88)$$

where,

$$\Delta\mathcal{E}_-(M^2, m_V^2) = \frac{9}{8} \left[\left(\frac{m_V^2}{M^2 + m_V^2} - \frac{3}{2} \right) M^2 + \frac{1}{2} m_V^2 \log \left(1 + \frac{M^2}{m_V^2} \right) \right] \quad (3.3.89)$$

And it must be noticed that the quadratic divergence that we had earlier (Eq. (3.2.62)) is much reduced now. If we consider the new matching scale that they obtained around $M \simeq m_V$, then we can see that the reduction in the strength of quadratic divergence is $\sim 38\%$ and as more and more resonances are taken into account this reduction will be even higher and presumably in the end leading to no quadratic divergence at all. In the light of discussion below Eq. (3.3.82), we can expect that even for value of $a = 2$, M^2 term will disappear, so in a sense the inclusion of more and more resonances is a limit where the coefficient of M^2 is expected eventually to become $(1 - a/2)$ in $f(M^2, m_V^2)$ given by Eq. (3.3.82). We will discuss below how vector mesons improve the matching.

3.3.3 Improved LD-SD Matching

The ratios given in Eq. (3.2.66) now improved by the vectors [11] look:

$$\frac{\gamma_{12}^M}{\gamma_{26}^M} = 8.7, \quad \frac{\gamma_{12}^{QG}}{\gamma_{26}^{QG}} = 9 \quad (3.3.90)$$

at $\mu = M = 0.8$ GeV.

Before we proceed to present our own work it is time we summarize their results:

1. In the range of M considered by them (0.6 - 1 GeV) the γ_{12}^M is larger than γ_{26}^M as in the case of short distance (QG) case.
2. Matching scale achieved with and without vector mesons are 0.8 and 0.7 GeV respectively and so they claim that the range 0.8 - 0.9 GeV is the most reliable range of matching scale.
3. They conclude that evolution is much faster in the long distance case than that in the short distance region of course because of the quadratically divergent term.

It is the matching of the anomalous dimension matrices or equivalently the renormalization group flow structure in the regions above and below 1 GeV that makes their approach so reliable and attractive and makes one tempted to apply it outside the process $K \rightarrow \pi\pi$ around which BBG built this scheme. In fact we will take this a bit further and will apply this to $K \rightarrow \pi e^+ e^-$ because in this process Q_- is one of the dominant operators.

Bibliography

- [1] G. Buchalla, A. J. Buras, and E. M. Lautenbacher. In: *Rev.Mod.Phys.* 68 (1996), pp. 1125–1144. eprint: [hep-ph/9512380](https://arxiv.org/abs/hep-ph/9512380).
- [2] K. Wilson. In: *Phys. Rev.* 179 (1969), p. 1499.
- [3] F. J. Gilman and M. B. Wise. In: *Phys. Rev. D* (1980).
- [4] W. A. Bardeen, A. J. Buras, and J. -M. Gerard. In: *Nucl.Phys. B* 293 (1987), p. 787.
- [5] W. A. Bardeen, A. J. Buras, and J. M. Gerard. In: *Phys.Lett. B* 180 (1986), p. 133.
- [6] W. A. Bardeen, A. J. Buras, and J. -M. Gerard. In: *Nucl.Phys. B* 192 (1987), p. 138.
- [7] F. J. Gilman and M. B. Wise. In: *Phys. Rev. D* 20 (1979), p. 2392.
- [8] W. A. Bardeen, A. J. Buras, and J. -M Gerard. In: *Phys. Rev. D* 20 (1979), p. 166.
- [9] G. 't Hooft and M Veltman. In: *Nucl. Phys. B* 153.365-401 (1979).
- [10] G. 't. Hooft. In: *Nucl. Phys. B* 72 (1974), pp. 461–473.
- [11] A. J. Buras, J. -M Gerard, and W. A. Bardeen. In: *Eur. Phys. J. C* 74 (2014), p. 2871.
- [12] J. -M Gerard. In: *Act. Phys. Pol. B* 21 (1990), pp. 257–305.
- [13] K. Kwarabayashi and M. Suzuki. In: *Phys. Rev. Lett.* 16 (1966), p. 225.
- [14] Riazuddin and Fayazuddin. In: *Phys. Rev.* 147 (1966), p. 1071.

Chapter 4

Application of BBG Scheme

This chapter is based solely on our own work [1] ¹ unless specified otherwise. But previous chapters also contain instances of our contributions, for example the calculations of section 2.7.2 of Chapter 2 was done by us in a different way, which of course we will continue again in this chapter. Then in the second chapter we also had our own inputs through interpretations, explanations and sometimes calculations but mostly last two chapters were reviews. Before we indulge ourselves in the detailed calculations, it will be better to have a blueprint of what we are going to do.

The Steps:

1. We start with the Gilman-Wise Hamiltonian given by Eq. (3.1.13).
2. Bosonize it at very low energy ² using BBG procedure.
3. Calculate the matrix element $\langle \pi e^+ e^- | \mathcal{Q}_{\pm,7}(0) | K \rangle$ at leading order in ChPT (Eq. (3.2.33)).
4. Evolve them using BBG scheme: $\langle \mathcal{Q}(0) \rangle \mapsto \langle \mathcal{Q}(M^2) \rangle$ and plug them with their corresponding Wilson coefficients to obtain the amplitude.

¹In Collaboration with G. D'Ambrosio, D. Greynat and E. Coluccio.

²Bosonization of \mathcal{Q}_{\pm} is already done in Eq. (3.2.40), here we will just do it for \mathcal{Q}_7

5. Set $\mu = M$ and look for the scale where the amplitude is scale independent. Obtain this matching scale M and evaluate “ a ” and “ b ” parameters (introduced in the end of Chapter 2) and predict their values.
6. We include the ρ -meson using Hidden Local Symmetry and repeat the steps described above.

As we discussed in the last chapter that one starts at a very high scale e.g. M_W scale and through OPE achieves an effective Hamiltonian at ~ 1 GeV. Gilman and Wise [2] constructed such a Hamiltonian through OPE, the final form of which ³ is given by Eq. (3.1.13). Then we consider the relevant operators, which are \mathcal{Q}_\pm and \mathcal{Q}_7 and bosonize them at the pion mass scale. Bosonization of \mathcal{Q}_\pm are given by Eq. (3.2.40) and using the current (Eq. (3.2.37)) we can bosonize \mathcal{Q}_7 (introduced in Eq. (3.1.12)) too:

$$\mathcal{Q}_7 = 2\alpha_e (\mathcal{L}_\mu^{BBG})_{32} [\bar{e}\gamma^\mu e] \quad (4.0.1)$$

These bosonization must be understood to be valid at the pion mass scale and is tagged by the argument “0” in $\mathcal{Q}_-(0)$. Which can only be taken to the higher scale (~ 1 GeV) through long distance evolution (check Eq. (3.2.62)), while \mathcal{Q}_7 cannot evolve and we discussed in section 3.1.1. We also consider the fact that $\mathcal{Q}_+(\mu)$ is suppressed in comparison to $\mathcal{Q}_-(\mu)$ in the short distance evolution due to Gilman and Wise [2], we consider only \mathcal{Q}_- and \mathcal{Q}_7 as our dominant operators. One can argue that as \mathcal{Q}_+ mixes with \mathcal{Q}_- as in Eq. (3.2.59) in the long distance evolution, \mathcal{Q}_- can pop out from \mathcal{Q}_+ then dropping of \mathcal{Q}_+ based on short distance evolution is not justified! Well it is, because looking the Wilson coefficients \tilde{C} given in Eq. (??) we can see that $\tilde{C}_+(1 \text{ GeV}) \ll \tilde{C}_-(1 \text{ GeV})$ and even if a \mathcal{Q}_- appears due to the LD evolution of \mathcal{Q}_+ it will be multiplied by C_+ and hence will still be sub-leading in comparison to \mathcal{Q}_- .

³For this study we took the four-quark model instead of six-quark.

$\Delta S = 1$ Effective Lagrangian

The effective Lagrangian at the order of ~ 1 GeV is the following:⁴

$$\mathcal{L}_{GW}^{\Delta S=1} = \frac{G_8}{g_8} \left[\tilde{C}_-(M) \mathcal{Q}_-(M) + \tilde{C}_7(M) \mathcal{Q}_7 \right] + h.c \quad (4.0.2)$$

Wilson coefficients $\tilde{C}_{i=-,7}$ are given in Eq (??) and here we have already implemented $\mu = M$ and used Eq. (2.5.64). The amplitude will be given by:

$$\mathcal{A}(K \rightarrow \pi e^+ e^-) = \langle \mathcal{L}_{GW}^{\Delta S=1} \rangle \quad (4.0.3)$$

4.0.4 Long Distance Mixing (Without Vectors)

Calculation of the amplitude requires the evaluations of $\langle \mathcal{Q}_{-,7} \rangle$ and before we do that we must set things in the context of BBG, we need to address what do we mean by $\langle \mathcal{Q}_i \rangle$.

Meaning of the matrix element notations:

$$\begin{aligned} \langle \mathcal{Q}_i(0) \rangle &= \langle \pi e^+ e^- | \mathcal{Q}_i | K \rangle && \text{Tree level matrix element.} \\ \langle \mathcal{Q}_i(M) \rangle &= \langle \pi e^+ e^- | \mathcal{Q}_i | K \rangle_{loop} && \text{Loop level matrix element where } M \text{ is the loop} \\ &&& \text{momentum cut-off.} \end{aligned} \quad (4.0.4)$$

When we have no vector mesons in the game the only tree level matrix element available for the process is coming from the \mathcal{Q}_7 operator. So it is clear that diagonal evolution of $\langle \mathcal{Q}_- \rangle$ is missing but there will be mixing among them due to evolution in M . And as we discussed earlier $\langle \mathcal{Q}_7 \rangle$ does not evolve at all so we can rephrase it by saying its evolution is always diagonal and the evolution operator is unity. The meaning is, in the absence of vector mesons we expect a relation like the following:

$$\begin{aligned} \langle \mathcal{Q}_-(M) \rangle &= 1 \times \left[\langle \mathcal{Q}_-(0) \rangle = 0 \right] + \eta_{-7}(M) \langle \mathcal{Q}_7(0) \rangle \\ \langle \mathcal{Q}_7(M) \rangle &= \langle \mathcal{Q}_7(0) \rangle + \left[\eta_{7-}(M) = 0 \right] \times \left[\langle \mathcal{Q}_-(0) \rangle = 0 \right] \end{aligned} \quad (4.0.5)$$

⁴Check Eq. (3.1.13)

Notice that there are two zeroes in the above equations, the first one is due to the fact that $\langle \mathcal{Q}_-(0) \rangle$ requires a photon exchange that, in the absence of vector resonances, can only occur at one loop⁵ while the other one is $\eta_{7-}(M) = 0$ because $\langle \mathcal{Q}_7 \rangle$ does not evolve and hence cannot have a scale dependence. Where $\eta_{ij}(M)$ is the off-diagonal mixing coefficient that connects $\langle \mathcal{Q}_i \rangle(M)$ with $\langle \mathcal{Q}_j(0) \rangle$. So we have:

$$\eta_{--}, \eta_{77} = 1, \quad \eta_{-7} \neq 0, \quad \eta_{7-} = 0 \quad (4.0.6)$$

So in general (with or without vectors) we will have the following mixing among matrix elements:

$$\begin{pmatrix} \langle \mathcal{Q}_-(M) \rangle \\ \langle \mathcal{Q}_7(M) \rangle \end{pmatrix} = \begin{pmatrix} 1 & \eta_{-7}(M) \\ 0 & 1 \end{pmatrix} \begin{pmatrix} \langle \mathcal{Q}_-(0) \rangle \\ \langle \mathcal{Q}_7(0) \rangle \end{pmatrix} \quad (4.0.7)$$

When we implement this to the amplitude given by Eq. (4.0.3) we get:

$$\mathcal{A}(K \rightarrow \pi e^+ e^-) = \frac{G_8}{g_8} \left\{ \tilde{C}_-(M) \langle \mathcal{Q}_-(0) \rangle + \left[\tilde{C}_-(M) \eta_{-7}(M) + \tilde{C}_7(M) \right] \langle \mathcal{Q}_7(0) \rangle \right\} \quad (4.0.8)$$

Next step is to follow the BBG scheme, that is writing down the loop matrix elements in terms of the tree level ones and extract the coefficient η_{-7} relevant in our case, which of course will contain the M dependence and at least the chiral logarithm, so even at this point looking at the above amplitude we can understand how the cancellation of scales will look like.

Scale Cancellation

As we discussed in the previous chapter that \mathcal{Q}_7 involves a conserved current and hence its matrix element cannot have a scale dependence but its Wilson coefficient $\tilde{C}_7(M)$ is scale dependent, hence to have a scale independent amplitude the scale dependence of \tilde{C}_7 must be cancelled by the total scale dependence of $\tilde{C}_7(M) \langle \mathcal{Q}_-(M) \rangle$.

⁵ $O(p^2)$ level must be understood because in BBG scheme we do not have higher order local operators.

That asks for a mixing of the matrix elements of \mathcal{Q}_- and \mathcal{Q}_7 . This is because, as counting of logarithms go,

$$\tilde{C}_-(M) \log M^2 \sim \tilde{C}_7(M) \quad (4.0.9)$$

Hence we must have:

$$\eta_{-7}(M) \sim \log M^2 \quad (4.0.10)$$

to have a cancellation of scale dependence of $C_7(M)$. This already tells us that Eq. (4.0.9) will be the form of the mixing coefficient η_{-7} . And this is expected because the mixing coefficient arises from the matrix elements in ChPT which will of course provide the so called chiral log.

4.0.5 $K^+ \rightarrow \pi^+ e^+ e^-$ Matrix Elements (No Vectors)

Tree Level Matrix Elements

As we already said there is only one tree level matrix element that is $\langle \mathcal{Q}_7 \rangle$ so let us calculate it. Considering the bosonized form of it from Eq. (4.0.1) and using the Feynman rule given by Eq. (A.3.23) we can directly write down the matrix element:

$$\langle \mathcal{Q}_7(0) \rangle = -\alpha_e [\bar{u}(p_-)(\not{k} + \not{p})v(p_+)] \quad (4.0.11)$$

One Loop Matrix Elements

This will be essentially a continuation of the calculation paused in section 2.7.2 of Chapter 2, the only difference is that we will be using cut-off regularization and instead of form factor, we will focus on the matrix element of \mathcal{Q}_- . Bosonized \mathcal{Q}_- in the context of this decay process has exactly the same structure as that of the one given by usual weak chiral Lagrangian Eq. (2.7.73) hence all the tricks of section 2.7.2 of Chapter 2 perfectly applies. In fact we do not have to calculate anything new, we can plug Eq. (2.7.87) into Eq. (2.7.76) applying the following substitutions:

$$B_{21}(q^2, m^2) \mapsto B_{21}(M^2, q^2, m^2)$$

where the new argument M^2 signals the cut-off scheme. The integrals are from Appendix B, given by Eq. (B.3.26) or (B.3.31) in NCR or SPCR schemes respectively, which comes down to choosing a value of θ , which is the only difference among DR ($\theta = 0$), NCR ($\theta = 5/18$) and SPCR ($\theta = 1/6$) schemes. We drop the coefficient G_8 , because we are calculating matrix element and not the amplitude, finally we write down the one loop matrix element of \mathcal{Q}_- as:⁶

$$\begin{aligned} \langle \mathcal{Q}_-(M) \rangle_{loop} &= \frac{\alpha_e}{4\pi} [\bar{u}(p_-)(\not{k} + \not{p})v(p_+)] \\ &\times \left\{ \chi(z/r_\pi^2) + \chi(z) + \frac{1}{6} \log \left[\left(1 + \frac{M^2}{m_\pi^2}\right) \left(1 + \frac{M^2}{m_K^2}\right) \right] - 2\theta \right\} \end{aligned} \quad (4.0.12)$$

And so the complete matrix element takes the form:

$$\begin{aligned} \langle \mathcal{Q}_-(M) \rangle &= \langle \mathcal{Q}_-(0) \rangle + \frac{\alpha_e}{4\pi} [\bar{u}(p_-)(\not{k} + \not{p})v(p_+)] \\ &\times \left\{ \chi(z/r_\pi^2) + \chi(z) + \frac{1}{6} \log \left[\left(1 + \frac{M^2}{m_\pi^2}\right) \left(1 + \frac{M^2}{m_K^2}\right) \right] - 2\theta \right\} \end{aligned} \quad (4.0.13)$$

Comparing Eq. (4.0.11) and Eq. (4.0.13) we can write down the following relation:

$$\langle \mathcal{Q}_-(M) \rangle = \langle \mathcal{Q}_-(0) \rangle + \eta_{-\tau}(M, z) \langle \mathcal{Q}_\tau(0) \rangle \quad (4.0.14)$$

Of course $\langle \mathcal{Q}_-(0) \rangle = 0$ in this case and,

$$\eta_{-\tau}(M, z) = -\frac{1}{4\pi} \left\{ \chi(z/r_\pi^2) + \chi(z) + \frac{1}{6} \log \left[\left(1 + \frac{M^2}{m_\pi^2}\right) \left(1 + \frac{M^2}{m_K^2}\right) \right] - 2\theta \right\} \quad (4.0.15)$$

Crucial Remark I: $\eta_{-\tau}(M, z)$ must not be seen as a Wilson-like long distance coefficient yet because it involves the photon transfer-momentum $z = q^2/m_k^2$, but the relation Eq. (4.0.14) should be seen as an evolution of matrix elements and not an operator level evolution equation that can be applied outside the context of the

⁶ $O(m_i^2/M^2)$ corrections in the loop integrals are neglected.

decay process considered. But if one wishes to extract the long distance anomalous matrix element as discussed in section 3.2.2 of Chapter 3, one will have to consider the appropriate scale for q^2 inside this coefficient η_{-7} and the z in the $\langle Q(0) \rangle$ should not be touched. This is in the spirit of BBG, where they took the chiral limit in the long distance mixing coefficients $c_{1,2}$ (Eq. (3.2.58)) but did not take this limit in the matrix elements. Because we are interested in the amplitude and hence matrix elements only, we do not intend to obtain an operator level evolution equation⁷ and hence we can keep the z dependence in the coefficient η_{-7} .

Crucial Remark II: It is clear that η_{-7} does not have a quadratic dependence in M , it has only log (which of course is needed based on the argument of section 4.0.4), therefore a long and short distance BBG-matching apparently is not possible. But actually that is not the case, we have to look at Eq. (3.2.57) to realize that M^2 can only appear at the next to leading order in large N correction. What we did so far is just the leading order calculation which is $O(f^0 \sim N^0)$ (because $K \rightarrow \pi\gamma^*$ amplitude starts at one loop in $O(p^2)$ chiral Lagrangian as we discussed in section 2.7.2 of Chapter 2) hence we have to include the $1/N$ corrections and only then we can expect a quadratic divergence. $1/N$ corrections can arise from three places, (i) Wavefunction renormalization⁸ factor $\sqrt{Z_K Z_\pi}$ given by Eq. (2.4.50), (ii) correction of the $K\pi\pi\pi$, $KKK\pi$ vertices in the diagram shown in Fig. (2.7) which can enter naturally through the BBG's evolution operator $\mathcal{E}_-(M^2)$ coming from $K\pi\pi$ analysis. (iii) Pion and Kaon electromagnetic form factor correction to the $\pi^+\pi^-\gamma^*$, $K^+K^-\gamma^*$ vertices given by Eq. 2.4.51. That is⁹

$$\eta_{-7}(M, z) \mapsto \eta_{-7}(M, z) (F_0(M^2) + z F_1(M^2)) \quad (4.0.16)$$

This of course does not enter the $\langle Q_7(0) \rangle$. But one must understand that these M^2 and/or accompanying extra logarithms do not spoil the cancellation of log argument

⁷Check Eq. (4.0.7) that we kept the mixing at the $K \rightarrow \pi e^+ e^-$ matrix element level.)

⁸Which of course in the leading order is unity.

⁹Please check Eq. (2.4.56) for $F_{0,1}$.

discussed section 4.0.4 because these extra corrections are sub-leading in large N . In the present case the whole coefficient η_{-7} is coming from the pion and kaon loop hence we can plug $\mathcal{E}(M^2)$ with it to obtain the quadratic divergence, which can also be viewed as a $K\pi\pi\pi$ and $KKK\pi$ vertex-corrections. Hence the next extension:

$$\eta_{-7}(M, z) \mapsto \mathcal{E}_-(M^2)\eta_{-7}(M, z) \quad (4.0.17)$$

A remark on g_8

Based on Eq. 4.0.17) and considering the Lagrangian given by Eq. (4.1.58) we can predict the scale dependence of g_8 (defined in Eq. (A.3.25)):

$$g_8(M) = \mathcal{E}_-(M^2) \tilde{C}_-(M) \quad (4.0.18)$$

This precisely gives the running of g_8 and is shown in Fig. 4.1.

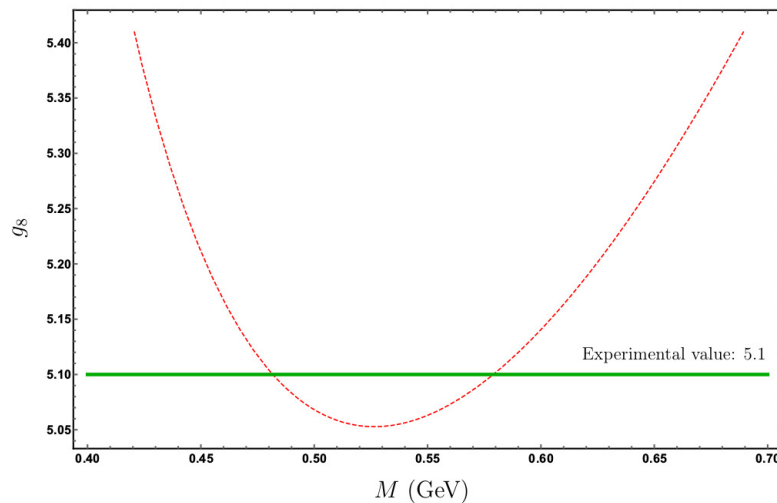


Figure 4.1: Variation of g_8 with scale M (in GeV).

Around the ρ mass (0.775 GeV) we have $g_8 \simeq 5.4$.

The Amplitude and a, b Parameters

Now that we have η_{-7} we can directly write down the amplitude using Eq. (4.0.8) and multiplying with the wavefunction renormalization (WFR) factors¹⁰:

$$\mathcal{A}(K \rightarrow \pi e^+ e^-) = \frac{G_8}{g_8} \left\{ \left[\tilde{C}_-(M) \mathcal{E}_-(M^2) \eta_{-7}(M, z) (F_0(M^2) + z F_1(M^2)) + \tilde{C}_7(M) \right] \langle \mathcal{Q}_7(0) \rangle \right\} \sqrt{Z_K Z_\pi} \quad (4.0.19)$$

where we have used $\langle \mathcal{Q}_-(0) \rangle = 0$. By comparing this with Eq. (2.7.76) and inserting $\langle \mathcal{Q}_7(0) \rangle$ from Eq. (4.0.11) we can obtain the form factor:

$$W_+(M^2, z) = -m_K^2 \frac{G_8}{g_8} \left(4\pi \tilde{C}_-(M) \mathcal{E}_-(M^2) \eta_{-7}(M, z) (F_0(M^2) + z F_1(M^2)) + 4\pi \tilde{C}_7 \right) \sqrt{Z_K Z_\pi}$$

(4.0.20)

Now that we have the full form factor we can look back to section 2.7.3 of Chapter 2 and try to predict the phenomenological parameters a and b introduced by D'Ambrosio *et al.* [3]. But fore the sake of completeness let us end this section by writing down the spectrum of the dilepton invariant mass:

$$\frac{d\Gamma}{dz} = \frac{\alpha_e^2 m_K}{12\pi(4\pi)^4} \lambda^{3/2}(1, z, r_\pi^2) \sqrt{1 - 4\frac{r_e^2}{z}} \left(1 + 2\frac{r_e^2}{z} \right) |W_+(M^2, z)|^2 \quad (4.0.21)$$

where $\lambda(a, b, c) = a^2 + b^2 + c^2 - 2(ab + bc + ca)$ and $4r_e^2 \leq z \leq (1 - r_\pi)^2$. Eq. (4.0.21) is unusual because it is apparently scale dependent ! But actually it is not, at this moment we can just insist that scale dependence of $\tilde{C}_-(M) \mathcal{E}_-(M) \langle \mathcal{Q}_-(0) \rangle$ conspire with $\tilde{C}_7 \langle \mathcal{Q}_7 \rangle$ to kill the scale dependence of the form factor, in fact this will be our demand to achieve the matching scale $\mu = M$ and the a and b parameters will play

¹⁰WFR factors are given in Eq. (2.4.50)

the fundamental role in this game. So let us proceed to extract the values of these parameters.

4.0.6 a Parameter and LD-SD Matching

To extract the these two parameters [3] introduced in Eq. (2.7.89) of Chapter 2, we must be careful because everything was calculated there in dimensional regularization and dispersive method but here we have ‘‘apparent’’ cut-off (M) dependence, so we expanded both $W_+(z)$ defined in Eq. (2.7.89) and our form factor $W_+(M^2, z)$ given by Eq. (4.0.20) in powers of z and equate the coefficients. To compare the coefficients we first expand their form factor given in Eq. (2.7.89), (2.7.90) and (2.7.93):

$$W_+(z) \underset{z \rightarrow 0}{\sim} G_F m_K^2 a_+ + \left(G_F m_K^2 b_+ + \frac{3r_\pi^2(\alpha_+ - \beta_+) - \beta_+}{180r_\pi^6} \right) z \quad (4.0.22)$$

And we expand also $W(M^2, z)$:

$$\begin{aligned} W_+(M^2, z) \underset{z \rightarrow 0}{\sim} & -m_K^2 \frac{G_8}{g_8} \left(4\pi \tilde{C}_-(M) \mathcal{E}_-(M^2) \eta_{-\tau}(M, 0) F_0(M^2) + 4\pi \tilde{C}_7 \right) \sqrt{Z_K Z_\pi} \\ & - m_K^2 \frac{G_8}{g_8} \left(4\pi \tilde{C}_-(M) \mathcal{E}_-(M^2) \eta_{-\tau}(M, 0) F_1(M^2) \right) \sqrt{Z_K Z_\pi} \\ & - m_K^2 \frac{G_8}{g_8} \left(\tilde{C}_-(M) \mathcal{E}_-(M^2) \sqrt{Z_K Z_\pi} \frac{(1 + r_\pi^2)}{60r_\pi^2} \right) z \end{aligned} \quad (4.0.23)$$

Comparing the coefficients of z in Eq. (4.0.22) and (4.0.23) we obtain a_+ :

$$a_+(M^2) = -\frac{4\pi V_{us}^* V_{ud}}{\sqrt{2}} \left(\tilde{C}_-(M) \mathcal{E}_-(M^2) \eta_{-\tau}(M, 0) F_0(M^2) + \tilde{C}_7 \right) \sqrt{Z_K Z_\pi} \quad (4.0.24)$$

and,

$$\begin{aligned} b_+(M^2) = & -\frac{V_{us}^* V_{ud}}{\sqrt{2}} \left(\tilde{C}_-(M) \mathcal{E}_-(M^2) \frac{(1 + r_\pi^2)}{60r_\pi^2} \right) \sqrt{Z_K Z_\pi} \\ & -\frac{V_{us}^* V_{ud}}{\sqrt{2}} \left(4\pi \tilde{C}_-(M) \mathcal{E}_-(M^2) \eta_{-\tau}(M, 0) F_1(M^2) \right) \sqrt{Z_K Z_\pi} \\ & -\frac{3r_\pi^2(\alpha_+ - \beta_+) - \beta_+}{G_F m_K^2 180r_\pi^6} \end{aligned} \quad (4.0.25)$$

where we have used Eq. (2.5.64) and the expansion of $\eta_-(M, z)$ around $z = 0$:

$$\begin{aligned} \eta_-(M, z) &\underset{z \rightarrow 0}{\simeq} \eta_-(M, 0) - \frac{1}{4\pi} \frac{z}{60r_\pi^2} (1 + r_\pi^2) \\ \eta_-(M, 0) &= -\frac{1}{4\pi} \left\{ \frac{1}{6} \log \left[\left(1 + \frac{M^2}{m_\pi^2}\right) \left(1 + \frac{M^2}{m_K^2}\right) \right] - 2\theta \right\} \end{aligned} \quad (4.0.26)$$

Let us put the final formulas inside a box:

$$\begin{aligned} a_+(M^2) &\simeq -\frac{4\pi V_{us}^* V_{ud}}{\sqrt{2}} \left(\tilde{C}_-(M) \mathcal{E}_-(M^2) \eta_{-\gamma}(M, 0) F_0(M^2) + \tilde{C}_\gamma \right) \sqrt{Z_K Z_\pi} \\ b_+(M^2) &\simeq -\frac{V_{us}^* V_{ud}}{\sqrt{2}} \frac{\tilde{C}_-(M) \mathcal{E}_-(M^2)}{60r_\pi^2} \sqrt{Z_K Z_\pi} \\ &\quad - \frac{V_{us}^* V_{ud}}{\sqrt{2}} \left(4\pi \tilde{C}_-(M) \mathcal{E}_-(M^2) \eta_{-\gamma}(M, 0) F_1(M^2) \right) \sqrt{Z_K Z_\pi} \\ &\quad - \frac{3r_\pi^2 (\alpha_+ - \beta_+) - \beta_+}{G_F m_K^2 180r_\pi^6} \end{aligned}$$

(4.0.27)

In the above formulas we have dropped r_π^2 in comparison to 1 and also $O(m_{K,\pi}^2/M^2)$ corrections have been neglected. Due to the product of wavefunction renormalization factors and $\mathcal{E}_-(M^2)$, $1/f^4$ term will also appear but for consistency we have to keep terms up to $1/f^2$ only. Notice that a_+ and b_+ are written with explicit M dependence which is of course superficial and will disappear due to the cancellation of scales displayed in Fig. (4.3) below.

Long and Short Distance Matching Through a_+

Schematically the matching can be represented by the diagram¹¹ shown in Fig. 4.2 shown below.

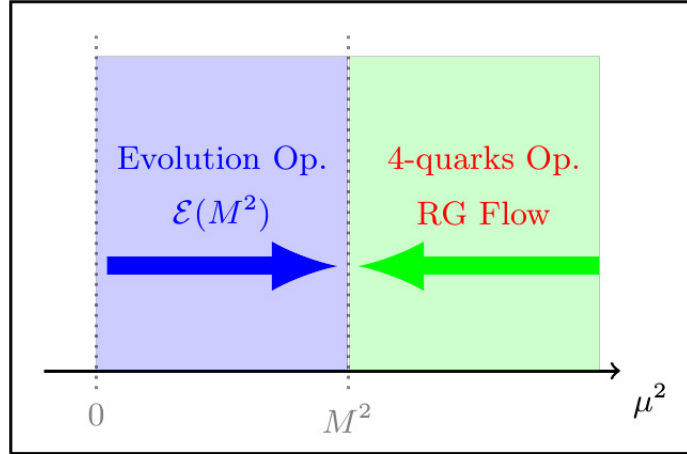


Figure 4.2: Schematic representation of LD-SD matching through a quadratic divergence.

The parameter a_+ is the value of the form factor at very low q^2 , hence demanding scale independence of the form factor can be achieved in the region where a_+ has extrema.

This gives the range of the matching scale in the range $M \simeq 0.9-1$ GeV which is much above the Bardeen, Buras and Gérard [4] matching scale $M = 0.7$ GeV (without vectors) ! But it is very clear from the figure that a_+ is almost scale independent in a much wider range that includes the BBG range, hence its value does not change much. Hence we can use the BBG scale to evaluate the parameters. Therefore, $a_+(0.7 \text{ GeV}) \simeq -0.17$ which is almost one third the experimental value 2.2. But $b_+(0.7 \text{ GeV}) \simeq 0.02$ which is basically the small kaon loop contribution factor $1/60!$ This can be blamed to the non-inclusion of vector resonances. Because vector exchange can generate a tree level \mathcal{Q}_- matrix element that presumably should

¹¹This diagram was produced by my colleague Dr. D. Greynat.

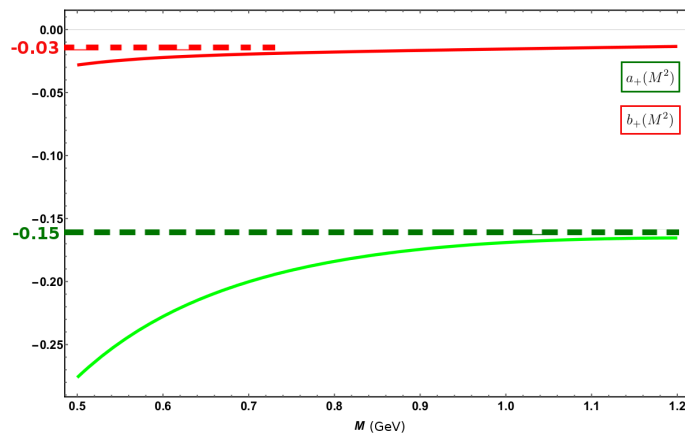


Figure 4.3: Long and short distance matching through $a_+(M^2)$. b_+ has been also shown (red) on this plot.

enhance both a_+ and b_+ . With this motivation we intend to include vectors in the next section.

4.1 Inclusion of Vector Meson Through Hidden Local Symmetry

The idea of massive vector mesons were well known even before QCD [5], in fact vector meson dominance [6] was based on this. But the notion that massive vector mesons can be actually gauge bosons, was never taken seriously even after the discovery of Higg's mechanism, because it was thought that they cannot be given mass through the spontaneous symmetry breaking. Finally Bando *et al.* [7, 8, 9, 10] had shown that a consistent description of massive vector mesons as gauge bosons of the Hidden Local Symmetry (HLS) is indeed possible. Present introduction is in the line of the elaborate review [11] where vector mesons were introduced as a nonlinear realization of the HLS, they had shown that a non-linear sigma model based on the coset space " G/H is equivalent to another model that has the symmetry group $G_{\text{global}} \times H_{\text{local}}$ ". They also review calculations showing that gauge bosons of the H_{local} (or the Hidden Symmetry) acquire kinetic terms through quantum effects

and become dynamical. We will mostly rely on a more recent and extensive review [12] (which is based on [11]) on HLS.

In the beginning of Chapter 2 we discussed how one can construct the Chiral Lagrangian from the non-linear realization of the coset space G/H where $G = SU(3)_L \times SU(3)_R$ and $H = SU(3)_V$, the well known fact stated in the last paragraph then tells us that there exists another equivalent model which has the symmetry $[SU(3)_L \times SU(3)_R]_{global} \times [SU(3)_V]_{local}$ and vector mesons can be accommodated in the later model as gauge bosons of the group $[SU(3)_V]_{local}$. This model does not have issues with the masses of the gauge bosons (vector mesons) because the masses arise through Higgs mechanism after fixing the (unitary) gauge of the hidden local group. Although the local hidden symmetry group breaks down and along with it breaks the global $[SU(3)_L \times SU(3)_R]_{global}$, the diagonal sum $[SU(3)_V]_{global}$ (light quark flavor symmetry) remains as a residual unbroken symmetry of the system.

4.1.1 Construction of The Lowest Order Lagrangian

In section 2.1.1 of the second chapter we discussed two special CCWZ parametrizations: Σ and ξ and we identified $\Sigma = \xi^2$, well this was a special case, in general Σ can be split into two quantities ξ_L and ξ_R as:

$$\Sigma = \xi_L^\dagger \xi_R \quad (4.1.28)$$

But even $\Sigma = \xi_L^\dagger \mathfrak{h}^\dagger(x) \mathfrak{h}(x) \xi_R$ would also be as good as the splitting defined in the above equation, so there is an ambiguity which can be understood as a local gauge freedom and the local transformation is nothing but an element of H_{local} . Considering the fact that $\Sigma \mapsto \mathfrak{g} \Sigma \mathfrak{g}^\dagger$ under the global chiral group if $\xi_{L,R}$ transform the following way under the full group $G_{global} \times H_{local}$:

$$\xi_{L,R}(x) \mapsto \mathfrak{h}(x) \xi_{L,R} \mathfrak{g}_{L,R} \quad (4.1.29)$$

where $\mathfrak{h}(x) \in H_{local}$ and $\mathfrak{g} \in G_{global}$. Under the above transformation splitting of Σ defined in Eq. (4.1.28) is ambiguous and this ambiguity is the hidden local symmetry

group $H_{local} = [SU(3)_V]_{local}$. ξ 's can be parametrized using CCWZ parametrization as:

$$\xi_L = \xi^\dagger e^{i\sigma/f_\sigma} \quad \xi_R = \xi e^{i\sigma/f_\sigma} \quad (4.1.30)$$

where $\xi = \exp[i\Pi/f]$ is of course the one defined in the second chapter (check sec. 2.1.1 of Chapter 2) with NG-Bosons $\Pi = \pi_a T^a$ of the broken global symmetry (G_{global}) while $\Sigma = \sigma_a T^a$ is the octet of NG-Bosons absorbed inside the gauge bosons of the local symmetry H_{local} . The ratio of the decay constants is defined as:

$$\frac{f_\sigma^2}{f^2} := \mathbf{a} \quad (4.1.31)$$

Invariants and The Leading Order Lagrangian

Two Maure-Cartan 1-forms can be built out of $\xi_{L,R}$ and they are the following:

$$\begin{aligned} \alpha_{\perp\mu} &= \frac{1}{2i} \left[(\partial_\mu \xi_R) \xi_R^\dagger - (\partial_\mu \xi_L) \xi_L^\dagger \right] \\ \alpha_{\parallel\mu} &= \frac{1}{2i} \left[(\partial_\mu \xi_R) \xi_R^\dagger + (\partial_\mu \xi_L) \xi_L^\dagger \right] \end{aligned} \quad (4.1.32)$$

And their transformations are:

$$\begin{aligned} \alpha_{\perp\mu} &\mapsto \mathfrak{h}(x) \alpha_{\perp\mu} \mathfrak{h}^\dagger \\ \alpha_{\parallel\mu} &\mapsto \mathfrak{h}(x) \alpha_{\parallel\mu} \mathfrak{h}^\dagger - i(\partial_\mu \mathfrak{h})(x) \mathfrak{h}^\dagger(x) \end{aligned} \quad (4.1.33)$$

Eq. (4.1.29) dictates the covariant derivative¹²

$$\mathcal{D}_\mu \xi_{L,R} = \partial_\mu \xi_{L,R} - i\mathcal{V}_\mu \xi_{L,R} \quad (4.1.34)$$

Where

$$\mathcal{V}_\mu = \mathcal{V}_{\mu a} T^a \quad (4.1.35)$$

¹²We used D as the covariant derivative of ChPT introduced in the Chapter 2 (Eq. (2.2.36)) that acts on Σ and we have used it so far before the introduction of HLS in this chapter. To avoid any confusion we will use the symbol \mathcal{D} for the covariant derivative of the HLS that act on ξ the way its defined here. Also the normalization is different than the one introduced in Eq. (3.3.68) in the BBG framework.

And they transform as:¹³

$$\mathcal{V}_\mu \mapsto \mathfrak{h}(x) \mathcal{V}_\mu \mathfrak{h}^\dagger - i(\partial_\mu \mathfrak{h}(x)) \mathfrak{h}^\dagger(x) \quad (4.1.36)$$

We can now use $\partial_\mu \mapsto \mathcal{D}_\mu$ in Eq. (4.1.32) to obtain their manifestly covariant form:

$$\begin{aligned} \hat{\alpha}_{\perp\mu} &= \frac{1}{2i} \left[(\mathcal{D}_\mu \xi_R) \xi_R^\dagger - (\mathcal{D}_\mu \xi_L) \xi_L^\dagger \right] \\ \hat{\alpha}_{\parallel\mu} &= \frac{1}{2i} \left[(\mathcal{D}_\mu \xi_R) \xi_R^\dagger + (\mathcal{D}_\mu \xi_L) \xi_L^\dagger \right] \end{aligned} \quad (4.1.37)$$

where

$$\hat{\alpha}_{\perp\mu} = \alpha_{\perp\mu}, \quad \hat{\alpha}_{\parallel\mu} = \alpha_{\parallel\mu} - \mathcal{V}_\mu \quad (4.1.38)$$

These covariantized quantities now transform homogeneously so invariant objects can be constructed in the most straight forward way. In the lowest order in derivatives we have the following two invariants (under $G_{global} \times H_{local}$):

$$\begin{aligned} \mathcal{L}_A &= f^2 \text{tr}[\hat{\alpha}_{\perp\mu} \hat{\alpha}_{\perp}^\mu] \\ \mathbf{a} \mathcal{L}_V &= f_\sigma^2 \text{tr}[\hat{\alpha}_{\parallel\mu} \hat{\alpha}_{\parallel}^\mu] = f_\sigma^2 \text{tr}[(\hat{\alpha}_{\parallel\mu} - \mathcal{V}_\mu)^2] \end{aligned} \quad (4.1.39)$$

The lowest order Lagrangian with full unbroken symmetry is then given by:

$$\mathcal{L}_{p^2}^{hls} = \mathcal{L}_A + \mathbf{a} \mathcal{L}_V - \frac{1}{2g_V^2} \text{tr}[\mathcal{V}_{\mu\nu} \mathcal{V}^{\mu\nu}] \quad (4.1.40)$$

If we are at very low energy scale (pion mass scale) then the vector mesons are frozen and hence the kinetic term for them can be dropped, in such a case the equation of motion for \mathcal{V}_μ is:

$$\mathcal{V}_\mu = \alpha_{\parallel\mu} \quad (4.1.41)$$

When this is substituted in Eq. (4.1.40), \mathcal{L}_V term disappear and \mathcal{L}_A is nothing but the usual ChPT Lagrangian in the absence of external fields, that is:

$$\mathcal{L}_A = \frac{f^2}{4} \text{tr}[\partial_\mu \Sigma \partial^\mu \Sigma^\dagger] \quad (4.1.42)$$

here we have shown (in a very sketchy way) how ChPT, which is based on the G_{global}/H_{global} is equivalent to the HLS Lagrangian which is built on $G_{global} \times H_{local}$.¹⁴

¹³Different normalization is used than the one used in Eq. (3.3.67)

¹⁴ $G = SU(3)_L \times SU(3)_R$ and $H = SU(3)_V$ was implied.

How do we know this is the physical vector meson ?

Physical ρ meson was defined in Eq. (7.3) of Weinberg's 1968 paper [13] and we will show how this transformation property arises naturally when one breaks the hidden local symmetry through (unitary) gauge fixing.

In the unitary gauge ($\sigma = 0$) we have:

$$\xi_R = \xi_L^\dagger = \xi = \exp[i\Pi/f] \quad (4.1.43)$$

But this *sigma*-less form is not preserved, σ comes back when we do a general global transformation shown in Eq. (4.1.29) which after gauge fixing of the H_{local} takes the form:

$$\begin{aligned} G_{global} : \xi &\mapsto \xi' = \mathfrak{g}_L x i = \xi \mathfrak{g}_R^\dagger \\ &= \exp[\pm i\sigma'/f_\sigma] \exp[i\Pi'/f] \end{aligned} \quad (4.1.44)$$

So to maintain the covariance under G_{global} we need a simultaneous local transformation that exactly cancels the σ' -exponential factor, that is for each such transformation defined above an unique local transformation of the following form:

$$\mathfrak{h} \in H_{local} = \exp[i\sigma'(\Pi, \mathfrak{g}_R, \mathfrak{g}_L)/f_\sigma] = \mathfrak{h}(\Pi, \mathfrak{g}_R, \mathfrak{g}_L) \quad (4.1.45)$$

is required. The system will have a global symmetry under $SU(3)_L \times SU(3)_R$ under the transformation:

$$G_{global} : \xi \mapsto \mathfrak{h}(\Pi, \mathfrak{g}_R, \mathfrak{g}_L) \xi \mathfrak{h}^\dagger(\Pi, \mathfrak{g}_R, \mathfrak{g}_L) \quad (4.1.46)$$

The gauge field \mathcal{V}_μ (of H_{local}) transforms now as:

$$\begin{aligned} G_{global} : \mathcal{V}_\mu &\mapsto \mathfrak{h}(\Pi, \mathfrak{g}_R, \mathfrak{g}_L) \mathcal{V}_\mu \mathfrak{h}^\dagger(\Pi, \mathfrak{g}_R, \mathfrak{g}_L) \\ &\quad - i[\partial_\mu \mathfrak{h}(\Pi, \mathfrak{g}_R, \mathfrak{g}_L)] \mathfrak{h}^\dagger(\Pi, \mathfrak{g}_R, \mathfrak{g}_L) \end{aligned} \quad (4.1.47)$$

Which is Weinberg's ρ meson and so in the unitary gauge of HLS we indeed have a theory of physical ρ meson. Now that it has been identified we can assign the physical particles namely:

$$V_\mu = \mathcal{V}_\mu/g_V = \frac{1}{\sqrt{2}} \begin{pmatrix} (\rho_\mu^0 + \omega_\mu)/\sqrt{2} & \rho_\mu^+ & K_\mu^{*+} \\ \rho_\mu^- & (-\rho_\mu^0 + \omega_\mu)/\sqrt{2} & K_\mu^{*0} \\ K_\mu^{*-} & \bar{K}_\mu^{*0} & \phi_\mu \end{pmatrix} \quad (4.1.48)$$

where we have switched to V_μ ¹⁵. from \mathcal{V}_μ .

We can now use the gauge fixed variables from Eq. (4.1.43) and substitute them in Eq. (4.1.40) to obtain the final form of the leading order Lagrangian that we are going to use:

$$\mathcal{L}^A = -\frac{f^2}{4} \text{tr} \left[(\mathcal{D}_\mu \xi^\dagger \xi - \mathcal{D}_\mu \xi \xi^\dagger)^2 \right] \quad (4.1.49)$$

$$\mathcal{L}^V = -\frac{f^2}{4} \text{tr} \left[(\mathcal{D}_\mu \xi^\dagger \xi + \mathcal{D}_\mu \xi \xi^\dagger)^2 \right] \quad (4.1.50)$$

where the final Lagrangian is the sum of the above two pieces and given by Eq. (4.1.40). Before we start the calculations it is crucial to specify the counting rules which are:

$$\begin{aligned} \mathfrak{a} f^2 &= f_\sigma^2 \sim O(p^0) \\ g_V &\sim O(p) \\ m_V^2 &\sim O(p^2) \\ \mathcal{V}_\mu &\sim O(p^0) \end{aligned} \quad (4.1.51)$$

We must also introduce the covariant derivative in terms of the external sources:

$$\begin{aligned} \mathcal{D}_\mu \xi &= \partial_\mu \xi - i g_V V_\mu \xi + i \xi r_\mu \\ \mathcal{D}_\mu \xi^\dagger &= \partial_\mu \xi^\dagger - i g_V V_\mu \xi^\dagger + i \xi^\dagger l_\mu \end{aligned} \quad (4.1.52)$$

Photon and W -bosons are introduced in the usual manner:

$$\begin{aligned} l_\mu &= -e Q \mathcal{A}_\mu - \frac{g_2}{2} W_\mu \\ r_\mu &= -e Q \mathcal{A}_\mu \end{aligned} \quad (4.1.53)$$

Following the procedure used in section 3.2.2 of the previous chapter we can identify the left current that couples to W -boson both in Eq. (2.5.59) and (4.1.40) and can extract it:

$$\mathcal{L}_\mu^{hls} = \mathcal{L}_\mu^A + \mathfrak{a} \mathcal{L}_\mu^V \quad (4.1.54)$$

¹⁵ V_μ was used in Chapter 3 for example check Eq. (3.3.67), (3.3.68) and (3.3.69).

Where,

$$\begin{aligned} [\mathcal{L}_\mu^A]_{ij} &= -\frac{if^2}{2} \left[\xi \left((\partial_\mu \xi^\dagger) \xi - (\partial_\mu \xi) \xi^\dagger \right) \xi^\dagger - i e \mathcal{A}_\mu [Q \Sigma^\dagger, \Sigma] \right]_{ji} \\ [\mathcal{L}_\mu^V]_{ij} &= -\frac{if^2}{2} \left[\xi \left((\partial_\mu \xi^\dagger) \xi + (\partial_\mu \xi) \xi^\dagger \right) \xi^\dagger - i e \mathcal{A}_\mu \{Q \Sigma^\dagger, \Sigma\} \right]_{ji} \\ &\quad - g_V f^2 \left[\xi V_\mu \xi^\dagger \right]_{ji} \end{aligned} \quad (4.1.55)$$

Total current can be cast into more transparent form:

$$[\mathcal{L}_\mu^{hls}]_{ij} = \frac{if^2}{2} (1 - \mathbf{a}) [(D_\mu \Sigma) \Sigma^\dagger]_{ji} + i \mathbf{a} f^2 [(\mathcal{D}_\mu \xi) \xi^\dagger]_{ji} \quad (4.1.56)$$

Based on the arguments of Bardeen, Buras and Gèrards [14] we can bosonize the operators Using these currents in the same manner as we explained in Chapter 3:

$$\begin{aligned} \mathcal{Q}_-^{hls} &= 4 \left\{ [\mathcal{L}_\mu^{hls}]_{31} [\mathcal{L}^{hls\mu}]_{12} - [\mathcal{L}_\mu^{hls}]_{32} [\mathcal{L}^{hls\mu}]_{11} \right\} \\ \mathcal{Q}_7^{hls} &= 2 \alpha_e [\mathcal{L}_\mu^{hls}]_{32} [\bar{e} \gamma^\mu e] \end{aligned} \quad (4.1.57)$$

And finally plug them into the $\Delta S = 1$ Lagrangian given by Eq. (4.0.2).¹⁶:

$$\mathcal{L}_{hls}^{\Delta S=1} = \frac{G_8}{g_8} \left[\tilde{C}_-(M) \mathcal{Q}_-^{hls}(M) + \tilde{C}_7(M) \mathcal{Q}_7^{hls} \right] + h.c \quad (4.1.58)$$

Once again the amplitude can be cast into the form similar to the one given by Eq. (4.0.8):

$$\mathcal{A}(K \rightarrow \pi e^+ e^-) = \frac{G_8}{g_8} \left\{ \tilde{C}_-(M) \langle \mathcal{Q}_-^{hls}(0) \rangle + \left[\tilde{C}_-(M) \eta_{-7}^{hls}(M, z) + \tilde{C}_7(M) \right] \langle \mathcal{Q}_7^{hls}(0) \rangle \right\} \quad (4.1.59)$$

where we have used the evolution equations:

$$\begin{aligned} \langle \mathcal{Q}_-^{hls}(M) \rangle &= \langle \mathcal{Q}_-^{hls}(0) \rangle + \eta_{-7}^{hls}(M, z) \langle \mathcal{Q}_7^{hls}(0) \rangle \\ \langle \mathcal{Q}_7^{hls}(M) \rangle &= \langle \mathcal{Q}_7^{hls}(0) \rangle + 0 \end{aligned} \quad (4.1.60)$$

¹⁶To avoid confusion we re-write the effective Lagrangian here tagging it with “hls”.

The only difference this time is that the diagonal evolution of $\langle \mathcal{Q}_- \rangle$ exists or simply put $\langle \mathcal{Q}_-^{hls}(0) \rangle \neq 0$, along with the usual mixing with $\langle \mathcal{Q}_7^{hls}(0) \rangle$ discussed in the last section. We expect an extension of the mixing coefficient in the following manner:

$$\eta_{-7}(M, z) \mapsto \eta_{-7}^{hls}(M, z) = \eta_{-7}(M, z) + \eta^V(M, z) \quad (4.1.61)$$

where the extra piece will encode the vector contributions to the mixing. Before we actually calculate it, we can have an idea about how this parameter should look like based on the argument of scale cancellation discussion in section Let us now repeat the steps of the last section but fortunately we will see that we will need to calculate only one diagram which is just the tree level matrix element of \mathcal{Q}_- , some of the other new diagrams can be shown to be non-contributing or identically zero and the rest can be built out of the one loop calculation of the last chapter based on arguments alone.

4.1.2 $K^+ \rightarrow \pi^+ e^+ e^-$ Matrix Elements (With Vectors)

Tree Level Matrix Elements

As we said earlier and is well known that vector resonances induce a non-zero tree level matrix element of \mathcal{Q}_- , then we also have $\langle \mathcal{Q}_7(0) \rangle$, so we have these two tree level matrix elements to take care.

Tree Level \mathcal{Q}_-^{hls} Matrix Element

There are two diagrams that contributes to $\langle \mathcal{Q}_7^{hls} \rangle$, one involves no vectors shown in Fig. (4.4), which in ChPT was zero but its presence here does not violate gauge invariance, in fact this diagram ensures gauge invariance, it combines with the Type-II^{hls} diagram shown in Fig. (4.5) to cancel the overall q^2 independent part and produces the final gauge invariant result. So we can apply the trick of Chapter 2, that is subtracting from Type-II^{hls} its $q^2 \rightarrow 0$ limit and obtain the complete result but we will not do it here because of two reasons:

1. Naturally one will be suspicious of the non-vanishing contribution of the diagram shown in Fig. (4.4), in the context of ChPT. So we need to prove that there is nothing spooky here inside HLS.
2. This proof will be valid off-shell which means we can apply this vertex even in the loop diagrams without thinking about violating ethics.

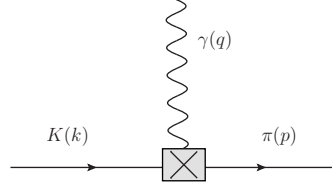


Figure 4.4: Type-I^{hls} diagram contributing to $\langle Q_-^{hls} \rangle$ in HLS.

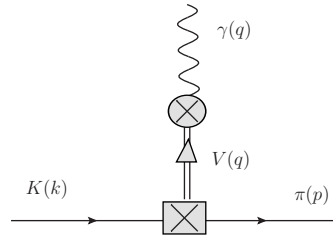


Figure 4.5: Type-II^{hls} diagram contributing to $\langle Q_-^{hls} \rangle$ in HLS. V stands for ρ , ω and ϕ

Using the vertices given by Eq. (A.5.34) and (A.6.45) from Appendix A¹⁷ we get the following contribution of Fig. 4.5:

$$\langle \pi^+ \gamma^* | Q_-^{hls}(0) | K^+ \rangle_{II} = e \epsilon^* \cdot (k + p) \mathbf{a} f^2 \left(\frac{2\mathbf{a} - 1}{3} \right) \frac{m_V^2}{m_V^2 - q^2} \quad (4.1.62)$$

where we have used the vector meson mass:

$$m_V^2 = \mathbf{a} f^2 g_V^2 \quad (4.1.63)$$

¹⁷We drop the factors \tilde{G}_8 because we are interested in matrix element of Q_-^{hls} and not in full amplitude.

And using Eq. (A.6.47) we calculate the matrix element corresponding to the diagram given in Fig. 4.4:

$$\langle \pi^+ \gamma^* | \mathcal{Q}_-^{hls}(0) | K^+ \rangle_I = -e \epsilon^* \cdot (k + p) \mathbf{a} f^2 \left(\frac{2\mathbf{a} - 1}{3} \right) \quad (4.1.64)$$

Adding Eq. (4.1.62) and (4.1.64) we find the full tree level contribution for $K^+ \rightarrow \pi \gamma$:

$$\langle \pi^+ \gamma^* | \mathcal{Q}_-^{hls}(0) | K^+ \rangle_{total} = e \epsilon^*(q) \cdot (k + p) \frac{2\mathbf{a} - 1}{3} \frac{z}{r_V^2 - z} \mathbf{a} f^2 \quad (4.1.65)$$

So this completes the proof that non- q^2 terms gets cancelled when the two diagrams added and the complete result is gauge invariant.

Now we can use Eq. (4.1.65) to obtain the final matrix element of interest:

$$\begin{aligned} \langle \mathcal{Q}_-^{hls}(0) \rangle &= \langle \pi^+ e^+ e^- | \mathcal{Q}_-(0) | K^+ \rangle \\ &= -\alpha_e [\bar{u}(p_-)(\not{k} + \not{p})v(p_+)] \frac{8\pi f^2}{m_V^2} F_V(z) \end{aligned} \quad (4.1.66)$$

where we have used $\mathbf{a} = 2$ and the definition of $F_V(z)$ given in Eq. (2.7.92).

Tree Level \mathcal{Q}_7 Matrix Element

As argued in section A.5.1 of Appendix A that the vertex due to \mathcal{Q}_7 just receives a factor of $F_V(z)$, hence using Eq. (A.5.39) we have:

$$\langle \mathcal{Q}_7^{hls}(0) \rangle = -\alpha_e [\bar{u}(p_-)(\not{k} + \not{p})v(p_+)] F_V(z) \quad (4.1.67)$$

We summarize the tree level matrix elements in our HLS based scheme:

$$\begin{aligned} \langle \mathcal{Q}_7^{hls}(0) \rangle &= -\alpha_e [\bar{u}(p_-)(\not{k} + \not{p})v(p_+)] F_V(z) \\ \langle \mathcal{Q}_-^{hls}(0) \rangle &= -\alpha_e [\bar{u}(p_-)(\not{k} + \not{p})v(p_+)] \frac{8\pi f^2}{m_V^2} F_V(z) \end{aligned} \quad (4.1.68)$$

Matching With Just Tree Level In Vectors ?

This is a right place to pause for a while and ask if it is possible to do the matching and calculate the a_+ and b_+ considering just the tree level contributions of vectors !

If we pause at tree level in vectors, and of course the earlier chiral loop (but without any vectors attached), we will not have the η^V introduced in Eq. (4.1.61) because $\eta^V(M, z)$ is the vector contribution to the $\langle \mathcal{Q}_- \rangle$ - $\langle \mathcal{Q}_7 \rangle$ mixing which can only appear if we consider vector involved loop diagrams. But there is another problem: due to the absolute vector meson dominance in the pion-pion and kaon-kaon electromagnetic form factors, “just a chiral loop” (Fig. 2.7) vanishes for $\mathbf{a} = 2$, because¹⁸

$$\begin{aligned}\mathcal{L}_{\pi^+\pi^-\gamma} &\propto (\mathbf{a} - 2) \\ \mathcal{L}_{K^+K^-\gamma} &\propto (\mathbf{a} - 2)\end{aligned}\tag{4.1.69}$$

Therefore we do not even have usual vector-less mixing coefficient $\eta_{-7}(M, z)$ defined in Eq. (4.0.5), therefore in view of the discussion in section 4.0.4 (Eq. (4.0.9,4.0.10)) nothing to cancel the scale of \tilde{C}_7 ! Therefore it is absolutely necessary that when we include vectors we must include at least loops with vectors attached such as the one shown in Fig. 4.9. On the other hand the same scale cancellation argument once again tells us how the $\eta^V(M, z)$ should look like. It must be of the following form:

$$\eta^V(M, z) \sim \log M^2 \left[\eta_0(m_\pi^2, m_K^2, m_V^2) + z \eta_1(m_\pi^2, m_K^2, m_V^2) + \dots \right]\tag{4.1.70}$$

Logarithm is essential based on the scale cancellation argument (Eq. (4.0.9)) while phenomenologically we know that a_+ and b_+ parameters must be enhanced by vectors, clearly η_0 will enhance a_+ and η_1 will enhance b_+ . Let us now explicitly calculate these constant coefficients (η_1, η_2) that supposedly should enhance a_i 's and b_i 's.

One Loop Matrix Element

Once again there is just \mathcal{Q}_- which will acquire a loop level matrix element. Before proving it explicitly let us claim that the result is the following:

$$\langle \mathcal{Q}_-^{hls}(M) \rangle_{loop} = \langle \mathcal{Q}_-(M) \rangle_{loop} \times F_V(z) + \Delta_\eta(M, z) \langle \mathcal{Q}_-^{hls}(0) \rangle\tag{4.1.71}$$

where $\langle \mathcal{Q}_-(M) \rangle_{loop}$ is the usual “without vector” matrix element given by Eq. (4.0.12)

¹⁸Please check Appendix A for details.

It is easy to see that our non-vector mixing coefficient will receive the following extension:

$$\eta_{-\gamma}(M, z) \mapsto \eta_{-\gamma}^{hls}(M, z) = \eta_{-\gamma}(M, z) + \frac{8\pi f^2}{m_V^2} (\Delta_\eta(M, z) - 1) \quad (4.1.72)$$

Therefore Eq. (4.1.61) tells us that

$$\eta^V(M, z) = \frac{8\pi f^2}{m_V^2} (\Delta_\eta(M, z) - 1) \quad (4.1.73)$$

One Loop \mathcal{Q}_-^{hls} Matrix Element: Proof Through Algebra of Diagrams

All the diagrams can be split into a few broad classes, let us call them Type-A,B,C... etc. Type-A diagrams are shown in Fig. (4.6), they are the $(\sqrt{Z_K} - 1)$ and $(\sqrt{Z_\pi} - 1)$ multiplied usual tree level matrix elements that we already have calculated but they will of course contribute to the η^V factor, so we write them down here as:

$$\begin{aligned} \langle \mathcal{Q}_-^{hls}(M) \rangle_A &= \langle \mathcal{Q}_-^{hls}(0) \rangle \left(\sqrt{Z_K} - 1 + \sqrt{Z_\pi} - 1 \right) \\ &= \langle \mathcal{Q}_-^{hls}(0) \rangle \left(\sqrt{Z_K Z_\pi} - 1 \right) + O(f^{-4}) \end{aligned} \quad (4.1.74)$$

Notice that we have subtracted 1 from $\sqrt{Z_{K,\pi}}$ because the 1 corresponds to tree level matrix element and here we are calculating only loop contributions. Then we have Type-B diagrams in Fig. (4.7) that are one of the usual ChPT Type-I diagrams (first two diagrams of Fig. 2.6) multiplied by $F_V(z)$ in the pion-pion-gamma (or kaon-kaon-gamma) vertex.

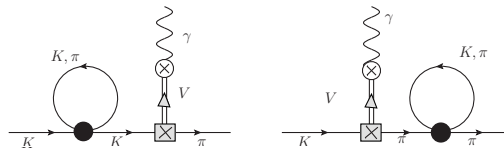


Figure 4.6: Type-A diagrams that just corrects the external meson propagators.

Then we have Type-C diagrams shown in Fig. 4.8, these upgrades the last diagram of Type-I (2.6) of the Chapter 2. The fourth kinds of diagrams are Type-D shown in Fig. 4.9, first and the last diagrams are zero because the $\pi\pi\gamma$ and $KK\gamma$ vertices

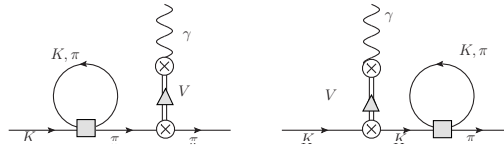


Figure 4.7: Type-B diagrams are just $F_V(z)$ corrected versions of first two diagrams of Type-I diagrams of ChPT.

come with a factor of $(1 - \alpha/2)$ so for $\alpha = 2$ they vanish. While the middle one is the usual ChPT times $F(z)$, this is because the $K\pi\pi\pi$ or $KKK\pi$ vertices are exactly the same as was before in non-vector case and is clear from the vertex rule given in Eq. (A.6.43). If we summarize this discussion into an equation, what it means is:

$$\text{Type-B} + \text{Type-C} = \text{Type-I} \times F_V(z) \quad (4.1.75)$$

And,

$$\text{Type-D} = \text{Type-II} \times F_V(z) \quad (4.1.76)$$

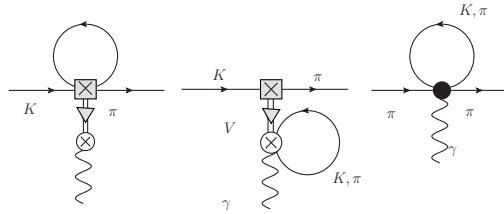


Figure 4.8: Type-C diagrams that upgrades the Type-I diagrams of ChPT.

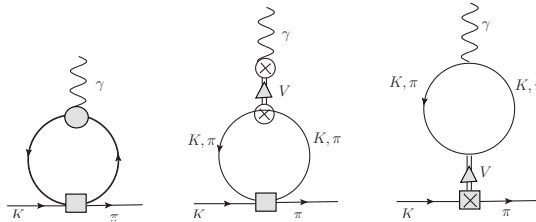


Figure 4.9: Type-D diagrams that upgrades the Type-II diagrams of ChPT.

where Type-I,II are the set of diagrams shown in Fig. 2.6, 2.7 respectively. As the whole structure of non-vector diagrams (Type-I and II) remains intact up to an

overall multiplicative function $F_V(z)$ we obtain an obvious update of our earlier result:

$$\langle \pi^+ \gamma^* | \mathcal{Q}_-^{hls}(M) | K^+ \rangle_D = \langle \pi^+ \gamma^* | \mathcal{Q}_-(M) | K^+ \rangle F_V(z) \quad (4.1.77)$$

where $\langle \pi^+ \gamma^* | \mathcal{Q}_-(M) | K^+ \rangle$ is given by Eq. (4.0.12). But this is not the whole $\langle \mathcal{Q}_-^{hls}(M) \rangle$ though! To realize this we have to look at the diagram of Fig. 2.5 (i), which gets removed by the diagonalization procedure discussed in section 2.7.2. But this diagram does not vanish in HLS, because, although the diagonalization procedure kills $K\pi$ mixing vertices, it does not remove $K\pi\gamma$ as was the case in pure ChPT or BBG (without vector). The reason for this is hidden in the form of the covariant derivative through which photon couples, a quick comparison of Eq. (4.1.52) and (2.2.36) makes it apparent. Hence there appears the fourth kinds of diagrams shown in Fig. 4.10, hence we need explicit calculation of these two diagrams.

Calculation of Type-E diagrams

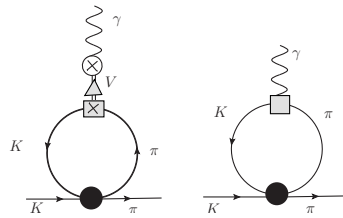
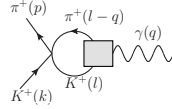


Figure 4.10: Type-E diagram that does not have a version in ChPT (after diagonalization of $K\pi$ terms).

Although it appears that we have to calculate two diagrams but actually we do not have to! Because when we add the two diagrams, the weak vertex that couples to photon directly and through a vector, adds up to produce a factor that has been already calculated through $\langle \mathcal{Q}_-(0) \rangle$, we just need to calculate the first diagram of Fig. 4.10 and use $\langle \pi^+ \gamma^* | \mathcal{Q}_-(0) | K^+ \rangle$ (Eq. (4.1.65)) as the photon vertex and evaluate the loop integral that employs the trick discussed in section 2.7.2 of Chapter 2. So we just need to replace $(k+p)$ in Eq. (4.1.65) by $2l$ (and of course an "i") and use the $K^+ K^- \pi^+ \pi^-$ vertex from Eq. (A.5.33) to obtain the following

integral:



$$= \frac{4ie f^2 z F_V(z)}{r_V^2} \int \frac{d^4 l}{(2\pi)^4} \frac{i \epsilon_V^*(k+p)_\mu}{4f^2} \frac{i l^\mu}{l^2 - m_K^2 + i0_+} \quad (4.1.78)$$

$$\times \frac{i l^\nu}{(l-q)^2 - m_K^2 + i0_+}$$

$$\implies \langle \pi^+(p) \gamma^*(q) | \mathcal{Q}_-(M) | K^+(k) \rangle_E = -e \epsilon^*(q) \cdot (k+p) \frac{z F_V(z)}{r_V^2} \quad (4.1.79)$$

$$\times q^2 B_{21}(M^2, q^2, m_K^2, m_\pi^2)$$

B_{21} is evaluated in Eq.(B.3.33) of Appendix B. Our discussion on Type-B-D proved that they were sufficient to upgrade all the ChPT Type-I and II diagrams by a multiplicative factor of $F(z)$ which means Type-D,E diagrams do not have any ChPT version to be added which in turn means that we should not subtract $q^2 \rightarrow 0$ limit of just calculated Type-E diagram from itself this time, like the way we did in Chapter 2 and also in the non-vector in this chapter, that would also mean that they must be automatically proportional to q^2 . And it is apparent from the explicit z factor in front which says that even if we subtract $q^2 \rightarrow 0$ limit, we would be subtracting a zero. This means there will appear quadratic divergence that got cancelled in non-vector case due to the just mentioned $q^2 \rightarrow 0$ subtraction. This finalizes the calculation of $\langle \pi^+ \gamma^* | \mathcal{Q}_-^{hls}(M) | K^+ \rangle$ that can be plugged in to the electron-positron pair to extract the final matrix element

$$\langle \pi^+ e^+ e^- | \mathcal{Q}_-^{hls}(M) | K^+ \rangle$$

:

$$\langle \mathcal{Q}_-^{hls}(M) \rangle_E = \alpha_e [\bar{u}(k + \not{p})] \times \frac{4\pi z F_V(z)}{r_V^2} B_{21}(M^2, q^2, m_K^2, m_\pi^2) \quad (4.1.80)$$

$$= -\frac{z m_K^2}{2f^2} B_{21}(M^2, q^2, m_K^2, m_\pi^2) \langle \mathcal{Q}_-^{hls}(0) \rangle$$

Now we add Type-A (4.1.74), E and tree contributions given by Eq. (4.1.66) to get the complete $\langle \mathcal{Q}_-^{hls}(M) \rangle$:

$$\langle \mathcal{Q}_-(M) \rangle = \langle \mathcal{Q}_-^{hls}(0) \rangle + \langle \mathcal{Q}_-^{hls}(M) \rangle_A + \langle \mathcal{Q}_-^{hls}(M) \rangle_D + \langle \mathcal{Q}_-^{hls}(M) \rangle_E \quad (4.1.81)$$

Comparison with Eq. (4.1.60) makes it apparent that the last three terms (A,D,E)

will contribute to η_{-7}^{hls} and is given by:

$$\eta_{-7}^{hls}(M, z) = \eta_{-7}(M, z) + \frac{8\pi f^2}{m_V^2} \left\{ -\frac{1}{2f^2} q^2 B_{21}(M^2, q^2, m_K^2, m_\pi^2) + \sqrt{Z_K Z_\pi} - 1 \right\} \quad (4.1.82)$$

Therefore the exact expression for η^V factor (introduced in Eq. (4.1.61) and restated in Eq (4.1.73)) will be:

$$\eta^V(M, z) = -\frac{8\pi f^2}{m_V^2} \left\{ 1 - \sqrt{Z_K Z_\pi} + \frac{1}{2f^2} q^2 B_{21}(M^2, q^2, m_K^2, m_\pi^2) \right\} \quad (4.1.83)$$

Plugging this in Eq. (4.1.72), we can get the vector upgraded mixing coefficient. We summarize the results of this section below:

$$\begin{aligned} \langle \mathcal{Q}_-^{hls}(M) \rangle &= \langle \mathcal{Q}_-^{hls}(0) \rangle + \eta_{-7}^{hls}(M, z) \langle \mathcal{Q}_7^{hls}(0) \rangle \\ \eta_{-7}^{hls}(M, z) &= \eta_{-7}(M, z) + \eta^V(M, z) \\ \eta^V(M, z) &\simeq -\frac{1}{24} \frac{\pi m_K^2}{m_V^2} \frac{1}{(4\pi)^2} \log \frac{M^2}{m_K^2} \times z \end{aligned} \quad (4.1.84)$$

The amplitude for the process $K^+ \rightarrow \pi^+ e^+ e^-$ will be given by Eq. (4.0.8) when we make the following replacements:

$$\begin{aligned} \langle \mathcal{Q}_{-,7}(0) \rangle &\mapsto \langle \mathcal{Q}_{-,7}^{hls}(0) \rangle \\ \eta_{-7}(M, z) &\mapsto \eta_{-7}^{hls}(M, z) \end{aligned} \quad (4.1.85)$$

And this time $F_{0,1}$ will be absent¹⁹. Which finally leads to the vector included form factor:

$$\begin{aligned} W_+^{hls}(M^2, z) &= 4\pi m_K^2 \frac{G_8}{g_8} \left\{ -\tilde{C}_-(M) \frac{2\pi f^2}{m_V^2} \right. \\ &\quad \left. + \tilde{C}_-(M) [\mathcal{E}_-(M^2, m_V^2) \eta_{-7}(M, z) + \eta^V(M, z)] \right. \\ &\quad \left. + \tilde{C}_7(M) \right\} \sqrt{Z_K Z_\pi} \times F_V(z) \end{aligned} \quad (4.1.86)$$

¹⁹ Please check Eq.(4.0.27)

Notice that we have plugged in the BBG evolution operator²⁰ $\mathcal{E}_-(M^2, m_V^2)$ just with the part that contains $K\pi\pi\pi$ or $KKK\pi$ vertex, that is $\eta_{-7}(M, z)$.

Note on counting: The wavefunction renormalization factor introduces a correction of $1/f^2$ and hence to keep the counting consistent we must drop any term of order lower than that, any formula presented must be viewed under this counting rule.

Vector Upgraded a and b

Once again expanding Eq. (4.1.86) around $z = 0$ and comparing with Eq. (4.0.22) we present the final forms of vector-included a_+ and b_+ :

$$\begin{aligned}
 a_+(M^2, m_V^2) &\simeq -\frac{V_{us}^* V_{ud}}{\sqrt{2}} \left\{ \tilde{C}_-(M) \frac{2(4\pi f)^2}{m_V^2} + \left[\tilde{C}_-(M) \mathcal{E}_-(M^2, m_V^2) \left(\frac{1}{3} \log \frac{M^2}{m_K m_\pi} - 2\theta \right) \right. \right. \\
 &\quad \left. \left. - 4\pi \tilde{C}_7(M) \right] \right\} \sqrt{Z_K Z_\pi} \\
 b_+(M^2, m_V^2) &\simeq \frac{a_+(M^2, m_V^2)}{r_V^2} - \frac{V_{us}^* V_{ud}}{\sqrt{2}} \left\{ \frac{1}{6} \frac{m_K^2}{m_V^2} \tilde{C}_-(M) \log \frac{M^2}{m_K^2} + \frac{\tilde{C}_-(M) \mathcal{E}_-(M^2, m_V^2)}{60 r_\pi^2} \right\} \\
 &\quad \times \sqrt{Z_K Z_\pi} - \frac{3r_\pi^2 (\alpha_+ - \beta_+) - \beta_+}{180 G_F m_K^2 r_\pi^6}
 \end{aligned}$$

(4.1.87)

²⁰This is the vector upgraded evolution operator defined in Eq. (3.3.88).

where $\theta = 1/6$ or $5/18$ depending on the cut-off scheme and $g_V \simeq 6.1$. Notice that both a_+ and b_+ receive corrections, but b_+ receives two corrections, one through a_+ as in a_+/r_V^2 which is obvious and expected, but it also receives an extra piece.

No-vector limit: It is easy to see that $m_V^2 \rightarrow \infty$ produces the vector-less results given by Eq. (4.0.27).

Long and Short Distance Matching Revisited

Once again we can look for the scale where $a_+(M^2)$ has the extrema and that will be our matching scale. The matching through a_+ is shown in Fig. (4.11).

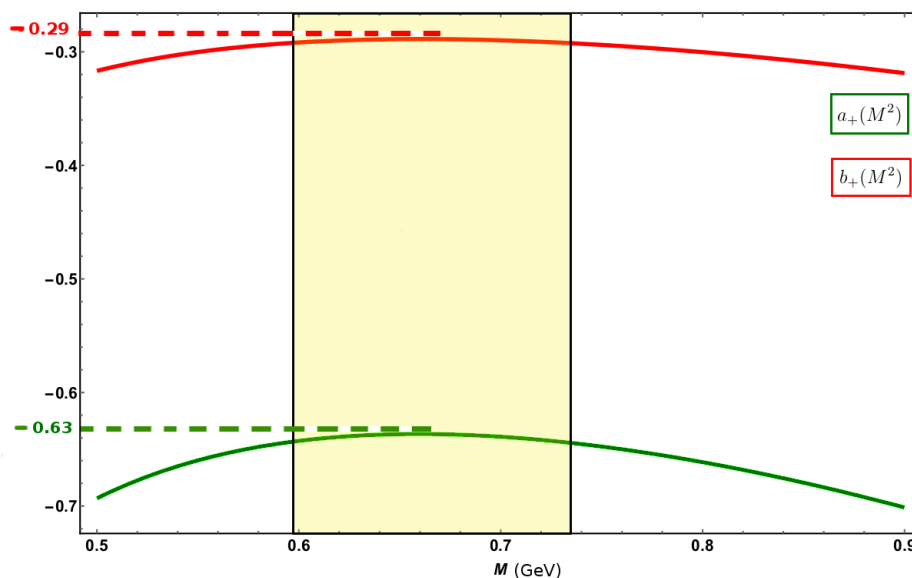


Figure 4.11: Long and short distance matching through vector upgraded $a_+(M^2)$. b_+ has also been plotted (red). The shaded region shows the matching range.

The matching scale is obtained around $M \sim 0.66$ GeV and at this scale $a_+ = -0.64$ ($\sim 280\%$ increase) and $b_+ = -0.29$ ($\sim 1300\%$ enhancement). Although there are huge enhancements in both parameters, a_+ matches well (up to 2σ) with experiment (2.2) but b_+ is missing almost a factor of 2.5, in fact the enhancement that will push $|b_+|$ beyond $|a_+|$ is missing ! The reason for this could be:

- The parameter \mathfrak{a} of Hidden Local Symmetry was fixed to 2 from VMD but as we are interpolating between long and short distance scales, more careful treatment would be to let it run with scale.
- So there is a need of new matchings: (i) HLS with Chpt and (ii) HLS with QCD. Construction of the weak Hamiltonian using HLS in the BBG framework needs the above mentioned matching to make the whole framework more powerful.

4.1.3 $K_S \rightarrow \pi^0 e^+ e^-$

For the decay $K_S \rightarrow \pi^0 l^+ l^-$, $K^0 \pi^0 \pi^+ \pi^-$ vertex is identically zero in the \mathcal{Q}_- sector, so we do not have pion loop in case of K_S decay but kaon loop is possible and there is a factor of $-\sqrt{2}$ in the $K^0 \pi^0 K^+ K^-$ vertex, hence from the definition of K_S :

$$K_S = \frac{1}{\sqrt{2}}(K^0 - \bar{K}^0) \quad (4.1.88)$$

it is apparent that the following substitution:

$$W_S(M^2, z) = - \lim_{m_\pi \rightarrow m_K} W_S(M^2, z) \quad (4.1.89)$$

will fix the form factor, additionally \mathcal{Q}_7 vertex also provides a factor of -2 that justifies above equation completely. Then the above definition provides the value of $a_S \simeq +1.2$ and the experimental value is $|1.08|_{-0.21}^{+0.26}$. So our approach successfully predicts a_i 's and also predicts huge enhancement in b_+ due to vector inclusion.

Bibliography

- [1] E. Coluccio et al. In: (2016). eprint: [arXiv:1522770](https://arxiv.org/abs/1522770).
- [2] F. J. Gilman and M. B. Wise. In: *Phys. Rev. D* (1980).
- [3] G. D'Ambrosio et al. In: *Journal of High Energy Physics* 1998 (1988). URL: <http://iopscience.iop.org/article/10.1088/1126-6708/1998/08/004>.
- [4] W. A. Bardeen, A. J. Buras, and J. -M. Gerard. In: *Nucl.Phys. B* 192 (1987), p. 138.
- [5] C. N. Yang and R. L. Mills. In: *Phys. Rev.* 96 (1954), p. 191.
- [6] J. J. Sakurai. *Currents and Mesons*. Ed. by L. Maiani, G. Pancheri, and N. Paver. University of Chicago Press, 1969.
- [7] M. Bando et al. In: *Phys. Rev. Lett.* 54.1215 (1985).
- [8] M. Bando, T. Kugo, and K. Yamawaki. In: *Nucl. Phys. B* 259 (1985), p. 493.
- [9] M. Bando, T. Kugo, and K. Yamawaki. In: *Prog. Theor. Phys.* 73 (1985), p. 1541.
- [10] T. Fujiwara et al. In: *Prog. Theor. Phys.* 73 (1985), p. 926.
- [11] M. Bando, T. Kugo, and K. Yamawaki. In: *Phys. Rept.* 164 (1988), p. 217.
- [12] M. Harada and K. Yamawaki. In: *Physics Reports* 381 (2003), pp. 1–233. eprint: [hep-ph/0302103](https://arxiv.org/abs/hep-ph/0302103).
- [13] S. Weinberg. In: *Phys. Rev.* 166 (1968), p. 1568.
- [14] W. A. Bardeen, A. J. Buras, and J. -M. Gerard. In: *Nucl.Phys. B* 293 (1987), p. 787.

Chapter 5

Conclusion

The motivation of this work was an attempt to understand the non-perturbative regime of QCD through long and short distance matching using rare Kaon decays as probes. The large N_c based framework of Bardeen, Buras and Gerard (discussed in details in Chap 3) looks promising in the light of their achievements in $K \rightarrow \pi\pi$ decay, especially for the bulk of the explanation for $\Delta I = 1/2$ rule. The agreement of their results with lattice simulations strengthened the ground to take this method seriously and to test it on the decay $K \rightarrow \pi e^+ e^-$, which is very well understood experimentally. In doing so we understood the inclusion of vector mesons in the usual Chiral Perturbation Theory (strong) and also proposed an extension to the weak sector through Bosonization of the Gilman-Wise Hamiltonian at the Chiral limit and then evolving it using BBG scheme. The successful prediction of the phenomenological parameters a_i and b_i suggests that such a weak Lagrangian can indeed be used to calculate the interactions of vector resonances with reasonable accuracy and so we intend to calculate other processes using such vector-extended weak Lagrangian in the context of BBG's meson evolution. Especially in the wake of this beautiful experiment NA62 [1] where 100 events of $K^+ \rightarrow \pi^+ \nu \bar{\nu}$ are expected and in the J-PARC KOTO [2] experiment with the goal of a few $K_L \rightarrow \pi^0 \nu \bar{\nu}$ SM events in 3-4 years run with Signal/Noise ratio ~ 2 . Since short contributions are essential for theoretical predictions of these processes, our approach looks sound to be applied. If the procedure produces consistent results then we can finally expect to put forward the standard model results and so indication of BSM physics. Indeed

Bardeen *et al.* are already indicating using their approach that there is a big (2-3 σ) difference between SM (backed by lattice [3, 4] group RBC and UKQCD) and experimental values of $Re(\epsilon'/\epsilon)$ demanding a BSM explanation. This is an exciting situation and we would like to be in tune with the experiments to produce results and test them.

Bibliography

- [1] In: (). URL: <http://na62.web.cern.ch/NA62/>.
- [2] In: (). URL: <http://koto.kek.jp/>.
- [3] J. Bai and *et al.* In: *Phys. Rev. Lett.* 115 (2015), p. 21.
- [4] N. H. Christ and *et al.* In: *Phys. Rev. Lett.* 92 (2015), p. 9.

Appendix A

Rules and Conventions

Notations

$$\begin{aligned}
 \epsilon & \quad \text{Photon polarization vector.} \\
 \bar{\epsilon}_{(V)} & \quad \text{Polarization vector of } V = \rho, \omega, \phi
 \end{aligned}
 \tag{A.0.1}$$

Space-Time Conventions

Propagators

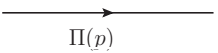
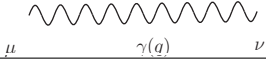
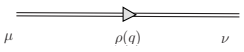
| Particle | Diagram | Value in Momentum Space |
|----------------------|---|--|
| Pseudo-scalar mesons |  | $\frac{i}{p^2 - m_\pi^2 + i\epsilon}$ |
| Photon |  | $\frac{-i}{q^2} \left(g_{\mu\nu} - \frac{q_\mu q_\nu}{q^2} \right)$ (LG) |
| ρ -meson |  | $\frac{-i}{q^2 - m_\rho^2} \left(g_{\mu\nu} - \frac{q_\mu q_\nu}{q^2} \right)$ (LG) |

Table A.1: Propagators of all the relevant particles. LG stands for the Lorentz-gauge.

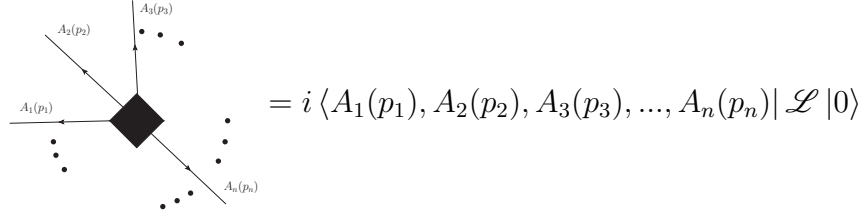
Vrtices

| QED | $\mathcal{L}_{p^2}^{\Delta S=0}$ | $\mathcal{L}_{p^2}^{hls}$ strong | \mathcal{L}_-^{hls} | $\mathcal{L}_{p^2}^{\Delta S=1}, \mathcal{L}_-$ | \mathcal{L}_7 |
|---|---|---|---|---|---|
|  |  |  |  |  |  |

Table A.2: Vertex symbols.

Vertex Conventions

- For a generic vertex, scalar fields $A_1, A_2, A_3, \dots, A_n$ all coming out of the vertex (diamond) carrying momenta $p_1, p_2, p_3, \dots, p_n$ respectively, governed by the Lagrangian \mathcal{L} has the following Feynman Vertex rule:



$$= i \langle A_1(p_1), A_2(p_2), A_3(p_3), \dots, A_n(p_n) | \mathcal{L} | 0 \rangle$$

- Conventions for incoming and outgoing scalar fields are:

$$\langle 0 | \partial^\mu A_j | A_i(p_i) \rangle = -i p_j^\mu \delta_{ij} \quad \langle A_i(p_i) | \partial^\mu A_j^* | 0 \rangle = -i p_j^\mu \delta_{ij}$$

A.1 Lagrangian Pieces and Feynman Rules For Chapter 2

A.1.1 Relevant Lagrangian Pieces Before Diagonalization

From Weak Lagrangian: Eq. (2.5.63)

Relevant pieces of Lagrangian are:

$$\begin{aligned} \mathcal{L}_{p^2}^{K^+ \pi^+ \pi^- \pi^-} &= \frac{G_8}{3} \left[(\pi^-)^2 \partial_\mu K^+ \partial^\mu \pi^+ + K^+ \pi^+ (\partial_\mu \pi^-)^2 \right. \\ &\quad \left. + K^+ \pi^- \partial_\mu \pi^- \partial^\mu \pi^+ - 3 \pi^- \pi^+ \partial_\mu K^+ \partial^\mu \pi^- \right] \\ \mathcal{L}_{p^2}^{K^+ K^+ K^- \pi^-} &= \frac{G_8}{3} \left[(K^+)^2 \partial_\mu K^- \partial^\mu \pi^- + K^- \pi^- (\partial_\mu K^+)^2 \right. \\ &\quad \left. + K^+ \pi^- \partial_\mu K^- \partial^\mu K^+ - 3 K^- K^+ \partial_\mu K^+ \partial^\mu \pi^- \right] \end{aligned} \tag{A.1.2}$$

and corresponding vertex rules are:

$$\begin{aligned}
\begin{array}{c} \pi^+(p_1) \\ \swarrow \\ \square \\ \searrow \\ \pi^-(p_3) \\ \swarrow \\ K^-(k_1) \\ \searrow \\ \pi^+(p_2) \end{array} &= -\frac{iG_8}{3} \left[2(k_1 \cdot p_3 + p_1 \cdot p_2) + (p_1 + p_2) \cdot (p_3 - 3k_1) \right] \\
\begin{array}{c} \pi^+(p_1) \\ \swarrow \\ \square \\ \searrow \\ K^-(k_3) \\ \swarrow \\ K^-(k_2) \\ \searrow \\ K^+(k_2) \end{array} &= -\frac{iG_8}{3} \left[2(k_1 \cdot k_3 + p_1 \cdot k_2) + (k_1 + k_3) \cdot (k_2 - 3p_1) \right]
\end{aligned} \tag{A.1.3}$$

From Strong Lagrangian: Eq. (2.2.43)

Relevant pieces of the strong Lagrangian:

$$\begin{aligned}
\mathcal{L}_{p^2}^{\pi^+\pi^-\gamma} &= ie (\pi^-\partial\pi^+ - \pi^+\partial\pi^-) \\
\mathcal{L}_{p^2}^{K^+K^-\gamma} &= ie (K^-\partial K^+ - K^+\partial K^-)
\end{aligned} \tag{A.1.4}$$

and corresponding vertex rules are:

$$\begin{aligned}
\begin{array}{c} \pi^-(p_2) \\ \swarrow \\ \circ \\ \searrow \\ \pi^+(p_1) \end{array} \begin{array}{c} \gamma(q) \\ \text{wavy line} \end{array} &= ie(p_2 - p_1)_\mu \epsilon^{*\mu}(q) \\
\begin{array}{c} K^-(k_2) \\ \swarrow \\ \circ \\ \searrow \\ K^+(k_1) \end{array} \begin{array}{c} \gamma(q) \\ \text{wavy line} \end{array} &= ie(k_2 - k_1)_\mu \epsilon^{*\mu}(q)
\end{aligned} \tag{A.1.5}$$

And specific to the loop such as the one defined in Eq. (2.7.82) we have,

$$\boxed{
\begin{array}{c} K^+, \pi^+(l-q) \\ \swarrow \\ \circ \\ \searrow \\ K^+, \pi^+(l) \end{array} \begin{array}{c} \gamma(q) \\ \text{wavy line} \end{array} = 2ie \epsilon_\nu^* \left(l^\nu - \frac{1}{2} q^\nu \right) = 2ie \epsilon_\nu^* l^\nu + \dots} \tag{A.1.6}$$

A.2 Simultaneous Diagonalization of Kinetic and Mass Terms

If we apply the following transformations[1] on the meson fields:

$$\begin{aligned}
\pi^+ &\mapsto \pi^+ - \frac{2m_K^2 f^2 G_8}{m_K^2 - m_\pi^2} K^+ \\
K^+ &\mapsto K^+ + \frac{2m_\pi^2 f^2 G_8^*}{m_K^2 - m_\pi^2} \pi^+ \\
\pi^0 &\mapsto \pi^0 + \frac{\sqrt{2}m_K^2 f^2 G_8}{m_K^2 - m_\pi^2} (G_8 K^0 + G_8^* \bar{K}^0) \\
K^0 &\mapsto K^0 - \frac{\sqrt{2}m_\pi^2 f^2 G_8^*}{m_K^2 - m_\pi^2} \pi^0 + \sqrt{\frac{2}{3}} \frac{m_\eta^2 f^2 G_8^*}{m_K^2 - m_\pi^2} \eta \\
\eta &\mapsto \eta - \sqrt{\frac{2}{3}} \frac{m_K^2 f^2}{m_\eta^2 - m_K^2} (G_8 K^0 + G_8^* \bar{K}^0)
\end{aligned} \tag{A.2.7}$$

Transformations of π^- , K^- and \bar{K}^0 are just the complex conjugate of the above transformations. We are dealing with cp conserving processes hence we can consider the G_8 to be real. These transformations when applied on the complete Lagrangian that is Eq. (2.2.43) + Eq. (2.5.63), they mix and cancel mixed quadratic (in meson fields) terms (Our interest is in K - π mixed terms) and as the kinetic terms contain photons through covariant derivatives, they also eliminate K - π - γ terms, resulting in a Lagrangian that does not have any K - π or K - π - γ terms and leaving the form of the kinetic and mass terms invariant. Once this has been done we need to worry about modifications in the original higher order (in number of meson fields) terms and the fact that we are working at $O(G_8)$ will help us simplify things enormously if we consider the following observations:

1. Weak Lagrangian (Eq. (2.5.63)) is already $O(G_8)$ so the extra terms that will appear due to above transformations will be at least $O(G_8^2)$ hence we do not have to touch the weak Lagrangian.
2. Consider a term from strong Lagrangian (Eq. (2.2.43)) which always has the form $\sim \pi^{2m} K^{2n}$ where m and n are positive integers and π and K represents their different isospin varieties and derivative etc are all included. This kind of terms will transform to:

$$\begin{aligned}
\pi^{2m} K^{2n} &\mapsto \pi^{2m} K^{2n} + G_8 (\pi^{2m-1} K^{2n+1} + \text{similar one field changing terms}) \\
&\quad + G_8^2 (\pi^{2m-2} K^{2n+2} + \text{similar two fields changing terms}) + O(G_8^3)
\end{aligned}$$

Of course also K transforms into π etc, we are just interested in the G_8 powers here and not the details of the structure of the terms. So the message is that at $O(G_8)$ we just have to consider one field flipping terms of the strong Lagrangian.

We have got just two relevant weak terms which are $K\pi\pi\pi$ and $KKK\pi$ and due to the above transformations they can receive just two contributions each, from the strong Lagrangian that involve single field transformations. That is $K\pi\pi\pi$ can come from $\pi\pi\pi\pi \mapsto G_8 K\pi\pi\pi$ and $KK\pi\pi \mapsto G_8 K\pi\pi\pi$. Similarly $KKK\pi$ can come from $KKKK \mapsto G_8 KKK\pi$ and $KK\pi\pi \mapsto G_8 KKK\pi$ and nothing else at this order. We introduce the following notations here:

$$\mathcal{L}_{p^2}^{\Delta S=0} \mapsto \mathcal{L}_{p^2}^{\Delta S=0} + G_8 \delta \mathcal{L}_{p^2}^{\Delta S=0} \quad (\text{A.2.8})$$

where $G_8 \delta \mathcal{L}_{p^2}^{\Delta S=0}$ is the extra piece of weak Lagrangian coming from the original strong Lagrangian due to the fields transformations described above. So we will keep the definition of strong Lagrangian intact, that is given by Eq. (2.2.43) but will redefine the weak Lagrangian as:

$$\mathcal{L}_{p^2}^{\Delta S=1} \mapsto \mathcal{L}'^{\Delta S=1} = \mathcal{L}_{p^2}^{\Delta S=1} + G_8 \delta \mathcal{L}_{p^2}^{\Delta S=0} \quad (\text{A.2.9})$$

We will keep this extra piece explicit so that we can track the mass ratios and expand in m_π^2/m_K^2 whenever it is necessary. From now on let us call this extra piece:

$$G_8 \delta \mathcal{L}_{p^2}^{\Delta S=0} = \delta \mathcal{L}_{p^2}^{\Delta S=1} \quad (\text{A.2.10})$$

A.2.1 Relevant Weak Lagrangian Pieces After Diagonalization

Terms coming from the weak Lagrangian given by Eq. (A.2.9) will be the original ones given by Eq. (2.5.63) plus the extra pieces coming from Eq. (A.2.10), so we will first write down only the extra terms below.

From $\delta\mathcal{L}_{p^2}^{\Delta S=1}$: Eq. (A.2.10)

$$\begin{aligned}\delta\mathcal{L}_{p^2}^{K^+\pi^+\pi^-\pi^-} &= -\frac{2G_8}{3}\left[(\pi^-)^2\partial_\mu K^+\partial^\mu\pi^+ + K^+\pi^+(\partial_\mu\pi^-)^2\right. \\ &\quad \left.- K^+\pi^-\partial_\mu\pi^+\partial^\mu\pi^- - \pi^-\pi^+\partial_\mu K^+\partial^\mu\pi^-\right] \\ \delta\mathcal{L}_{p^2}^{K^+K^+K^-\pi^-} &= -\frac{2G_8}{3}\left[(K^+)^2\partial_\mu K^-\partial^\mu\pi^- + K^-\pi^-(\partial_\mu K^+)^2\right. \\ &\quad \left.- K^+\pi^-\partial_\mu K^-\partial^\mu K^+ - K^-\pi^+\partial_\mu K^+\partial^\mu\pi^-\right]\end{aligned}\tag{A.2.11}$$

and corresponding vertex rules are:

$$\begin{aligned}\delta\begin{array}{c} \pi^+(p_1) \\ \swarrow \\ \square \\ \searrow \\ \pi^-(p_3) \\ \swarrow \\ \pi^+(p_2) \\ \swarrow \\ K^-(k_1) \end{array} &= \frac{2iG_8}{3}\left[2(k_1\cdot p_3 + p_1\cdot p_2) - (p_1 + p_2)\cdot(k_1 + p_3)\right] \\ \delta\begin{array}{c} \pi^+(p_1) \\ \swarrow \\ \square \\ \searrow \\ K^-(k_3) \\ \swarrow \\ K^+(k_2) \\ \swarrow \\ K^-(k_1) \end{array} &= \frac{2iG_8}{3}\left[2(k_1\cdot k_3 + p_1\cdot k_2) - (p_1 + k_2)\cdot(k_1 + k_3)\right]\end{aligned}\tag{A.2.12}$$

Note: Of course there are other $\Delta S = 1$ terms which do not involve any derivatives, they are coming from the χ (mass) term of the strong Lagrangian given by Eq. (2.2.43) due to the above diagonalization process, but as we discussed in Section 2.7.2 of Chapter 2. These terms are unimportant for our calculations and that is why we have not written down the Feynman rules for them.

Vertices Coming From The Total Weak Lagrangian: Eq. (A.2.9)

Adding the extra pieces given in Eq. (A.2.12) to the original weak terms in Eq. (A.1.3) we obtain the following vertex rule corresponding to full weak Lagrangian given by Eq. (A.2.9):

$$\begin{aligned}\begin{array}{c} \pi^+(p_1) \\ \swarrow \\ \square \\ \searrow \\ \pi^-(p_3) \\ \swarrow \\ \pi^+(p_2) \\ \swarrow \\ K^-(k_1) \end{array} &= \frac{iG_8}{3}\left[2(k_1\cdot p_3 + p_1\cdot p_2) + (p_1 + p_2)\cdot(5k_1 + p_3)\right] \\ \begin{array}{c} \pi^+(p_1) \\ \swarrow \\ \square \\ \searrow \\ K^-(k_3) \\ \swarrow \\ K^+(k_2) \\ \swarrow \\ K^-(k_1) \end{array} &= \frac{iG_8}{3}\left[2(p_1\cdot k_2 + k_1\cdot k_3) - (k_1 + k_3)\cdot(k_2 + 5p_1)\right]\end{aligned}\tag{A.2.13}$$

Vertices specific to the loop integral Eq. (2.7.82):

$$= iG_8 (k + p)_\mu l^\nu + \dots \quad (\text{A.2.14})$$

Ellipses represent the terms that are not linear in l and they do not contribute.

A.3 Lagrangian Pieces and Feynman Rules For Chapter 4

Remark I: Because we will be calculating the matrix elements in Chapter 4, we can directly derive the Feynman rules for the bosonized operators $\mathcal{Q}_{-,7}$ without referring to the Lagrangians given by Eq. (4.0.2) and/or (4.1.58). But to implement the diagonalization procedure to remove $K\pi$ mixing vertices etc discussed and implemented in the last section, we need to do things in terms of Lagrangians. Hence we will split the Lagrangian into two pieces due to the obvious reason that we have two operators only. We will do this for both non-vector and vector included Lagrangians. So let us split the weak Lagrangian of Eq. (4.0.2):

$$\mathcal{L}_{GW}^{\Delta S=1} = \mathcal{L}_- + \mathcal{L}_7 + h.c \quad (\text{A.3.15})$$

where,

$$\mathcal{L}_- = \frac{G_8}{g_8} \tilde{C}_-(M) \mathcal{Q}_-(0) \quad (\text{A.3.16})$$

$$\mathcal{L}_7 = \frac{G_8}{g_8} \tilde{C}_7(M) \mathcal{Q}_7 \quad (\text{A.3.17})$$

And similarly in the vector included case we split the Lagrangian given by Eq. (4.1.58):

$$\mathcal{L}_{hls}^{\Delta S=1} = \mathcal{L}_-^{hls} + \mathcal{L}_7^{hls} + h.c \quad (\text{A.3.18})$$

where,

$$\mathcal{L}_-^{hls} = \frac{G_8}{g_8} \tilde{C}_-(M) \mathcal{Q}_-^{hls}(0) \quad (\text{A.3.19})$$

$$\mathcal{L}_7^{hls} = \frac{G_8}{g_8} \tilde{C}_7(M) \mathcal{Q}_7^{hls} \quad (\text{A.3.20})$$

Then after deriving the final Feynman vertex rules using diagonalization and everything we can remove G_8 , g_8 and the Wilson coefficients $\tilde{C}_{-,7}$ to obtain the rules for the operators ($\mathcal{Q}_{-,7}$) only.

Remark II: Rules of last section cannot be naively applied to Chapter 4 because the effective weak Lagrangian is apparently different now. About the strong Lagrangian, despite the fact that it has an extra piece given by Eq. (3.2.33) which in any case does not contribute in the decay we are studying, it does not affect $\pi\pi\gamma$ and $KK\gamma$ vertices in the Lorentz gauge, so the vertices given by Eq. (A.1.5) and (A.1.6) will still be applicable. But the weak Lagrangian is different in two ways: firstly, because of extra piece in the Lagrangian mentioned above which will add an extra piece to the left current too but it does not affect the $K \rightarrow \pi\gamma^*$ through pion/or loop calculation because of the Lorentz structure of the integral and gauge invariance. And secondly, usual chiral weak Lagrangian is of the form:

$$\mathcal{L}_{2i}\mathcal{L}_{i3}, \quad i = 1, 2, 3$$

While our weak Lagrangian involves \mathcal{Q}_- operator and in fact just \mathcal{Q}_2 that contributes to this process, that means $i = 2, 3$ of the above Lagrangian are missing. But these are just superficial observations. We will see that indeed the relevant piece of the weak Lagrangian for $K\pi\pi\pi$ and $KKK\pi$ vertices have the same structure of ChPT case.

A.3.1 Relevant Lagrangian Pieces Before Diagonalization

Relevant Pieces of Lagrangian From \mathcal{L}_7 : Eq. (A.3.17)

$$\begin{aligned} \mathcal{L}_7^{K^+\pi^-e^+e^-} = i\alpha_e \frac{G_8}{g_8} \tilde{C}_7(M) & \left[(K^+\partial_\mu\pi^- - \pi^-\partial_\mu K^+) \right. \\ & \left. - \frac{m_K^2 - m_\pi^2}{2\Lambda^2} (K^+\partial_\mu\pi^- + \pi^-\partial_\mu K^+) \right] (\bar{e}\gamma^\mu e) \end{aligned} \quad (\text{A.3.21})$$

Corresponding vertex rule is:

$$\begin{aligned} \begin{array}{c} \pi^+(p_1) \nearrow \\ \searrow K^-(k_1) \\ \blacksquare \\ \nearrow e^+(p_+) \\ \searrow e^-(p_-) \end{array} & = i\alpha_e \frac{G_8}{g_8} \tilde{C}_7(M) \left[(k_1 - p_1)_\mu + \frac{m_K^2 - m_\pi^2}{2\Lambda^2} (k_1 + p_1)_\mu \right] \\ & \times \left[\bar{u}(p_-)\gamma^\mu v(p_+) \right] \end{aligned} \quad (\text{A.3.22})$$

And specific to the decay we have,

$$\begin{aligned} \begin{array}{c} \pi^+(p) \nearrow \\ \searrow K^+(k) \\ \blacksquare \\ \nearrow e^+(p_+) \\ \searrow e^-(p_-) \end{array} & = -i\alpha_e \frac{G_8}{g_8} \tilde{C}_7(M) [(k+p)_\mu] [\bar{u}(p_-)\gamma^\mu v(p_+)] + \dots \end{aligned} \quad (\text{A.3.23})$$

Ellipses represents the q_μ term that does not contribute.

Relevant Pieces of Lagrangian From \mathcal{L}_- : Eq. (A.3.16)

We will not consider \mathcal{L}^Λ given in Eq. (3.2.33) because it is irrelevant for the present study. So the currents involved in the Lagrangian are usual currents without the Λ -term (check Eq. (2.2.37)).

$$\begin{aligned} \mathcal{L}_-^{K^+\pi^+\pi^-\pi^-} & = \frac{G_8}{3g_8} -(M^2)\tilde{C}_-(M) \left[(\pi^-)^2\partial_\mu K^+\partial^\mu\pi^+ + K^+\pi^+(\partial_\mu\pi^-)^2 \right. \\ & \quad \left. + K^+\pi^-\partial_\mu\pi^-\partial^\mu\pi^+ - 3\pi^-\pi^+\partial_\mu K^+\partial^\mu\pi^- \right] \\ \mathcal{L}_-^{K^+K^+K^-\pi^-} & = \frac{G_8}{3g_8} -(M^2)\tilde{C}_-(M) \left[(K^+)^2\partial_\mu K^-\partial^\mu\pi^- + K^-\pi^-(\partial_\mu K^+)^2 \right. \\ & \quad \left. + K^+\pi^-\partial_\mu K^-\partial^\mu K^+ - 3K^-K^+\partial_\mu K^+\partial^\mu\pi^- \right] \end{aligned} \quad (\text{A.3.24})$$

This is exactly the same as in Eq. (A.1.2) if

$$G_8 \mapsto \frac{G_8}{g_8} \tilde{C}_-(M) := \tilde{G}_8(M) \quad (\text{A.3.25})$$

This is precisely the relation that defines g_8 within our approach and shows the scale dependence of the ChPT weak coupling g_8 defined in Eq. (2.5.64) when the BBG evolution operator $\mathcal{E}_-(M^2)$ is multiplied when $K\pi\pi\pi$ vertex is present, scale dependence has been explicitly shown in Fig. (4.1). It has been discussed in section 4.0.5 in more details.

Applying above substitution (Eq. (A.3.25)) ¹

$$\begin{aligned}
\begin{array}{c} \pi^+(p_1) \\ \swarrow \\ \square \\ \nwarrow \\ \pi^-(p_3) \\ \swarrow \\ \pi^+(p_2) \\ \searrow \\ K^-(k_1) \end{array} &= -\frac{i}{3} \tilde{G}_8(M) \left[2(k_1 \cdot p_3 + p_1 \cdot p_2) + (p_1 + p_2) \cdot (p_3 - 3k_1) \right] \\
\begin{array}{c} \pi^+(p_1) \\ \swarrow \\ \square \\ \nwarrow \\ K^-(k_3) \\ \swarrow \\ K^+(k_2) \\ \searrow \\ K^-(k_1) \end{array} &= -\frac{i}{3} \tilde{G}_8(M) \left[2(k_1 \cdot k_3 + p_1 \cdot k_2) + (k_1 + k_3) \cdot (k_2 - 3p_1) \right]
\end{aligned} \quad (\text{A.3.26})$$

Which are of course same as that in Eq. (A.1.3) under the substitution mentioned above.

A.4 Diagonalization In Chapter 4

We have to modify the diagonalizing transformation given in Eq. (A.2.7) using the substitution defined in Eq. (A.3.25) and as we have realized that the weak chiral Lagrangian Eq (A.1.2) and \mathcal{L}_- given by Eq. (A.3.24) are exactly the same under the substitution Eq. (A.3.25), we do not have to go through everything that we did in section A.4 to obtain the rotated Lagrangian. All we have to do is apply the

¹In this section and the following ones, we will always need this quantity and to save space we will use $\tilde{G}_8(M)$ for $G_8\tilde{C}_-(M)/(M^2)/g_8$

substitution. Hence the weak vertices after diagonalization (Eq. (A.2.7)) become:

$$\begin{aligned}
 \begin{array}{c} \pi^+(p_1) \\ \swarrow \\ \square \\ \nwarrow \\ K^-(k_1) \end{array} & \begin{array}{c} \pi^-(p_3) \\ \nearrow \\ \square \\ \searrow \\ \pi^+(p_2) \end{array} = \frac{i}{3} \tilde{G}_8(M) \left[2(k_1 \cdot p_3 + p_1 \cdot p_2) + (p_1 + p_2) \cdot (5k_1 + p_3) \right] \\
 \begin{array}{c} \pi^+(p_1) \\ \swarrow \\ \square \\ \nwarrow \\ K^-(k_1) \end{array} & \begin{array}{c} K^-(k_3) \\ \nearrow \\ \square \\ \searrow \\ K^+(k_2) \end{array} = \frac{i}{3} \tilde{G}_8(M) \left[2(p_1 \cdot k_2 + k_1 \cdot k_3) - (k_1 + k_3) \cdot (k_2 + 5p_1) \right]
 \end{aligned} \tag{A.4.27}$$

Vertices specific to the loop integral Eq. (2.7.82):

$$\boxed{
 \begin{array}{c} \pi^+(p) \\ \swarrow \\ \square \\ \nwarrow \\ K^+(k) \end{array}
 \begin{array}{c} K^+, \pi^+(l-q) \\ \nearrow \\ \square \\ \searrow \\ K^+, \pi^+(l) \end{array}
 = i \tilde{G}_8(M) (k+p)_\mu l^\nu + \dots
 } \tag{A.4.28}$$

Note: As no $K\pi\bar{e}\gamma^\mu e$ terms cannot be generated from the strong Lagrangian (Eq. (3.2.32)) by applying Eq. (A.2.7), \mathcal{L}_7 remains unchanged.

A.5 Rules and Conventions After Vector Inclusion

A.5.1 Relevant Lagrangian Pieces Before Diagonalization

Relevant Pieces of Lagrangian From Strong Lagrangian $\mathcal{L}_{p^2}^{hls}$: Eq. (4.1.40)

$$\begin{aligned}
 \mathcal{L}_{p^2}^{\gamma V} &= \frac{1}{3} e \mathbf{a} f^2 g_V \mathcal{A}_\mu (3\rho^\mu + \omega^\mu - \sqrt{2}\phi^\mu) \\
 \mathcal{L}_{p^2}^{\pi^+ \pi^- V} &= \frac{i}{2} \mathbf{a} g_V \rho_\mu (\pi^- \partial^\mu \pi^+ - \pi^+ \partial^\mu \pi^-) \\
 \mathcal{L}_{p^2}^{K^+ K^- V} &= \frac{i}{2} \mathbf{a} g_V \left(\frac{\rho_\mu + \omega_\mu}{2} - \frac{\phi}{\sqrt{2}} \right) (K^- \partial^\mu K^+ - K^+ \partial^\mu K^-) \\
 \mathcal{L}_{p^2}^{K^+ K^- \pi^+ \pi^-} &= \frac{3\mathbf{a} - 4}{24f^2} \left\{ \partial_\mu \pi^+ \partial^\mu \pi^- K^+ K^- + \partial_\mu K^+ \partial^\mu K^- \pi^+ \pi^- \right. \\
 &\quad + \partial_\mu \pi^+ \partial^\mu K^- K^+ \pi^- + \partial_\mu K^+ \partial^\mu \pi^- K^- \pi^+ \\
 &\quad \left. - 2 (\partial_\mu K^+ \partial^\mu \pi^+ K^- \pi^- + \partial_\mu K^- \partial^\mu \pi^- K^+ \pi^+) \right\}
 \end{aligned} \tag{A.5.29}$$

$\pi\pi\gamma$ and $KK\gamma$ terms are very special in this case so we write them separately below:

$$\begin{aligned}\mathcal{L}_{p^2}^{\pi^+\pi^-\gamma} &= i e \left(1 - \frac{\mathbf{a}}{2}\right) \mathcal{A}_\mu \left(\pi^- \partial^\mu \pi^+ - \pi^+ \partial^\mu \pi^-\right) \\ \mathcal{L}_{p^2}^{K^+K^-\gamma} &= i e \left(1 - \frac{\mathbf{a}}{2}\right) \mathcal{A}_\mu \left(K^- \partial^\mu K^+ - K^+ \partial^\mu K^-\right)\end{aligned}\quad (\text{A.5.30})$$

Note: Notice that for $\mathbf{a} = 2$ these vertices disappear ! But there is no reason to panic because pion or kaon pair annihilation to photon gets dominated by a ρ exchange which restores the charge in the pion and kaon electromagnetic form factors. Schematically:

$$= i e \epsilon^* \cdot (p_1 + p_2) + O\left(\frac{q^2}{m_\rho^2}\right) \quad (\text{A.5.31})$$

This becomes very clear once we notice the vertices corresponding to Eq. (A.5.29) and (A.5.30):

$$\begin{aligned}\begin{array}{c} \pi^+(p_1) \\ \diagdown \\ \otimes \\ \diagup \\ \pi^-(p_2) \end{array} \begin{array}{c} V(q) \\ \longrightarrow \\ \triangleright \end{array} &= \frac{i}{2} \mathbf{a} g_V \bar{\epsilon}^{*\mu}(q) \cdot (p_2 - p_1) \\ \begin{array}{c} K^+(k_1) \\ \diagdown \\ \otimes \\ \diagup \\ K^-(k_2) \end{array} \begin{array}{c} V(q) \\ \longrightarrow \\ \triangleright \end{array} &= \frac{i}{2} \mathbf{a} g_V \bar{\epsilon}^{*\mu}(q) \cdot (k_2 - k_1) \\ \begin{array}{c} \pi^+, K^+(p_1) \\ \diagdown \\ \bullet \\ \diagup \\ \pi^-, K^-(p_2) \end{array} \begin{array}{c} \gamma(q) \\ \longrightarrow \\ \text{wavy} \end{array} &= i e \left(1 - \frac{\mathbf{a}}{2}\right) \epsilon^*(q) \cdot (p_1 - p_2)\end{aligned}\quad (\text{A.5.32})$$

Vertex rules for the strong vertex $K^+K^-\pi^+\pi^-$ specific to the loop integral defined in Eq. (4.1.78) is:

$$\begin{array}{c} \pi^+(p) \\ \diagdown \\ \bullet \\ \diagup \\ K^+(k) \end{array} \begin{array}{c} K^+(l) \\ \diagdown \\ \bullet \\ \diagup \\ \pi^+(l-\gamma) \end{array} = i \frac{3\mathbf{a} - 4}{8f^2} (k + p) \cdot l + \text{irrelevant } q_\mu \text{ term.} \quad (\text{A.5.33})$$

And we write the V - γ separately:

$$\begin{array}{c} \rho(q_1) \\ \longrightarrow \\ \triangleleft \end{array} \begin{array}{c} \otimes \\ \longrightarrow \\ \text{wavy} \end{array} \begin{array}{c} \gamma(q_2) \\ \longrightarrow \\ \text{wavy} \end{array} = \frac{i e}{3} \mathbf{a} f^2 g_V \epsilon^* \cdot (3\bar{\epsilon}^*(\rho) + \bar{\epsilon}^*(\omega) - \sqrt{2}\bar{\epsilon}^*(\phi)) \quad (\text{A.5.34})$$

Relevant Pieces of Lagrangian From \mathcal{L}_- : Eq. (A.3.19)

$$\begin{aligned}
\mathcal{L}_-^{K^+\pi^+\pi^-\pi^-} &= -\frac{\tilde{G}_8(M)}{12} \left[(3\mathbf{a}^2 - 4) \left((\pi^-)^2 \partial_\mu K^+ \partial^\mu \pi^+ + K^+ \pi^+ (\partial_\mu \pi^-)^2 \right) \right. \\
&\quad \left. + (6\mathbf{a} - 3\mathbf{a}^2 - 4) K^+ \pi^- \partial_\mu \pi^- \partial^\mu \pi^+ + 3(4 - 2\mathbf{a} - \mathbf{a}^2) \pi^- \pi^+ \partial_\mu K^+ \partial^\mu \pi^- \right] \\
\mathcal{L}_-^{K^+K^+K^-\pi^-} &= -\frac{\tilde{G}_8(M)}{12} \left[(3\mathbf{a}^2 - 4) \left((K^+)^2 \partial_\mu K^- \partial^\mu \pi^- + K^- \pi^- (\partial_\mu K^+)^2 \right) \right. \\
&\quad \left. + (6\mathbf{a} - 3\mathbf{a}^2 - 4) K^+ \pi^- \partial_\mu K^+ \partial^\mu K^- + 3(4 - 2\mathbf{a} - \mathbf{a}^2) K^- K^+ \partial_\mu K^+ \partial^\mu \pi^- \right] \\
\mathcal{L}_-^{K^+\pi^-V} &= i \tilde{G}_8(M) \mathbf{a} f^2 g_V \left(1 - \frac{\mathbf{a}}{2} \right) (\rho_\mu + \omega_\mu) (\partial^\mu K^+ \pi^- - \partial^\mu \pi^- K^+) \\
\mathcal{L}_-^{K^+\pi^-\gamma} &= -2i e f^2 \left(1 + \frac{\mathbf{a}(\mathbf{a} - 1)}{3} \right) \mathcal{A}_\mu (\partial^\mu K^+ \pi^- - \partial^\mu \pi^- K^+)
\end{aligned} \tag{A.5.35}$$

Corresponding vertices are:

$$\begin{aligned}
\begin{array}{c} \pi^+(p_1) \\ \swarrow \\ \square \\ \searrow \\ \pi^-(p_3) \\ \swarrow \\ \pi^+(p_2) \\ \searrow \\ K^-(k_1) \end{array} &= \frac{i \tilde{G}_8(M)}{12} \left[2(3\mathbf{a}^2 - 4) (k_1 \cdot p_3 + p_1 \cdot p_2) \right. \\
&\quad \left. + (p_1 + p_2) \cdot \left(p_3(6\mathbf{a} - 3\mathbf{a}^2 - 4) + 3k_1(4 - 2\mathbf{a} - \mathbf{a}^2) \right) \right] \\
\begin{array}{c} \pi^+(p_1) \\ \swarrow \\ \square \\ \searrow \\ K^-(k_3) \\ \swarrow \\ K^+(k_2) \\ \searrow \\ K^-(k_1) \end{array} &= \frac{i \tilde{G}_8(M)}{12} \left[2(3\mathbf{a}^2 - 4) (k_1 \cdot k_3 + p_1 \cdot k_2) \right. \\
&\quad \left. + (k_1 + k_3) \cdot \left(k_2(6\mathbf{a} - 3\mathbf{a}^2 - 4) + 3p_1(4 - 2\mathbf{a} - \mathbf{a}^2) \right) \right] \tag{A.5.36} \\
\begin{array}{c} \rho, \omega(q) \\ \uparrow \\ \triangle \\ \downarrow \\ \square \\ \leftarrow K^-(k_1) \quad \rightarrow \pi^+(p_1) \end{array} &= -i (k_1 - p_1) \cdot (\tilde{\epsilon}_\rho^* + \tilde{\epsilon}_\omega^*) (\mathbf{a} f^2 g_V) \left(1 - \frac{\mathbf{a}}{2} \right) \\
\begin{array}{c} \gamma(q) \\ \uparrow \\ \circ \\ \downarrow \\ \square \\ \leftarrow K^-(k_1) \quad \rightarrow \pi^+(p_1) \end{array} &= 2i \epsilon^*(q) \cdot (k_1 - p_1) e f^2
\end{aligned}$$

Relevant Pieces of Lagrangian From \mathcal{L}_7 : Eq. (A.3.20)

$$\mathcal{L}_7^{K^+\pi^-e^+e^-} = i \alpha_e \left(1 - \frac{\mathbf{a}}{2} \right) \frac{G_8}{g_8} \tilde{C}_7(M) \left(K^+ \partial_\mu \pi^- - \pi^- \partial_\mu K^+ \right) \tag{A.5.37}$$

It of course is the same as in Eq. (A.3.21) when $\mathbf{a} = 0$ but when $\mathbf{a} = 2$, this vertex disappears. This does not mean that $\langle \pi e^+ e^- | \mathcal{L}_7^{hls} | K \rangle$, here we must recall

the vertex given by Eq. (A.5.31), where we saw that $\pi^+\pi^-\gamma$ vertex also has the same factor in front $1 - \alpha/2$ and hence vanishing at $\alpha = 2$, but we saw how another tree diagram where the vertex got a correction due to a vector propagator and we summed up the two diagrams we recovered pure ChPT $\pi\pi\gamma$ form factor which is 1 in the low momentum transfer limit. For the same reason, at very low momentum transfer, where vectors are completely decoupled, we must get back our usual α -independent $\langle \mathcal{L}_7 \rangle$ given by Eq. (A.3.21). Like we found in pion electromagnetic form factor case:

$$1 \mapsto F_V(z) = \frac{r_V^2}{r_V^2 - z}, \quad r_V = \frac{m_V}{m_K} \quad (\text{A.5.38})$$

same should be in this case also, so the full vertex rule will take the following form:

$$\begin{aligned}
\begin{array}{c} \pi^+(p_1) \\ \swarrow \\ \blacksquare \\ \nwarrow \\ K^-(k_1) \end{array} \begin{array}{c} e^+(p_+) \\ \swarrow \\ \blacksquare \\ \nwarrow \\ e^-(p_-) \end{array} &= i \alpha_e F_V(z) \frac{G_8}{g_8} \tilde{C}_7(M) \left[(k_1 - p_1) \right] \\ &\times \left[\bar{u}(p_-) \gamma^\mu v(p_+) \right] \quad (\text{A.5.39})
\end{aligned}$$

And specific to the decay we have,

$$\begin{aligned}
\begin{array}{c} \pi^+(p) \\ \swarrow \\ \blacksquare \\ \nwarrow \\ K^+(k) \end{array} \begin{array}{c} e^+(p_+) \\ \swarrow \\ \blacksquare \\ \nwarrow \\ e^-(p_-) \end{array} &= -i \alpha_e F_V(z) \frac{G_8}{g_8} \tilde{C}_7(M) [(k + p)_\mu] [\bar{u}(p_-) \gamma^\mu v(p_+)] + \dots \\ & \quad (\text{A.5.40})
\end{aligned}$$

A.6 Diagonalization In Chapter 4: HLS

The diagonalization transformation will be carried out with the same replacement defined in Eq. (A.3.25) because the same form of $K\pi$ term in the weak Lagrangian in Eq. (A.3.19) and (A.3.16) when expanded, but due to the presence of extra terms in the four-meson terms the result will now be different than we had in section A.4. We will therefore write down the relevant Lagrangian pieces and also the vertex rules originating from \mathcal{L}_-^{hls} defined in Eq. (A.3.19) and of course \mathcal{L}_7^{hls} does not change due to the reasons discussed in section A.4.

Relevant Pieces of Lagrangian From \mathcal{L}_-^{hls} After Diagonalization

$$\begin{aligned}
\mathcal{L}_-^{K^+\pi^+\pi^-\pi^-} &= -\frac{\tilde{G}_8(M)}{12} \left[(4 - 6\mathbf{a} + 3\mathbf{a}^2) \left((\pi^-)^2 \partial_\mu K^+ \partial^\mu \pi^+ + K^+ \pi^+ (\partial_\mu \pi^-)^2 \right) \right. \\
&\quad \left. - 3(\mathbf{a} - 2)^2 K^+ \pi^- \partial_\mu \pi^- \partial^\mu \pi^+ + (4 - 3\mathbf{a}^2) \pi^- \pi^+ \partial_\mu K^+ \partial^\mu \pi^- \right] \\
\mathcal{L}_-^{K^+K^+K^-\pi^-} &= -\frac{\tilde{G}_8(M)}{12} \left[(4 - 6\mathbf{a} + 3\mathbf{a}^2) \left((K^+)^2 \partial_\mu K^- \partial^\mu \pi^- + K^- \pi^- (\partial_\mu K^+)^2 \right) \right. \\
&\quad \left. - 3(\mathbf{a} - 2)^2 K^+ \pi^- \partial_\mu K^+ \partial^\mu K^- + (4 - 3\mathbf{a}^2) K^- K^+ \partial_\mu K^+ \partial^\mu \pi^- \right]
\end{aligned} \tag{A.6.41}$$

We will write down $K\pi V$ and $K\pi\gamma$ terms in a moment, but before that we write down the following vertices:

$$\begin{aligned}
\begin{array}{c} \pi^+(p_1) \\ \downarrow \\ \square \\ \uparrow \\ K^-(k_1) \end{array} \begin{array}{c} \pi^-(p_3) \\ \uparrow \\ \square \\ \downarrow \\ \pi^+(p_2) \end{array} &= \frac{i\tilde{G}_8(M)}{12} \left[2(4 - 6\mathbf{a} + 3\mathbf{a}^2)(k_1 \cdot p_3 + p_1 \cdot p_2) \right. \\
&\quad \left. + (p_1 + p_2) \cdot \left(k_1(4 - 3\mathbf{a}^2) - 3p_3(\mathbf{a} - 2)^2 \right) \right] \\
\begin{array}{c} \pi^+(p_1) \\ \downarrow \\ \square \\ \uparrow \\ K^-(k_3) \end{array} \begin{array}{c} K^-(k_3) \\ \uparrow \\ \square \\ \downarrow \\ K^+(k_2) \end{array} &= \frac{i\tilde{G}_8(M)}{12} \left[2(4 - 6\mathbf{a} + 3\mathbf{a}^2)(k_1 \cdot k_3 + p_1 \cdot k_2) \right. \\
&\quad \left. + (k_1 + k_3) \cdot \left(p_1(4 - 3\mathbf{a}^2) - 3k_2(\mathbf{a} - 2)^2 \right) \right]
\end{aligned} \tag{A.6.42}$$

Vertices specific to the loop integral in Eq. (2.7.82) are:

$$\boxed{
\begin{array}{c} \pi^+(p) \\ \downarrow \\ \square \\ \uparrow \\ K^+(k) \end{array} \begin{array}{c} K^+, \pi^+(l-q) \\ \uparrow \\ \square \\ \downarrow \\ K^+, \pi^+(l) \end{array} = i\tilde{G}_8(M) (k+p)_\mu l^\nu \left[1 + \frac{3\mathbf{a}}{2} \left(\frac{\mathbf{a}}{2} - 1 \right) \right] + \dots
} \tag{A.6.43}$$

Notice that $a = 0, 2$ reduces the vertices to the ChPT case which says that there is no modification to the usual ‘‘only meson’’ weak vertex.

The $K\pi\rho$ term is given by:

$$\begin{aligned}
\mathcal{L}_-^{K^+\pi^-V} &= -i \frac{\tilde{G}_8(M) \mathbf{a} f^2 g_V}{2(m_K^2 - m_\pi^2)} (\partial^\mu K^+ \pi^- - \partial^\mu \pi^- K^+) \\
&\quad \times \left([m_\pi^2 + \mathbf{a}(m_K^2 - m_\pi^2)] \rho_\mu + [(\mathbf{a} - 2)m_K^2 + (1 - \mathbf{a})m_\pi^2] \omega_\mu + [\sqrt{2}m_\pi^2] \phi_\mu \right)
\end{aligned} \tag{A.6.44}$$

Corresponding vertex rule is:

$$\begin{aligned}
&= i\mathbf{a}f^2 g_V \tilde{G}_8(M) (k_1 - p_1) \left([m_\pi^2 + \mathbf{a}(m_K^2 - m_\pi^2)] \bar{\epsilon}_{(\rho)}^* \right. \\
&\quad \left. + [(\mathbf{a} - 2)m_K^2 + (1 - \mathbf{a})m_\pi^2] \bar{\epsilon}_{(\omega)}^* + [\sqrt{2}m_\pi^2] \bar{\epsilon}_{(\phi)}^* \right)
\end{aligned} \tag{A.6.45}$$

And $K\pi\gamma$ term and corresponding vertex rule are:

$$\mathcal{L}_-^{K^+\pi^-\gamma} = i\tilde{G}_8(M) e \mathbf{a} f^2 \frac{1 - 2\mathbf{a}}{3} \mathcal{A}_\mu (\partial^\mu K^+ \pi^- - \partial^\mu \pi^- K^+) \tag{A.6.46}$$

$$= i \tilde{G}_8(M) e \epsilon^*(q) \cdot (k_1 - p_1) \mathbf{a} f^2 \frac{2\mathbf{a} - 1}{3} \tag{A.6.47}$$

Bibliography

- [1] G. Ecker, A. Pich, and E. de Rafael. In: *Nucl. Phys. B* 303 (1988), pp. 665–702.

Appendix B

Loop Integrals and Functions

| | |
|-------------|--|
| <i>DR</i> | Dimensional Regularization |
| <i>CR</i> | Hard or Naive Cut-off Regularization |
| <i>SPCR</i> | Symmetry Preserving Cut-off Regularization |

B.1 Notations Specific To Loop Integrations

| | |
|-----------------|--|
| \mathfrak{d} | space-time dimension used to evaluate loop integrals. |
| ε | $= 4 - \mathfrak{d}$ |
| 0_+ | An infinitesimal positive number. |
| γ_E | Euler's constant $\simeq 0.577\dots$ |
| R_ε | $= -2/\varepsilon + \gamma_E - \log(4\pi) - 1$ |
| μ | scale introduced in DR to keep the dimension of the integrals right. |
| M | Momentum cut-off used in CR and SPCR. |
| r_M | $= M/m_K$ |

(B.1.1)

B.2 List of Relevant Analytic Functions

$$\mathcal{F}(z, x) = 1 + z x(x - 1) \quad (\text{B.2.2})$$

$$\mathcal{H}(z) = \int_0^1 dx \log[\mathcal{F}(z, x)] = -2 + 2G(z) \quad (\text{B.2.3})$$

$$\chi(z) = \frac{4}{9} - \frac{4}{3z} - \frac{1}{3} \left(1 - \frac{4}{z}\right) G(z) \quad (\text{B.2.4})$$

$$G(z) = \left. \begin{aligned} & \sqrt{\frac{4}{z} - 1} \arcsin \sqrt{\frac{z}{4}}, & z \leq 4 \\ & = -\frac{1}{2} \sqrt{1 - \frac{4}{z}} \left(\log \frac{1 - \sqrt{1 - 4/z}}{1 - \sqrt{1 - 4/z}} + i\pi \right), & z \geq 4 \end{aligned} \right\} \quad (\text{B.2.5})$$

Rest of the symbols like r_i , z etc are all defined in Eq. (1.1.1).

B.2.1 Behavior of The Functions Around $z = 0$

$$\mathcal{H}(z) = -\frac{z}{6} + O(z^{3/2}) \quad (\text{B.2.6})$$

$$\chi(z) = \frac{z}{60} + O(z^2) \quad (\text{B.2.7})$$

$$G(z) = 1 - \frac{z}{12} + O(z^{3/2}) \quad (\text{B.2.8})$$

B.3 Loop Integrals

The one and two point functions are evaluated in dimensional regularization in [1] and are given in numerous places, so we will just provide with the definitions and the results in dimensional regularization but evaluate them explicitly in cut-off.

B.3.1 Definitions of All The Integrals

A_0 Integral

$$A_0(m_i^2) = i \int \frac{d^4 l}{(2\pi)^4} \frac{1}{l^2 - m_i^2 + i0_+} \quad (\text{B.3.9})$$

B₀ Integral

$$B_0(q^2, m_1^2, m_2^2) = i \int \frac{d^4 l}{(2\pi)^4} \frac{1}{l^2 - m_1^2 + i0_+} \frac{1}{(l - q)^2 - m_2^2 + i0_+} \quad (\text{B.3.10})$$

For $m_1 = m_2 = m$ we get:

$$B_0(q^2, m^2, m^2) = B_0(q^2, m^2) = \int_0^1 dx \left. \frac{\partial A_0(t^2)}{\partial t^2} \right|_{t^2 = m^2 + q^2 x(x-1)} \quad (\text{B.3.11})$$

B_{20,21} Integrals

B_{20,21} are actually functions of one point and two point functions and we feel the need to list them down here.

$$q^2 B_{20}(q^2, m^2) = \frac{1}{\mathfrak{d} - 1} \left[\frac{\mathfrak{d} - 2}{2} A_0(m^2) + \left(\frac{\mathfrak{d} q^2}{4} - m^2 \right) B_0(q^2, m^2) \right] \quad (\text{B.3.12})$$

$$q^2 B_{21}(q^2, m^2) = \frac{1}{\mathfrak{d} - 1} \left[\frac{1}{2} A_0(m^2) + \left(m^2 - \frac{q^2}{4} \right) B_0(q^2, m^2) \right] \quad (\text{B.3.13})$$

B_{μν} Integral

$$\begin{aligned} B_{\mu\nu}(q^2, m^2) &= i \int \frac{d^4 l}{(2\pi)^4} \frac{l_\mu}{l^2 - m^2 + i0_+} \frac{l_\nu}{(l - q)^2 - m^2 + i0_+} \\ &= q_\mu q_\nu B_{20}(q^2, m^2) + g_{\mu\nu} q^2 B_{21}(q^2, m^2) \end{aligned} \quad (\text{B.3.14})$$

B.3.2 The Values of The Integrals In Dimensional Regularization (DR)

A₀ Integral In DR:

$$A_0(m_i^2) = \frac{m_i^2}{16\pi^2} \left(R_\varepsilon - \log \frac{\mu^2}{m_i^2} \right) + O(\varepsilon) \quad (\text{B.3.15})$$

B₀ Integral In DR:

$$B_0(q^2, m_i^2) = \frac{1}{16\pi^2} \left(R_\varepsilon - \log \frac{\mu^2}{m_i^2} + 1 + \mathcal{H}(z/r_i^2) \right) + O(\varepsilon) \quad (\text{B.3.16})$$

B_{μν} Integral In DR:

It will be enough to give the value of B₂₁ and that will determine B_{μν} because we will see later when we calculate everything in cut-off scheme, that B₂₁ and B₂₀ are related and we will provide exact expressions later. But B₂₁ is expressed in terms of A₀ and B₀ in Eq. (B.3.13) and so B_{μν} is already known in dimensional regularization.

B.3.3 The Values of The Integrals In Naive Cut-off Regularization (NCR)

A₀ is trivial so we will just write down the results below but we will evaluate all B integrals in details.

A₀ Integral In NCR:

$$A_0(m^2) \mapsto A_0(M^2, m^2) = \frac{1}{16\pi^2} \left[M^2 - m^2 \log \left(1 + \frac{M^2}{m^2} \right) \right] \quad (\text{B.3.17})$$

B₀ Integral In NCR:

Using the derived definition Eq. (B.3.11) we can write down:

$$\begin{aligned} B_0(q^2, m_i^2, m_i^2) &\mapsto B_0(M^2, q^2, m_i^2) \\ &= B_0^{(0)}(q^2, m_i^2, m_i^2) + \delta^{(1)} B_0(M^2, q^2, m_i^2) + \delta^{(2)} B_0(M^2, q^2, m_i^2) \end{aligned} \quad (\text{B.3.18})$$

where the first term is the value of B₀(M², q², m_i²) when M ≫ m_i and in fact this result is well known:

$$B_0^{(0)}(M^2, q^2, m_i^2) = \frac{1}{16\pi^2} \left[1 - \log \frac{M^2}{m_i^2} + \mathcal{H}(z/r_i^2) \right] \quad (\text{B.3.19})$$

But there are corrections $\delta^{(1,2)}B_0$ due to the fact that M is not so large (for example when $m_i = m_K$). Before we evaluate their values we expect that $\delta^{(1,2)}B_0(M^2, q^2, m_i^2)$ must vanish by cancelling each other or each separately when $M^2 \gg m_i^2$ limit is taken. Our expectation is that the scale M will be close to 1 GeV and in that case this correction should be very small and we can easily neglect it. But we do not know yet where exactly M stands and in fact these corrections to B_0 will affect the matching hence value of M itself so better we calculate the correction exactly because it is not so difficult. These corrections are simple to calculate when we notice that they involve integration of $\mathcal{F}(z')$, where z' is a scaling of z due to the presence of non-zero m_i^2/M^2 , precisely:

$$z \mapsto \frac{z m_i^2}{m_i^2 + M^2} \quad (\text{B.3.20})$$

and this helps cast the corrections into the following form:

$$\begin{aligned} \delta^{(1)}B_0(M^2, q^2, m_i^2) &= \frac{1}{16\pi^2} \int_0^1 dx \left\{ \left(1 + \frac{m_i^2}{M^2}\right)^{-1} \frac{1}{\mathcal{F}\left(\frac{z m_i^2}{M^2 + m_i^2}, x\right)} - 1 \right\} \\ &= \frac{1}{16\pi^2} \left\{ \frac{\left(1 + \frac{m_i^2}{M^2}\right)^{-1} G\left(\frac{z m_i^2}{m_i^2 + M^2}\right)}{1 - \frac{z}{4} \frac{m_i^2}{m_i^2 + M^2}} - 1 \right\} \end{aligned} \quad (\text{B.3.21})$$

$$\begin{aligned} \delta^{(2)}B_0(M^2, q^2, m_i^2) &= -\frac{1}{16\pi^2} \left[\log\left(1 + \frac{m_i^2}{M^2}\right) + \int_0^1 dx \log\left[\mathcal{F}\left(\frac{z m_i^2}{M^2 + m_i^2}, x\right)\right] \right] \\ &= -\frac{1}{16\pi^2} \left[\log\left(1 + \frac{m_i^2}{M^2}\right) + \mathcal{H}\left(\frac{z m_i^2}{M^2 + m_i^2}\right) \right] \end{aligned} \quad (\text{B.3.22})$$

Expansion around $z = 0$

$$B_0^{(0)}(M^2, q^2, m_i^2) = \frac{1}{16\pi^2} \left(1 - \log\frac{M^2}{m_i^2} - \frac{z}{6}\right) + O(z^{3/2}) \quad (\text{B.3.23})$$

$$\delta^{(1)}B_0(M^2, q^2, m_i^2) = \frac{1}{16\pi^2} \left(\frac{m_i M}{m_i^2 + M^2}\right)^2 \frac{z}{6} + O(z^{3/2}) \quad (\text{B.3.24})$$

$$\begin{aligned} \delta^{(2)}B_0(M^2, q^2, m_i^2) &= -\frac{1}{16\pi^2} \log\left(1 + \frac{m_i^2}{M^2}\right) \\ &\quad + \frac{1}{16\pi^2} \left(\frac{m_i M}{m_i^2 + M^2}\right)^2 \frac{z}{6} + O(z^{3/2}) \end{aligned} \quad (\text{B.3.25})$$

B₂₁ Integral In NCR:

Now that we know $A_0(m^2)$ and $B_0(M^2, q^2, m^2)$ integrals so substituting them in Eq. (B.3.13) one can easily obtain the value of $B_{21}(M^2, q^2, m^2)$, but we will rather write down the value of the following quantity which is the one we need in our calculation:

$$\frac{32\pi^2}{q^2} \left[q^2 B_{21}(M^2, q^2, m_i^2) - \lim_{q^2 \rightarrow 0} q^2 B_{21}(M^2, q^2, m_i^2) \right] = \chi(z/r_i^2) + \frac{1}{6} \log \frac{M^2}{m_i^2} - \theta_{ncr} + O\left(\frac{m_i^2}{M^2}\right)$$

(B.3.26)

where $\theta_{ncr} = \frac{5}{18}$, $O(m_i^2/M^2)$ corrections are due to $\delta^{(1,2)}B_0(M^2, q^2, m_i^2)$ given by Eq. (B.3.21) and (B.3.22).

B.3.4 Integrals in Symmetry Preserving Cut-off Regularization (SPCR)

Naive momentum cut-off violates gauge symmetry but this problem can be avoided if we introduce cut-off through a symmetry preserving procedure. Harada and Yamawaki [2] used the fact realized by 't Hooft and Veltman [3] that $\mathfrak{d} = 4$ poles correspond to logarithmic while $\mathfrak{d} = 2$ ones are the origins of quadratic divergences and evaluated the integrals in a way that preserve symmetries and still carries quadratic divergences which are crucial in matching long and short distance physics through BBG [4] scheme. We will not illustrate on the proof but will state the procedure which is simple, one starts with the usual dimensional regularization and then uses the following correspondence:

$$\frac{2}{4 - \mathfrak{d}} - \gamma_E + \log(4\pi) + 1 \mapsto \log M^2 \quad (\text{B.3.27})$$

And the quadratic divergence comes from:

$$\begin{aligned} \int \frac{d^{\mathfrak{d}}l}{(2\pi)^{\mathfrak{d}}} \frac{i}{l^2} &\mapsto \frac{M^2}{(4\pi)^2} \\ \int \frac{d^{\mathfrak{d}}l}{(2\pi)^{\mathfrak{d}}} \frac{i l^\mu l^\nu}{l^2} &\mapsto g^{\mu\nu} \frac{M^2}{(4\pi)^2} \end{aligned} \quad (\text{B.3.28})$$

Results of basic loop integrals are listed in many places for example in [], we will state the results of A_0 and A_0 and finally will write down the value of the quantity defined in Eq. (B.3.26). The only difference it makes in this quantity is that instead of the constant $-5/18$ we will have $-1/6$ (Compare Eq. (B.3.26) and (B.3.31)). We will abbreviate this method as SPCR (symmetry preserving cut-off regularization).

A_0 Integral In SPCR:

$$A_0(M^2, m^2) = \frac{1}{16\pi^2} \left[M^2 - m^2 \log \frac{M^2}{m^2} \right] + O\left(\frac{m^2}{M^2}\right) \quad (\text{B.3.29})$$

B_0 Integral In SPCR:

$$B_0(M^2, q^2, m_i^2) = \frac{1}{16\pi^2} \left[1 - \log \frac{M^2}{m_i^2} + \mathcal{H}(z/r_i^2) \right] + O\left(\frac{m^2}{M^2}\right) \quad (\text{B.3.30})$$

And using A_0 and B_0 we finally calculate the following quantity:

$$\begin{aligned} \frac{32\pi^2}{q^2} \left[q^2 B_{21}(M^2, q^2, m_i^2) - \lim_{q^2 \rightarrow 0} q^2 B_{21}(M^2, q^2, m_i^2) \right] &= \chi(z/r_i^2) + \frac{1}{6} \log \frac{M^2}{m_i^2} - \theta_{spcr} \\ &+ O\left(\frac{m_i^2}{M^2}\right) \end{aligned}$$

(B.3.31)

where $\theta_{spcr} = 1/6$. Comparing the above equation with Eq. (B.3.26) we can see the difference in the constant term θ , this is coming from the factor $1/(\mathfrak{d} - 1)$ sitting in front in the definition of B_{21} integral in Eq. (B.3.13) which gets replaced by just $1/3$ in naive momentum cut-off case and finally leads to a constant factor of $-5/18$ but if special care is taken in the view of Eq. (B.3.27) we get $-1/6$ instead.

$$\mathbf{B}_{\mu\nu}(M^2, m_K^2, m_\pi^2, q^2)$$

In section B.3.1 we defined the $B_{\mu\nu}(q^2, m^2)$ loop integral when two propagators have the same mass, we will now repeat the calculation of this integral with two different masses and also the relevant integrals that come with it, that is B_0 , B_{21} and B_{20} . The following extension must be understood:

$$\begin{aligned} B_{\mu\nu}(q^2, m^2) &\mapsto B_{\mu\nu}(q^2, m_1^2, m_2^2) \\ B_0(q^2, m^2) &\mapsto B_0(q^2, m_1^2, m_2^2) \\ B_{20}(q^2, m^2) &\mapsto B_{20}(q^2, m_1^2, m_2^2) \\ B_{21}(q^2, m^2) &\mapsto B_{21}(q^2, m_1^2, m_2^2) \end{aligned} \tag{B.3.32}$$

We will just need B_{21} for the integral in Eq. (4.1.78) and just the divergent part numerically is relevant for us. We can directly obtain this from Appendix A of [2] and after applying our conventions and normalizations we obtain:

$$B_{21}(M^2, q^2, m_K^2, m_\pi^2) \simeq \frac{1}{16\pi^2} \left[\frac{M^2}{2} - \frac{m_K^2}{4} \log \frac{M^2}{m_K^2} + \frac{z m_K^2}{12} \log \frac{M^2}{m_K^2} \right] \tag{B.3.33}$$

Bibliography

- [1] G. 't Hooft and M Veltman. In: *Nucl. Phys. B* 153.365-401 (1979).
- [2] M. Harada and K. Yamawaki. In: *Physics Reports* 381 (2003), pp. 1–233.
eprint: [hep-ph/0302103](https://arxiv.org/abs/hep-ph/0302103).
- [3] G. 't Hooft and M Veltman. In: *Nucl. Phys. B* 44.189-213 (1972).
- [4] W. A. Bardeen, A. J. Buras, and J. -M. Gerard. In: *Nucl.Phys. B* 192 (1987),
p. 138.

Appendix C

Large N Structure of Wilson Coefficients

This appendix is based on the Gilman-Wise paper [1], where they have calculated the anomalous dimension matrix and so the Wilson coefficients at around 1 GeV, coming down from the scale of W while obtaining the effective Hamiltonian for $K \rightarrow \pi e^+ e^-$. But large N_c counting was irrelevant in their paper hence they did not keep $N_c = N$ explicit. In this appendix we will equip their calculation with explicit N structure right from the beginning ($f = 4$ quark case).

As this calculation is a straight forward revision of Gilman-Wise paper (referred above) improved with N structure, we will not go into details, one can refer to the paper, we will just revive the four quark case given in Appendix A of their paper with the intention of extracting N explicit form of $\tilde{C}_7(\mu)$ which is the coefficient of the operator $O_- = \mathcal{Q}_-$ in Eq. A15 of their paper. Following notations will help us a lot in the calculation:

$$\begin{aligned} A_+ &= 2/9\pi, & A_- &= -1/9\pi, & B_+ &= -2, & B_- &= 4, & \Gamma^{(+)} &= 1, & \Gamma^{(-)} &= -2, \\ \delta_N^{(f)} &= 11N - 2f, & \beta^{(f)}(g) &= -\delta_N^{(f)} \frac{g^3}{48\pi^2}, & \gamma^{(\pm)} &= \Gamma^{(\pm)} \frac{g^2}{4\pi^2}, & a_{\pm}^{(f)} &= \frac{6\Gamma^{(\pm)}}{\delta_N^{(f)}}, \\ b_{\pm}^{(f)} &= 1 - 3B_{\pm}/\delta_N^{(f)}, & g &= g(f=4) = \sqrt{4\pi\alpha_s(\mu^2)}, & \bar{g} &= \bar{g}(m_c/\mu, g) = \sqrt{4\pi\alpha_s(m_c^2)}, \\ g'(1, \bar{g}) &\simeq \bar{g}. \end{aligned}$$

In Gillman-Wise (GW) language, no-prime means original theory with full f that

can be either $f = 6$ for six-quark theory, or $f = 4$ for four-quark theory, that is the number of quarks (f) in the full theory. Single prime means $f - 1$, double prime means $f - 2$ and so on.

List of Integrals

$$\mathcal{I}_{\pm 0} = \int_g^{\bar{g}} dx \frac{\gamma^{(\pm)}(x)}{\beta(x)} = -a_{\pm}^{(4)} \log \frac{\bar{g}^2}{g^2} = \log \left(\frac{\alpha_s(m_c^2)}{\alpha_s(\mu^2)} \right)^{-a_{\pm}^{(4)}} \quad (\text{C.0.1})$$

$$I_7^{B_{\pm}} = B_{\pm} \int_z^{g'(1, \bar{g})} dx \frac{x^2}{8\pi^2 \beta'(x)} \simeq -\frac{6B_{\pm}}{\delta_N^{(3)}} \int_z^{\bar{g}} dx \frac{1}{x} = \log \left(\frac{\bar{g}}{z} \right)^{-6B_{\pm}/\delta_N^{(3)}} \quad (\text{C.0.2})$$

$$I_7^{(\pm 0)} = e^{\Gamma^{(\pm)} \mathcal{I}_{\pm 0}} = \left(\frac{\alpha_s(m_c^2)}{\alpha_s(\mu^2)} \right)^{-a_{\pm}^{(4)}} \quad (\text{C.0.3})$$

$$\begin{aligned} I_{7\pm}^{(A_{\pm}, B_{\pm})} &= A_{\pm} \int_{g'}^{g'(1, \bar{g})} dz \left(\frac{1}{\beta'(z)} \right) e^{I_7^{B_{\pm}}} \\ &= A_{\pm} \int_{g'}^{g'(1, \bar{g})} dz \left(\frac{8}{\beta'(z)} \right) \left(\frac{\bar{g}}{z} \right)^{-6B_{\pm}/\delta_N^{(3)}} \\ &= \frac{48\pi}{\delta_N^{(3)}} A_{\pm} (\alpha_s(m_c^2))^{-3B_{\pm}/\delta_N^{(3)}} \frac{(\alpha_s(m_c^2))^{-b_{\pm}^{(3)}} - (\alpha'_s(\mu^2))^{-b_{\pm}^{(3)}}}{b_{\pm}^{(3)}} \end{aligned} \quad (\text{C.0.4})$$

We redefine their[1] Eq. A11 the following way:

$$L_7^{(\pm)} \left(\frac{m_c}{\mu}, g \right) = I_7^{(\pm 0)} \left\{ I_{7+}^{(\pm)} L_+^{(\pm)}(1, \bar{g}) + I_{7-}^{(\pm)} L_-^{(\pm)}(1, \bar{g}) + L_7^{(\pm)}(1, \bar{g}) \right\} \quad (\text{C.0.5})$$

In leading logarithmic approximation $L_{\pm,7}^{(\pm)}(1, g)$ can be replaced by their free field values, the free field values are: $L_1^{(\pm)}(1, 0) = \pm 1$, $L_2^{(\pm)}(1, 0) = +1$, $L_7^{(\pm)}(1, \bar{g}) = 0$, that makes $L_+^{(\pm)} = (1 \pm 1)/2$ and $L_-^{(\pm)} = (1 \mp 1)/2$, last two can be expressed as $L_i^{(l)} = \delta_{li}$ also given in Eq. (42) of their previous paper[2]. Hence,

$$L_7^{(\pm)} \left(\frac{m_c}{\mu}, g \right) = I_7^{(\pm 0)} I_{7\pm}^{(\pm)}(A_{\pm}, B_{\pm}) \quad (\text{C.0.6})$$

Then using Eq. A1 of [1], we get:

$$H_{eff} = -\frac{G_F}{2\sqrt{2}} V_{us}^* V_{ud} \left(\tilde{C}_+ Q_+ + \tilde{C}_- Q_- + \tilde{C}_7 Q_7 \right) \quad (\text{C.0.7})$$

As large N expansion of \tilde{C}_- is given in many places but not \tilde{C}_7 we focus on \tilde{C}_7 only. Here,

$$\tilde{C}_7 = \left(\frac{\alpha_s(m_W^2)}{\alpha_s(\mu^2)} \right)^{-a_+^{(4)}} L_7^{(+)} + \left(\frac{\alpha_s(m_W^2)}{\alpha_s(\mu^2)} \right)^{-a_-^{(4)}} L_7^{(-)} \quad (\text{C.0.8})$$

As everything is expressed in terms of no. of colors (N), we can easily expand \tilde{C}_7 in large N .

$$\tilde{C}_7(\mu^2) = -\frac{4}{9\pi} \left[\log \frac{\mu^2}{m_c^2} + \frac{2}{11N} A(\mu^2) \right] + O(1/N^2) \quad (\text{C.0.9})$$

where,

$$\begin{aligned} A(\mu^2) &= \log \frac{m_c^2}{\Lambda^2} \left\{ 13 + 12 \log \left(\frac{\log \frac{m_W^2}{\Lambda^2}}{\log \frac{m_c^2}{\Lambda^2}} \right) \right\} \\ &\quad - 12 \log \frac{\mu^2}{\Lambda^2} \left\{ 1 + \log \frac{m_c^2}{\Lambda^2} + \log \left(\frac{\log \frac{m_W^2}{\Lambda^2}}{\log \frac{m_c^2}{\Lambda^2}} \right) \right\} \end{aligned} \quad (\text{C.0.10})$$

And,

$$\tilde{C}_-(\mu) = \frac{1}{2} \left[\frac{\alpha'_s(\mu^2)}{\alpha_s(m_c^2)} \right]^{-a_-^{(3)}} \left[\frac{\alpha_s(\mu^2)}{\alpha_s(m_W^2)} \right]^{-a_-^{(4)}} \quad (\text{C.0.11})$$

$$= 1 - \frac{12}{11N} \log \left[\frac{\log(m_W^2/\Lambda^2)}{\log(\mu^2/\Lambda^2)} \right] + O(N^{-2}) \quad (\text{C.0.12})$$

Although it is not needed here¹ but still one must use the N -explicit quark charge matrix too in relevant calculations:

$$Q = \frac{1}{2} \begin{bmatrix} 1 & 0 & 0 \\ 0 & -1 & 0 \\ 0 & 0 & -1 \end{bmatrix} + \frac{\mathbb{1}}{2N} \quad (\text{C.0.13})$$

¹Charge enters as $(Q_{11} - Q_{22,33})$ in our decay process hence the N dependence cancels out precisely.

Bibliography

- [1] F. J. Gilman and M. B. Wise. In: *Phys. Rev. D* (1980).
- [2] F. J. Gilman and M. B. Wise. In: *Phys. Rev. D* 20 (1979), p. 2392.